

LSPE: a large-scale polarization survey of the CMB

Silvia Masi

Sapienza Università di Roma & INFN Roma

for the LSPE collaboration

B-mode from Space

@ Max-Planck-Institut für Astrophysik
Munich, December 16–19, 2019



The LSPE collaboration

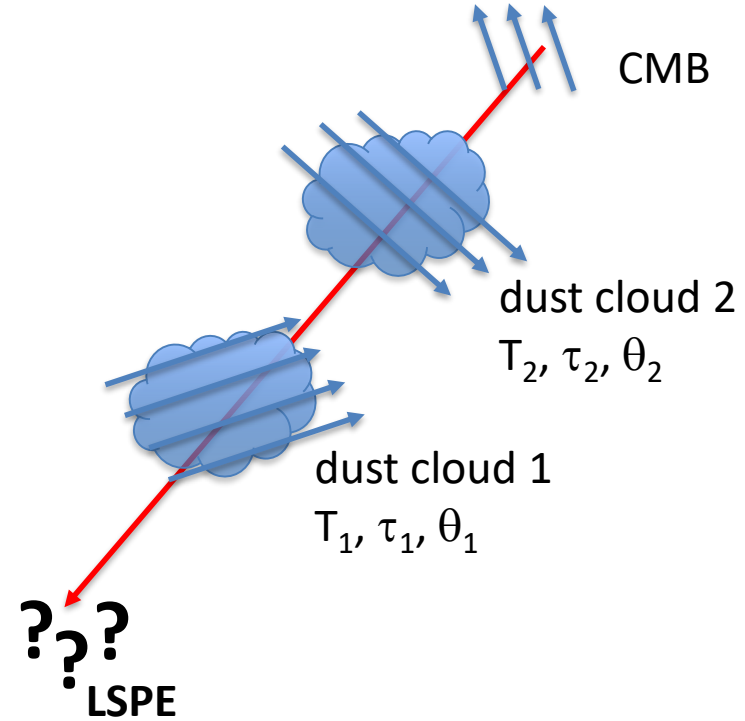
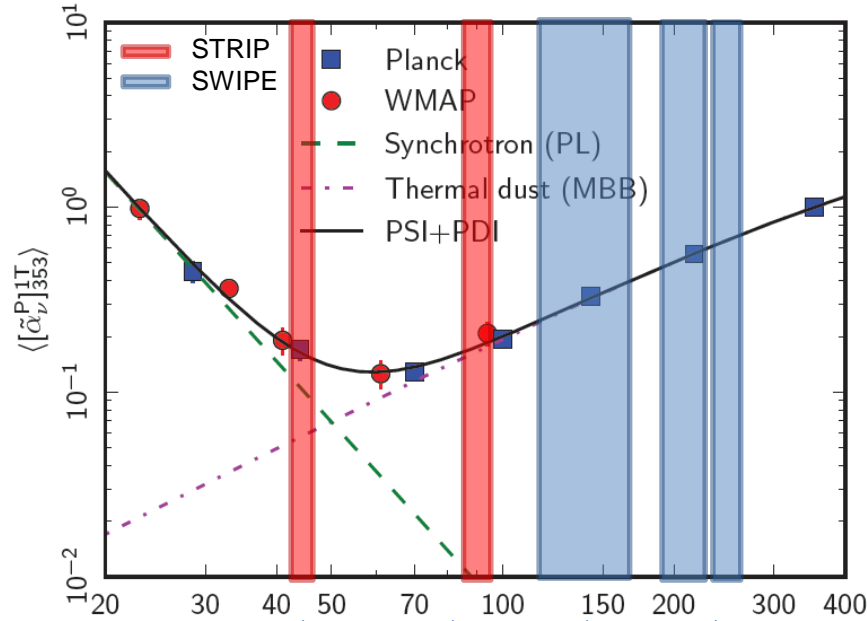
Scientists from institutions in Italy, UK, USA, Spain, Chile:

Addamo	G.	Gregorio	A.	Biasotti	M.
Farooqui	Z.	Maris	M.	Boragno	C.
Lumia	M.	Sartor	S.	Ceriale	V.
Paonessa	F.	Zacchei	A.	Corsini	D.
Peverini	O.A.	Hill-Valler	J.	Fontanelli	F.
Virone	G.	Jew	L.	Fumagalli	E.
Battaglia	P.	Jones	M.	Gatti	F.
Bersanelli	M.	Taylor	A.	Giovannini	M.
Caccianiga	B.	Watkins	B.	Grosso	D.
Caprioli	S.	Gaier	T.	Siri	B.
Cavaliere	F.	Soria	M.	Baldini	A. M.
Colombo	L.	Cleary	K.	Cei	F.
Franceschet	C.	Genova-Santos	R.	Galli	L.
Incardona	F.	González Escalera	V.	Grassi	M.
Maino	D.	Hoyland	R.	Incagli	M.
Mandelli	S.	Perez	A.	Moggi	A.
Mandelli	L.	Rebolo	R.	Nicolò	D.
Mennella	A.	Rubiño-Martin	J. A.	Piendibene	M.
Paradiso	S.	Mena	P.	Signorelli	G.
Pezzotta	F.	Pizarro	J.	Spinella	F.
Realini	S.	Reyes	N.	Tartari	D.
Tomasi	M.	Tapia	V.	Vaccaro	D.
Viganò	D.	Amico	G.	Ade	P.A.R.
Baschirotto	A.	Battistelli	E. S.	Pisano	G.
Baù	A.	Columbro	F.	Tucker	C.
De Matteis	M.	Coppi	G.	Coppi	G.
Gervasi	M.	Coppolecchia	A.	Martinis	L.
Ghigna	T.	D'Alessandro	G.	May	A.
Mainini	R.	de Bernardis	P.	McCulloch	M.
Nati	F.	De Petris	M.	Melhuish	S.
Passerini	A.	Lamagna	L.	Piccirillo	L.
Pincella	C.	Marchetti	T.	Baccigalupi	C.
Tartari	A.	Masi	S.	Farsian	F.
Zannoni	M.	Paiella	A.	Krachmalnicoff	N.
Cuttaia	F.	Panico	F.	Puglisi	G.
De Rosa	A.	Piacentini	F.	Matarrese	S.
Morgante	G.	Presta	G.		
Ricciardi	S.	Schillaci	A.		
Sandri	M.	Boscaleri	A.		
Terenzi	L.				
Villa	F.				

CNR-TO
UniMI, INFN-MI
UniMIB, INFN-MIB
INAF-BO
INAF-OAT
UniTS
Oxford
JPL
Caltech
IAC
UniChile
UniGE, INFN Ge
INFN Pi
Sapienza Roma, INFN Roma
IFAC CNR
UniCardiff
UniManchester
SISSA
UniPD
UniFE, INFN Fe
Tor Vergata, INFN RM2
ASI

- The **Large-Scale Polarization Explorer** is an experiment **to measure the polarization of the CMB at large angular scales.**
- **Science drivers / targets :**
 - The B-modes from inflation are mainly at large scales (r)
 - Polarization signatures from reionization (τ) are mainly at large scales
 - Rotation of the polarization angles (related to new physics)
 - Sensitive polarized dust survey at l close to the CMB ones
 - Sensitive polarized synchrotron survey at l close to the CMB ones
- **Instrumental approach :**
 - Frequency coverage: 40 – 250 GHz (5 bands)
 - 2 instruments covering the same northern sky
 - **STRIP** is a ground-based instrument working at 43 and 90 GHz
 - **SWIPE** works from near-space (balloon) at 145, 210, 240 GHz

LSPE : frequency coverage



43 GHz (ground)
Monitor polarized
synchrotron

90 GHz (ground)
Atmospheric monitor

145 GHz (balloon)
Main CMB channel

210 + 240 GHz (balloon)
Monitor **level, slope and possible rotation**
with frequency of polarized dust emission.
To date: extrapolated from single frequency (Planck 353 GHz)

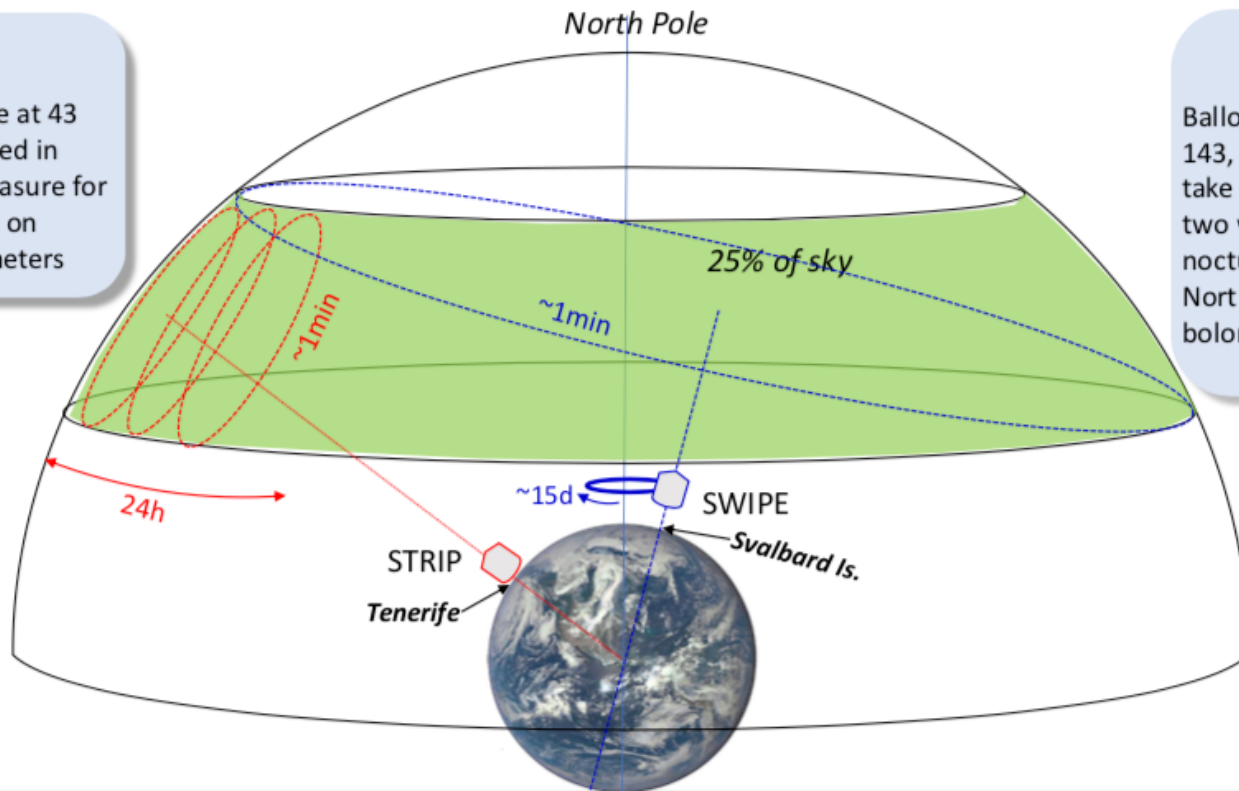
LSPE : Sky Coverage

STRIP

Ground telescope at 43 and 95 GHz located in Tenerife. Will measure for two years. Based on coherent polarimeters

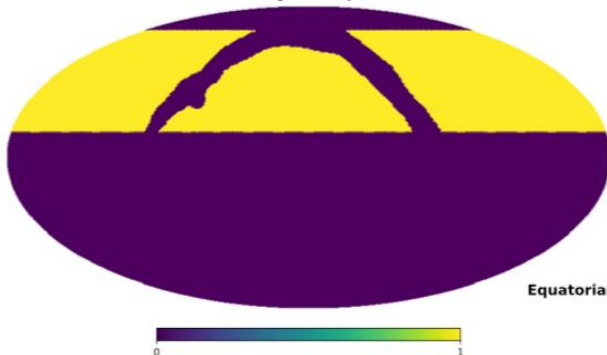
SWIPE

Balloon borne telescope at 143, 220 and 240 GHz. Will take measurements for two weeks during a LDB nocturnal flight around the North Pole. Based on TES bolometers

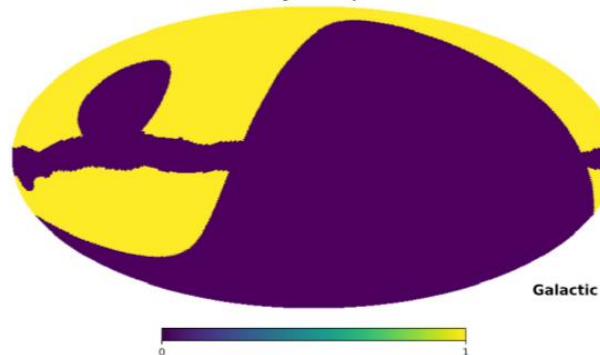


Credit A. Mennella

Mask covB + foreground - sky fraction: 0.303

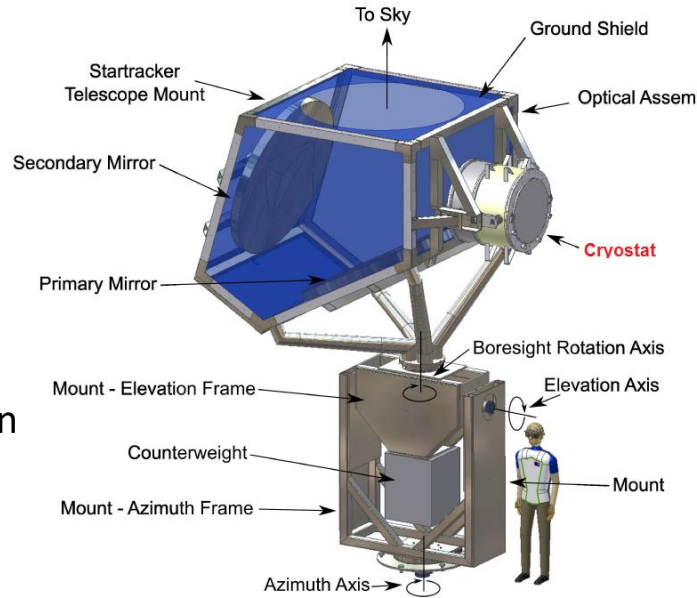


Mask covB + foreground - sky fraction: 0.303

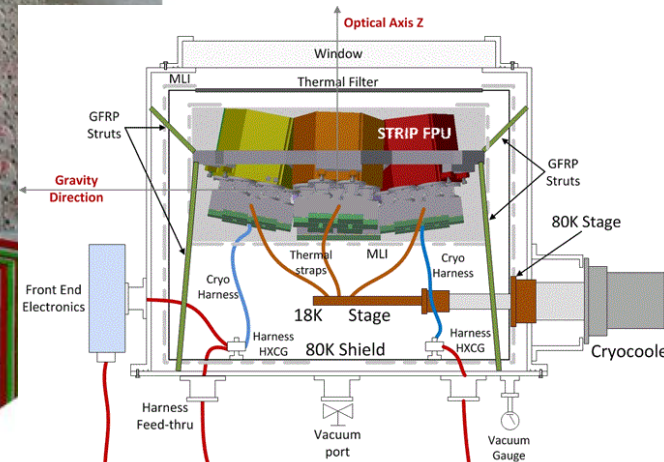
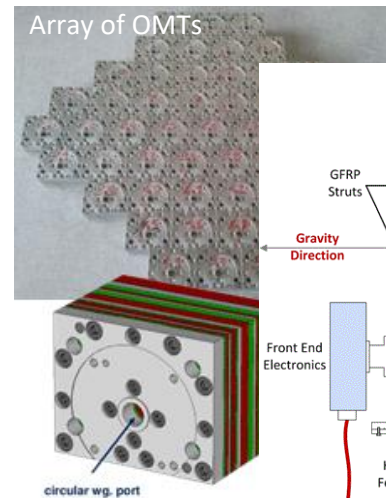


Credit L. Pagano,
F. Piacentini

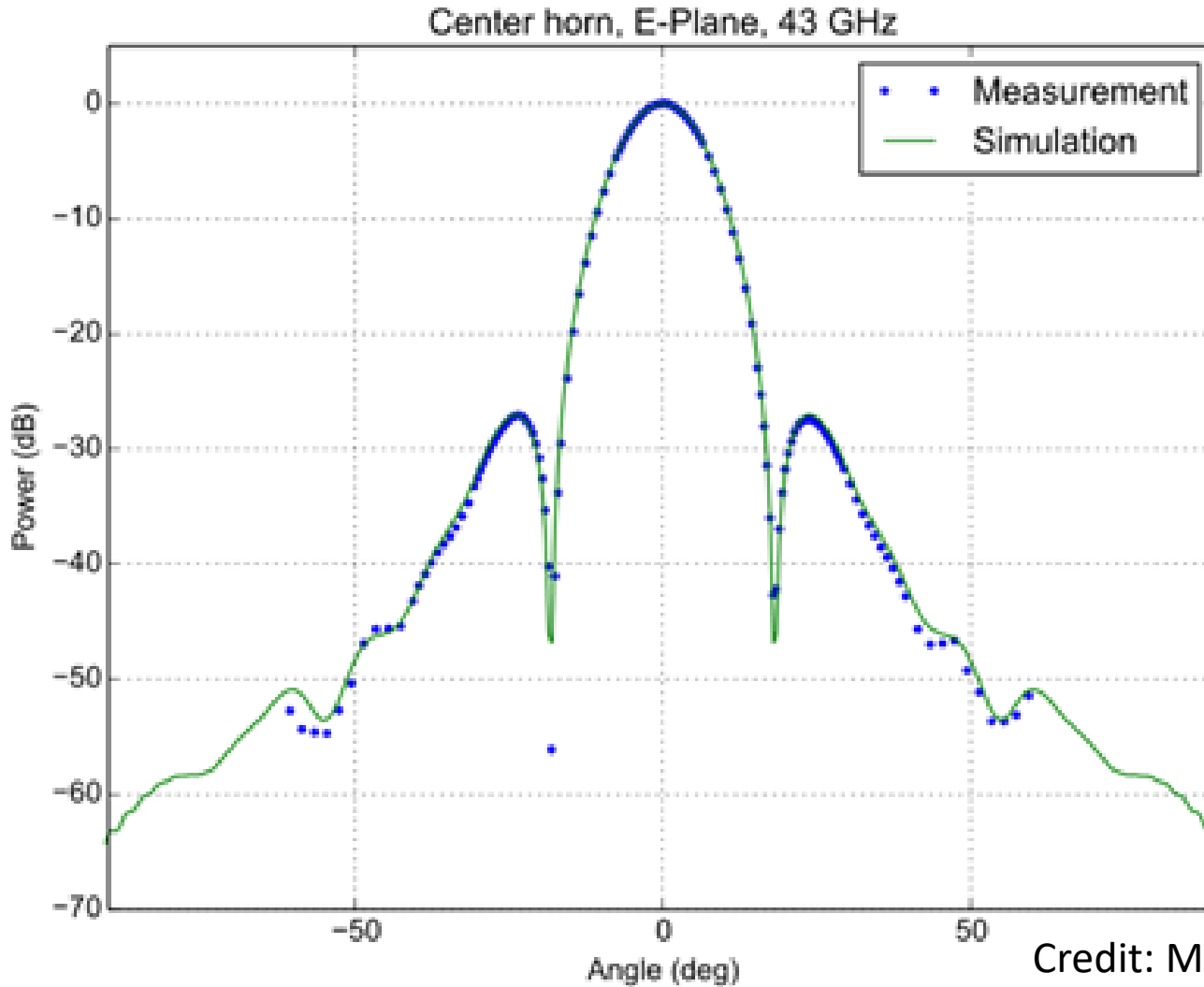
- Survey TeneRife Polarimeter
- Target: Polarized Synchrotron
- Two arrays of coherent polarimeters: 49 @44 GHz (QUIET) plus 7 @ 90 GHz.
- The measured response of the corrugated feedhorns confirms the expected performance down to -55 dB
- 1.5 m telescope (Clover)
- PI M. Bersanelli UNIMI



Instrument	STRIP	
Site	Tenerife	
Freq (GHz)	43	90
Bandwidth	17%	8%
Angular resolution FWHM (arcmin)	20	10
Detectors technology	HEMT	
Number of detectors N_{det}	49	6
Detector NET ($\mu K_{CMB} \sqrt{s}$)	515	1139
Mission duration	2 years	
Duty cycle	50%	
Sky coverage f_{sky}	37%	
Map sensitivity $\sigma_{Q,U}$ ($\mu K_{CMB} \cdot arcmin$)	102	777
Noise power spectrum ($N_{\ell}^{E,B}$) ^{1/2} ($\mu K_{CMB} \cdot arcmin$)	171	1330



Provides essential information on polarized synchrotron

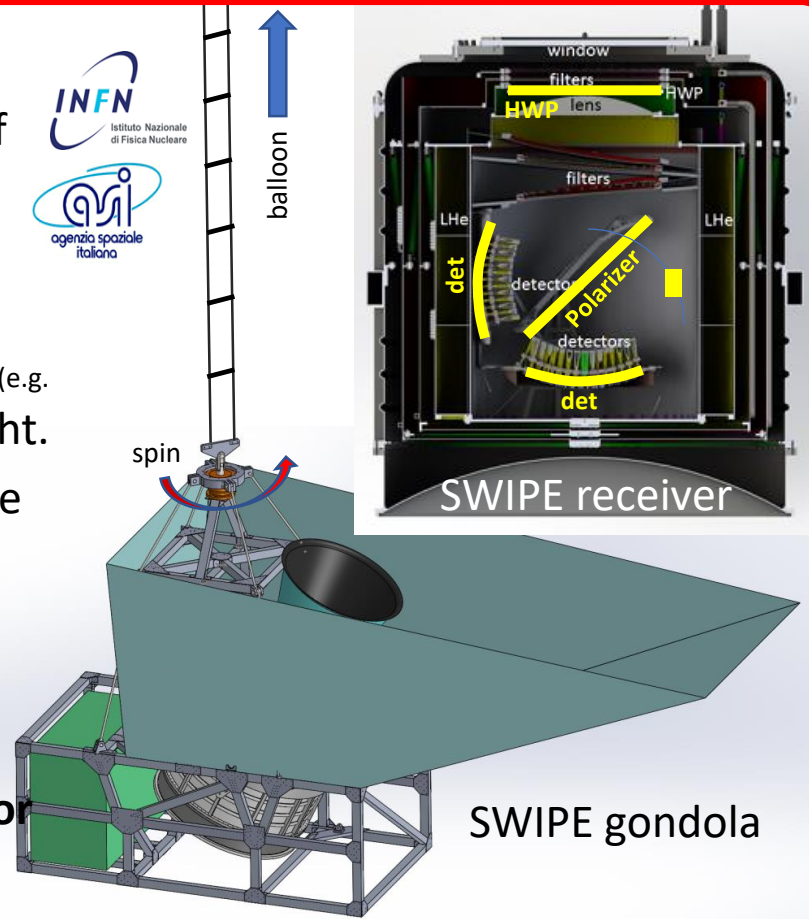


Credit: Mennella

Receiver under test. Telescope being finalized.

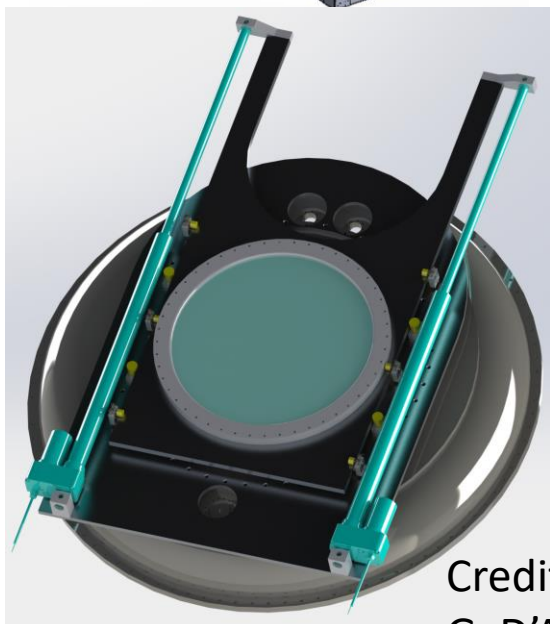
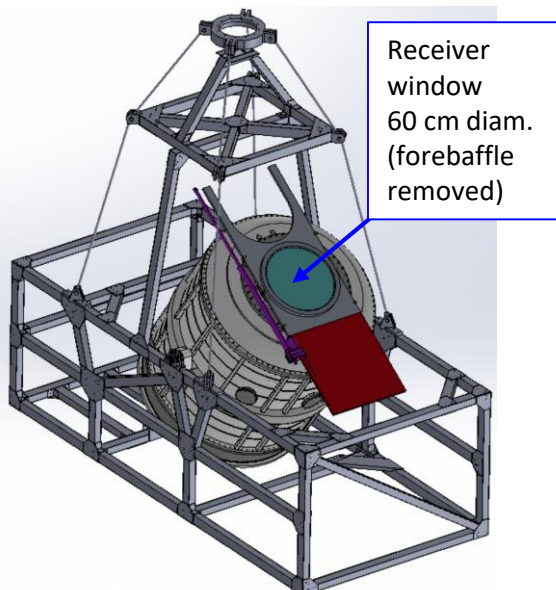
LSPE-SWIPE in a nutshell

- SWIPE is a multiband (145, 210, 220 GHz) array of Stokes polarimeters (163).
- Is flown on a stratospheric **balloon**, to avoid atmospheric noise at high f , including polarized radiation from ice crystals in tropospheric clouds (e.g. Takakura et al. 2018). **38%** of the sky covered in a 15d flight.
- SWIPE uses 326 **multimoded detectors** to improve the sensitivity wrt to Planck-HFI. The focal planes collect 8800 radiation modes. The resolution of each multimoded beam is 1.4° FWHM.
- Combined sensitivity: **10 $\mu\text{K arcmin}$ per flight**
- SWIPE uses an **HWP-based polarization modulator as the first optically active element**, to solve several issues important at large scales (beam asymmetry leakage, bandpass mismatch, $1/f$ noise ... etc.)
- SWIPE uses a **single large polarizer, common to the entire focal plane**, to define the main axis of the polarimeter with high precision ($< 0.1^\circ$): accurate absolute reconstruction of the pol. directions.
- PI P. de Bernardis (Sapienza)

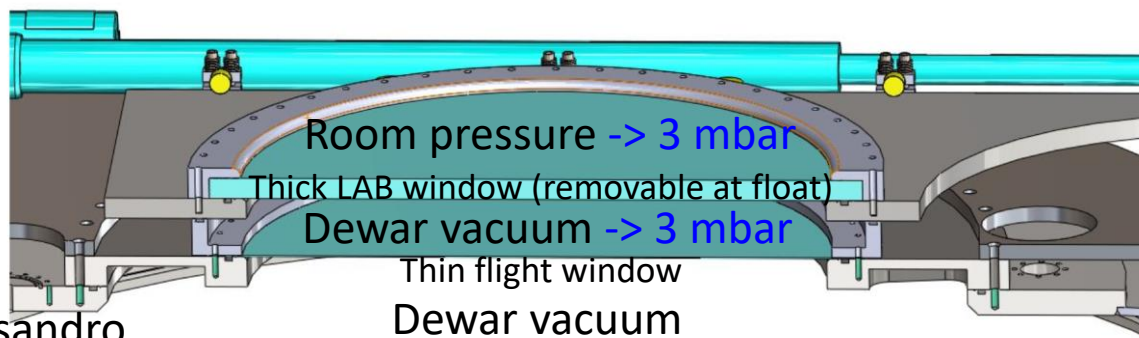
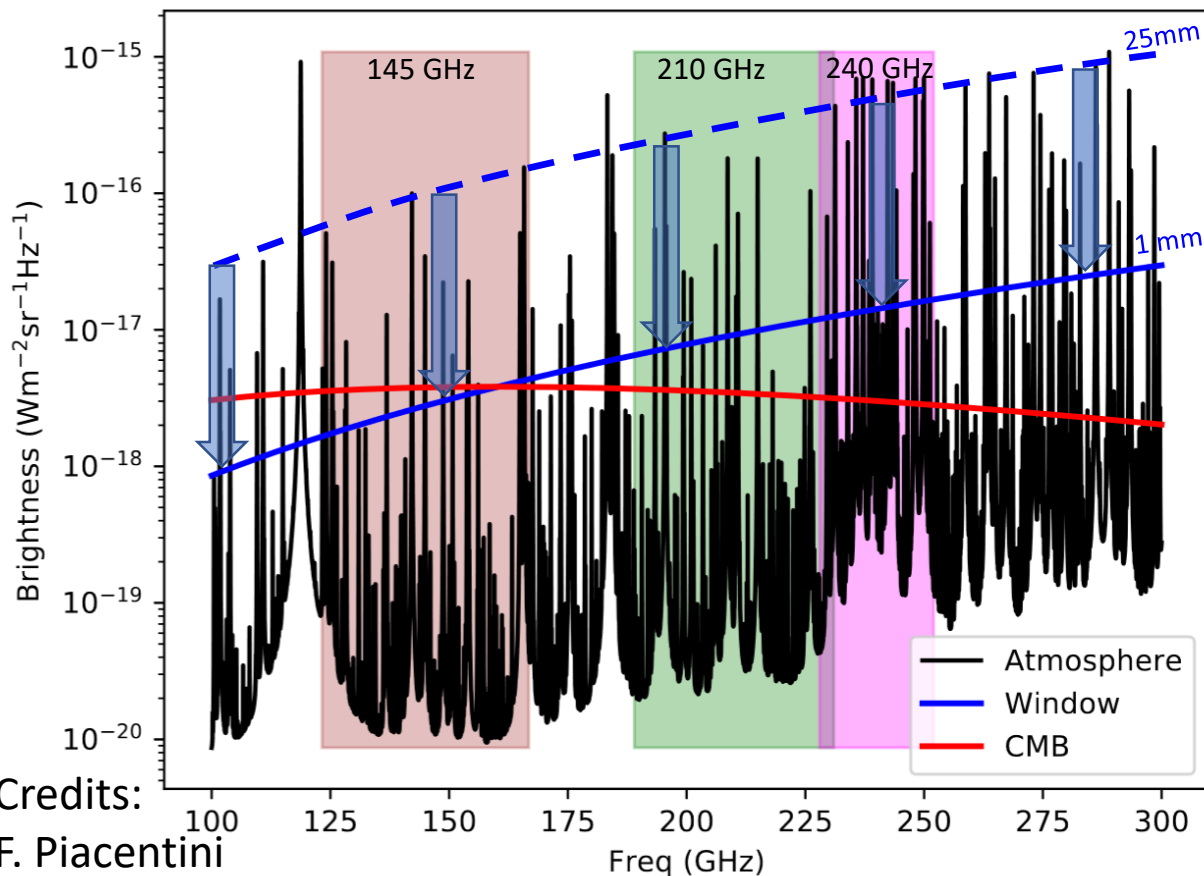


Instrument	SWIPE		
Site	balloon		
Freq (GHz)	145	210	240
Bandwidth	30%	20%	10%
Angular resolution FWHM (arcmin)	85		
Detectors technology	TES multimoded		
Number of detectors N_{det}	162	82	82
Detector NET ($\mu\text{K}_{\text{CMB}} \sqrt{\text{s}}$)	12.7	15.7	30.9
Mission duration	8 - 15 days		
Duty cycle	90%		
Sky coverage f_{sky}	38%		
Map sensitivity $\sigma_{Q,U}$ ($\mu\text{K}_{\text{CMB}} \cdot \text{arcmin}$)	10	17	34
Noise power spectrum ($N_\ell^{E,B}$) ^{1/2} ($\mu\text{K}_{\text{CMB}} \cdot \text{arcmin}$)	16	28	55

To fully exploit the low radiative background: thin window



Credits:
G. D'Alessandro



Background power on each detector :

$$W = \int f_\nu \alpha A \Omega I_\nu d\nu$$

Optical throughput :

$$A \Omega = n_{\text{modes}} \lambda^2$$

Photon noise :

$$\text{NEP}_{\text{ph}}^2 = 2 \int f_\nu \alpha A \Omega I_\nu h\nu \left(1 + \frac{f_\nu \alpha c^2 I_\nu}{h\nu^3} \right) d\nu.$$

Detector noise :

$$\text{NEP}_{\text{detector}} = \sqrt{4k_B T_c^2 G F}$$

Ideal noise performance estimate

band (GHz).....	145	210	240
bandwidth.....	30%	20%	10%
n_{modes}	[10,17]	[23,32]	[32,39]
$A \Omega$ (m ² sr).....		$n_{\text{modes}} \lambda^2$	
efficiency α	0.3	0.3	0.3
Power on cryostat entrance			
W_{CMB} (pW).....	9.1	7.9	3.9
W_{atm} (pW).....	0.9	1.9	9.8
W_{window} (pW).....	6.9	21.4	18.4
W_{total} (pW).....	16.9	31.2	32.1
Power on detector			
$W_{\text{total-detector}}$ (pW).....	5.1	9.4	9.6
Noise on detector			
$\text{NEP}_{\text{ph-CMB}}$ (aW/√Hz).....	23.5	25.9	19.3
$\text{NEP}_{\text{ph-atm}}$ (aW/√Hz).....	8.4	13.7	38.5
$\text{NEP}_{\text{ph-window}}$ (aW/√Hz)....	20.6	43.3	42.8
$\text{NEP}_{\text{ph-total}}$ (aW/√Hz).....	32.3	52.3	60.8
Thermal cond. G (pW/K) ...	86.2	158.9	163.5
$\text{NEP}_{\text{detector}}$ (aW/√Hz).....	37.9	51.5	52.3
$\text{NEP}_{\text{total}}$ (aW/√Hz).....	49.8	73.4	80.1
Optical noise			
$\text{NEP}_{\text{optical-total}}$ (aW/√Hz)....	166	245	267
NET ($\mu\text{K}_{\text{CMB}} \sqrt{\text{s}}$).....	12.7	15.7	30.9

The power of multimoded bolometers ...

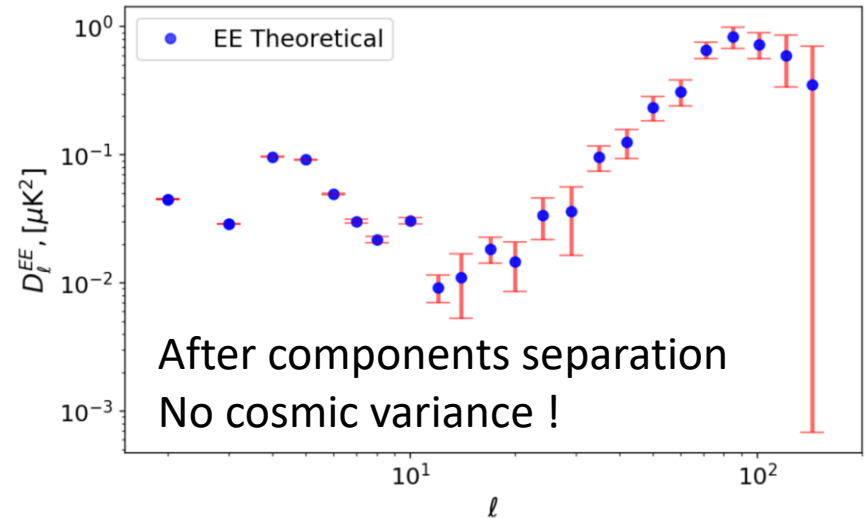


- TOD simulations > Components separation > Power spectra > Parameters (r , τ)
- Forthcoming LSPE paper. Preview of Results:

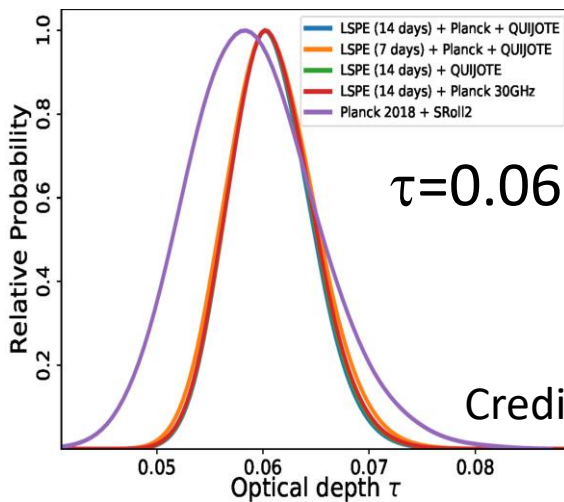
Table 7. Component separation weights for each component in each channel for the minimal case: Planck + LSPE (STRIP, SWIPE).

f (GHz)	Probes	W_{CMB}	W_{Dust}	W_{Synch}
30	P	-1.5×10^{-2}	2.7×10^{-3}	8.7×10^{-1}
43	ST	-2.6×10^{-3}	-4.5×10^{-4}	3.9×10^{-1}
145	SW	1.4	-4.1×10^{-1}	-1.6
210	SW	-1.9×10^{-1}	2.4×10^{-1}	2.8×10^{-2}
240	SW	-2.02×10^{-1}	1.6×10^{-1}	3.4×10^{-1}

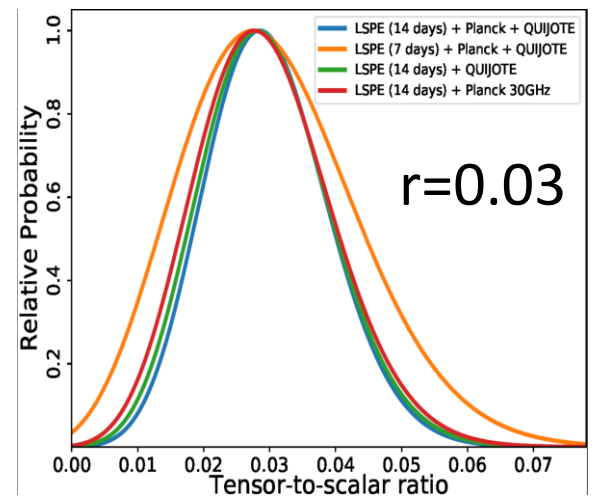
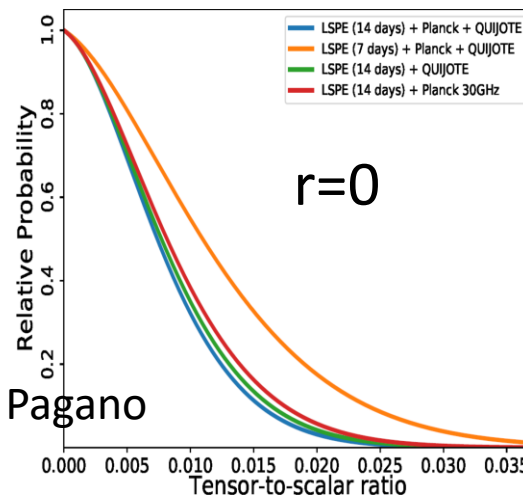
Credit: Piacentini



Credit: Krachmalnicoff, Farsian



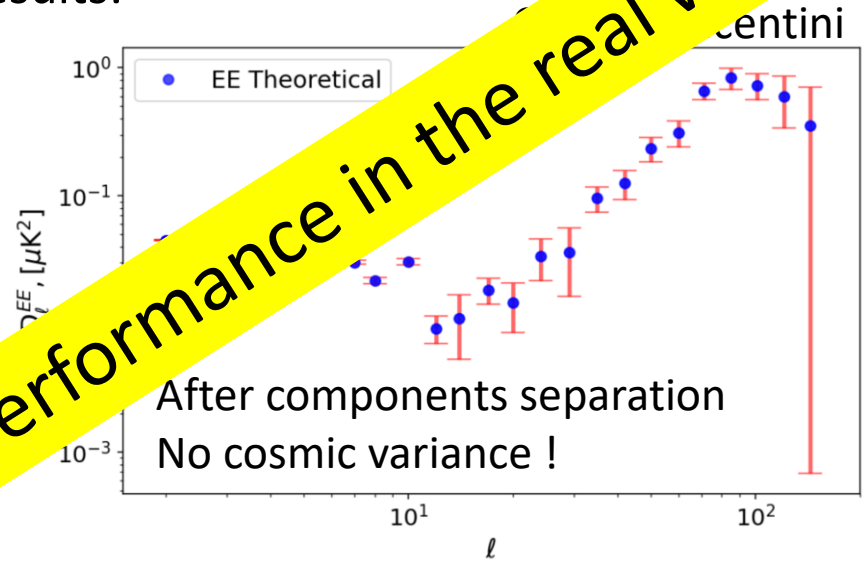
Credit: Pagano



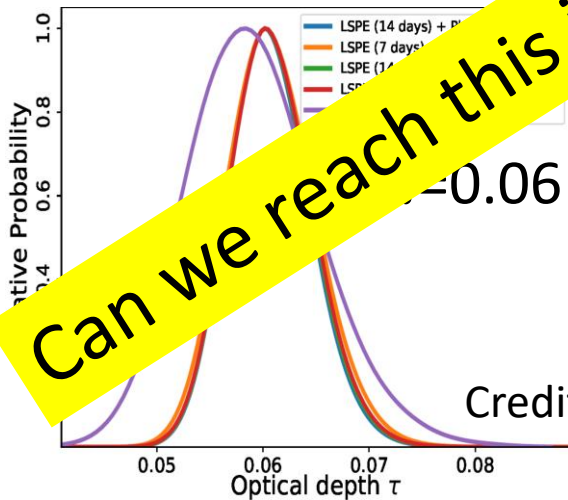
- TOD simulations > Components separation > Power spectra > Parameters
- Forthcoming LSPE paper. Preview of Results:

Table 7. Component separation weights for each component in each channel for the minimal case: Planck + LSPE (STRIP, SWIPE).

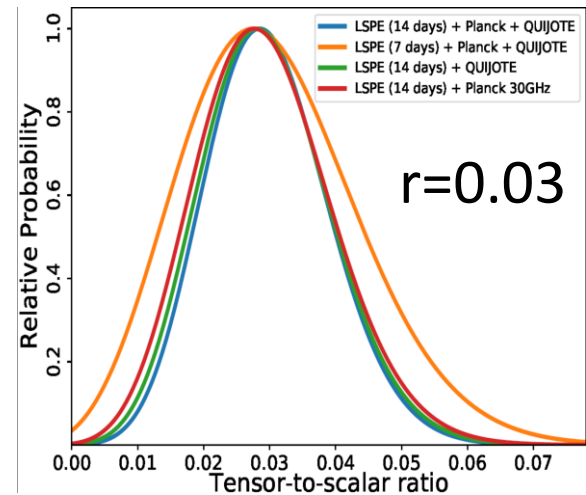
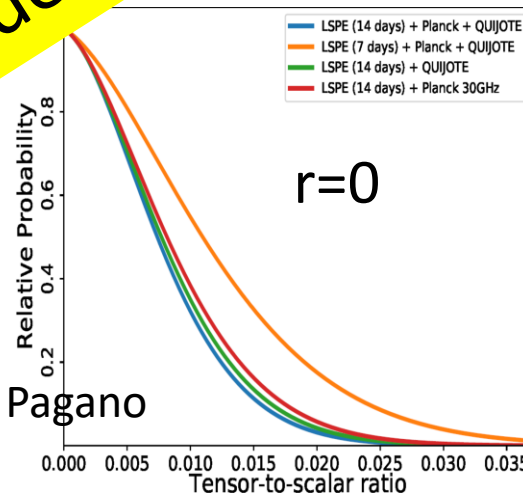
f (GHz)	Probes	W _{CMB}	W _{Dust}	W _{Synch}
30	P	-1.5×10^{-2}	2.7×10^{-3}	8.7×10^{-1}
43	ST	-2.6×10^{-3}	-4.5×10^{-4}	3.9×10^{-1}
145	SW	1.4	-4.1×10^{-1}	-1.6
210	SW	-1.9×10^{-1}	2.4×10^{-1}	2.8×10^{-2}
240	SW	-2.02×10^{-1}	1.6×10^{-1}	3.4



Credit: Krachmalnicoff, Farsi



Credit: Pagano



Can we reach this idealized performance in the real world ?

- Ideal operation: staring at a given sky pixel with polarization vector (I_s, Q_s, U_s, V_s) , the signal W measured by the detectors (sensitive to horizontal or vertical polarization) is

$$\Rightarrow W_H = \frac{1}{2} [I_s + Q_s \cos(4\gamma + 2\theta) + U_s \sin(4\gamma + 2\theta)]$$

$$\Rightarrow W_V = \frac{1}{2} [I_s - Q_s \cos(4\gamma + 2\theta) - U_s \sin(4\gamma + 2\theta)]$$

γ = angle of the fast HWP axis wrt the instrument vertical (geometrical, mechanical)

θ = angle of the instrument vertical wrt the meridian

- So, the measured signal should be at $f_{HWP,opt} = 4f_{HWP,mech}$
- However, real HWPs are nonideal ...
- and optical systems are also not ideal.
- Real-world nonidealities produce spurious optical signals at $f_{HWP}, 2f_{HWP}, 3f_{HWP}, 4f_{HWP}, 5f_{HWP}, 6f_{HWP} \dots$
- Moreover, the sky scan modulates the input signal, encoding the sky polarization signal in *two narrow sidebands* of $4f$. These must be free from spurious signals.
- We have adjusted f_{HWP} and f_{scan} to approximate this condition.

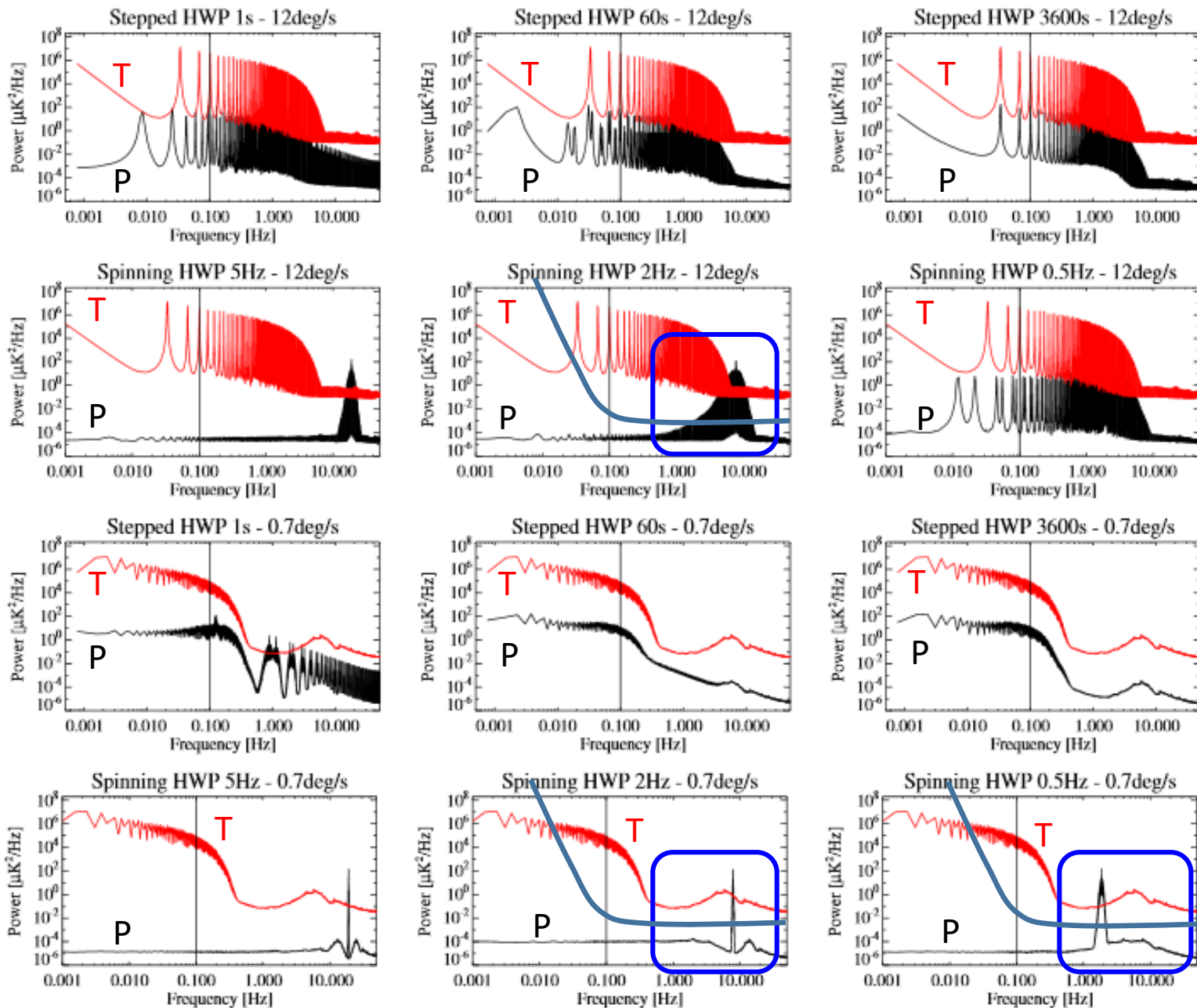
- Bolometric detectors are slow (especially the large area ones used for multimode detectors, with $\tau \sim 30$ ms)
- So $4f_{\text{HWP}}$ should be low enough that a 30 ms delay in the response of the bolometer is nearly irrelevant, or can be corrected precisely.
- Otherwise, such a delay would mimic a systematic offset $\Delta\gamma$ in the knowledge of the rotation angle γ of the HWP: this would result in a leakage of E-modes in B-modes

(see e.g. Pagano et al. 2009):

$$C_{\ell}^{BB,L} = C_{\ell}^{EE} \sin^2(2\Delta\gamma)$$

- In order to target $\sigma_r=0.01$, the rotation angle must be known better than **$\Delta\gamma=10$ arcmin.**
- The delay due to the time constant of the bolometer can be compensated deconvolving the bolometer transfer function in the analysis pipeline. This procedure, however, requires a precise knowledge of the time constant.
- In our case, if $\tau=30$ ms and $f_{\text{HWP}}=0.5$ Hz, it is required **$\sigma_{\tau}<1$ ms**, a reasonable target for both ground-based and in-flight calibration.
- This drives us to select **$f_{\text{HWP}}=0.5$ Hz** (0.5 rps, $T_{\text{HWP}}=2$ s), with an optical signal around 2Hz.
- The payload spin in azimuth (scan frequency f_{scan}) is adjusted so that most of the signal of interest is well within the $[3f_{\text{HWP}} - 5f_{\text{HWP}}]$ interval. In this way it is not cut by the notch filters used to remove synchronous systematics.

Signal-only simulations of SWIPE signals for different HWP & scan strategies:



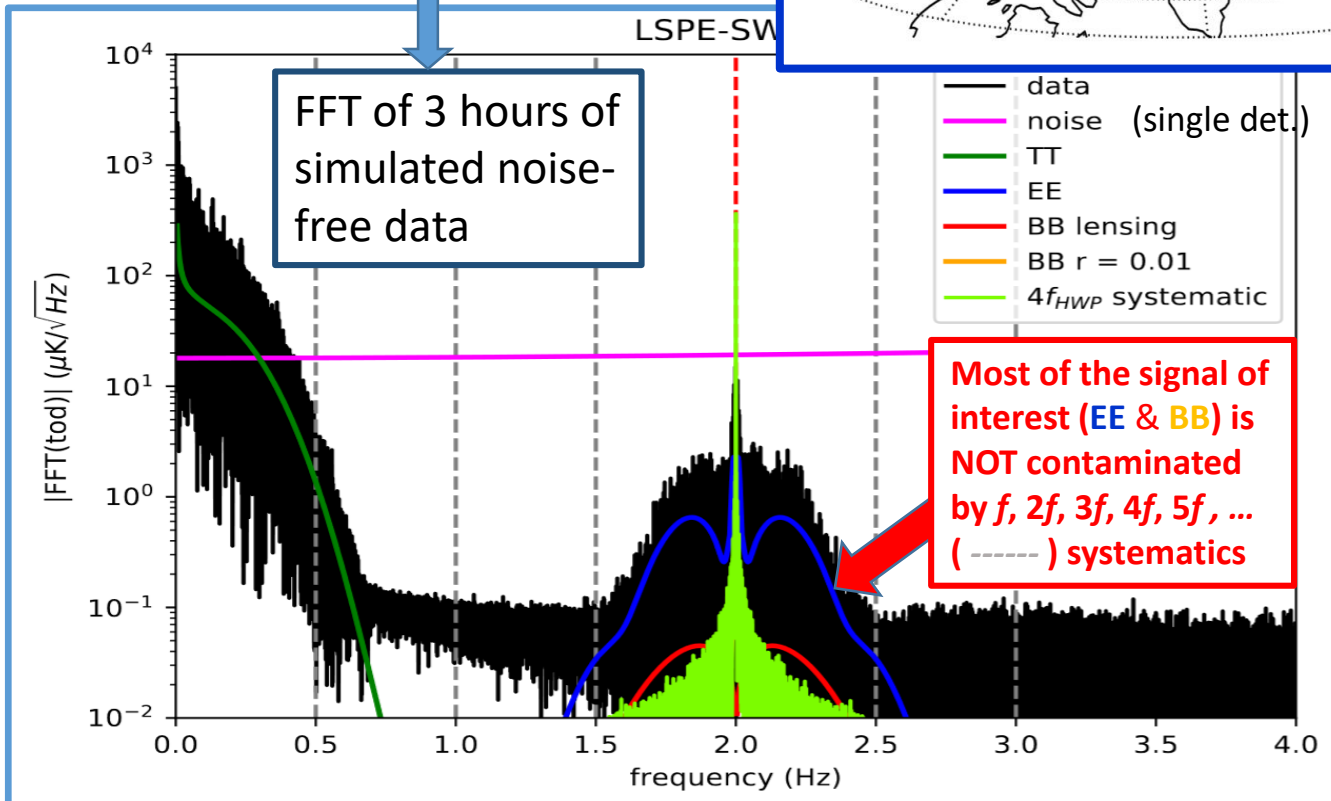
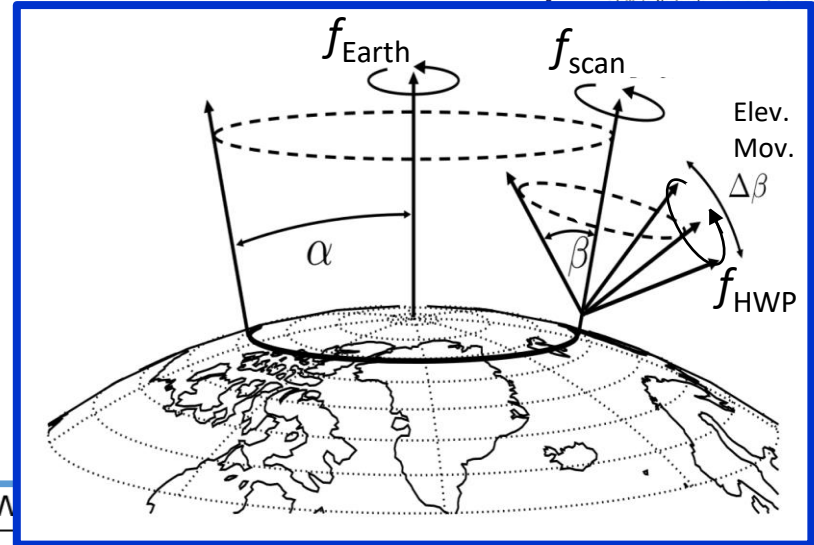
Based on $\tau_{bol}=30\text{ms}$:

$f_{HWP} = 0.5 \text{ Hz mech.} \rightarrow 2\text{ Hz optical}$
 TOD simulations suggest

$f_{scan} = 1.93 \text{ mHz}$
 ($0.7^\circ/\text{s}$, $T_{scan}=8.6 \text{ min}$)

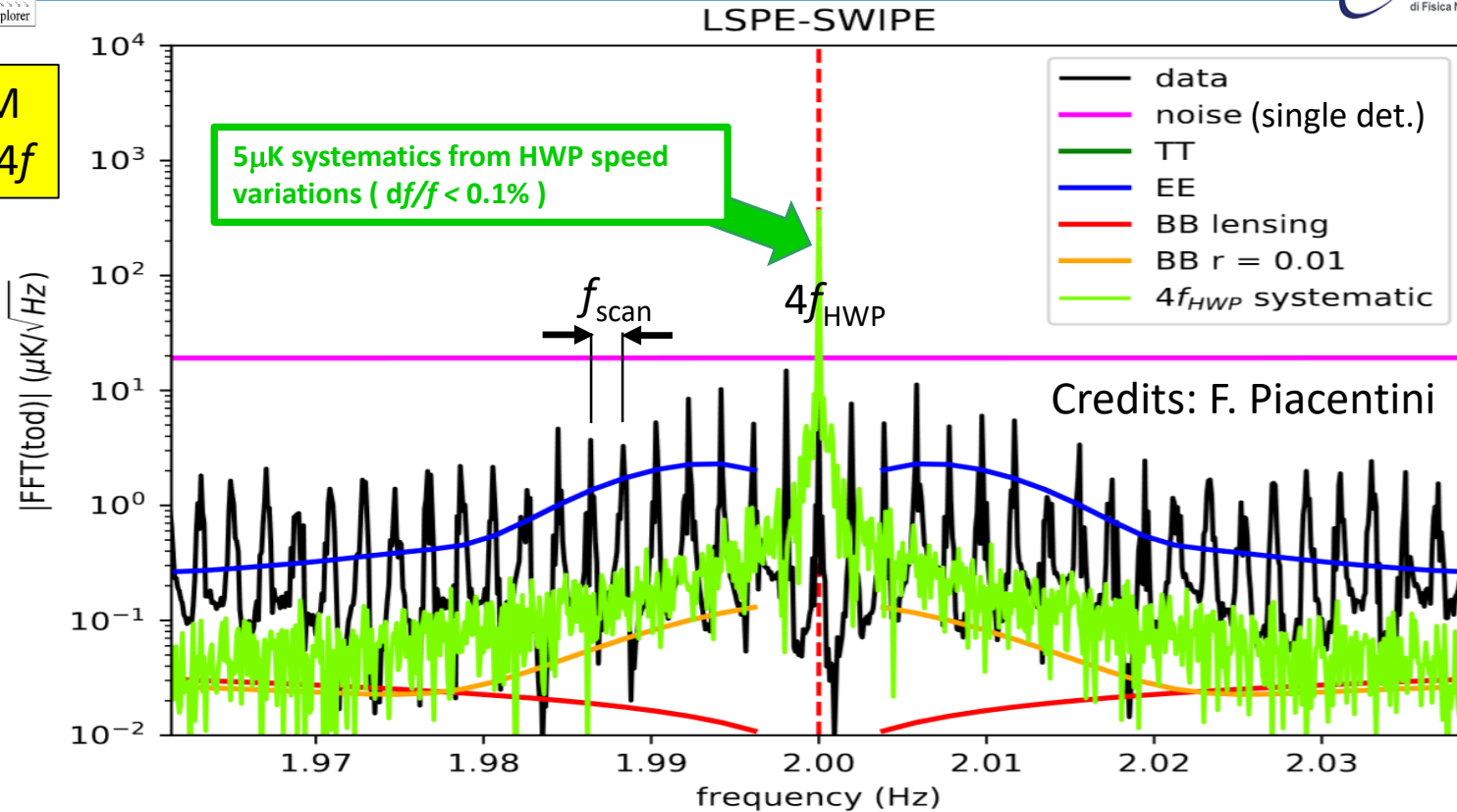
#modulations per FWHM = 4.5.

With this choice..



Credits:
 F. Piacentini

ZOOM
near $4f$

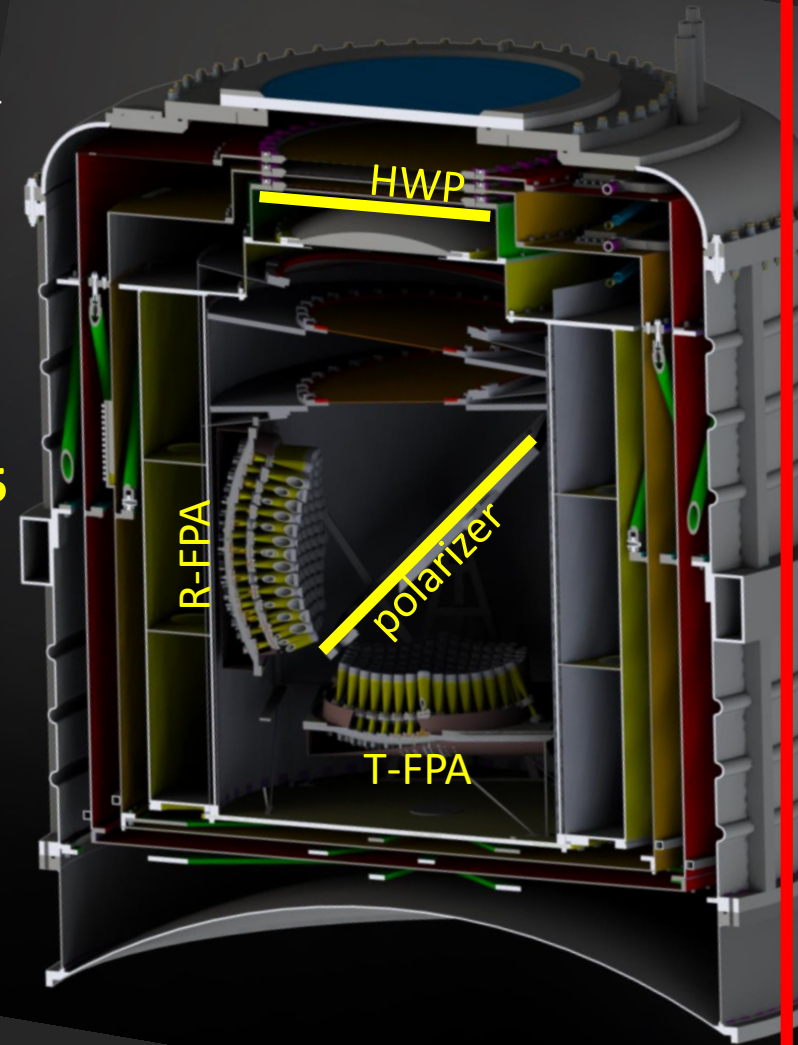


- The signal of interest (black line) is encoded in the peaks at $4f_{HWP} \pm f_{scan} \pm 2f_{scan} \pm 3f_{scan} \pm \dots$. The intermediate frequencies contain only noise, and can be filtered out using custom notch filters (for example removing the interval $[4f_{HWP} - f_{scan} \dots 4f_{HWP} + f_{scan}]$).
- The noise from both the detector (magenta) and the speed instability (green) are for 1s of integration and are reduced when increasing the integration time, while the signals (black, blue, red, orange) will remain where they are.
- Detector noise (magenta) will also decrease including data from more than 1 detector.

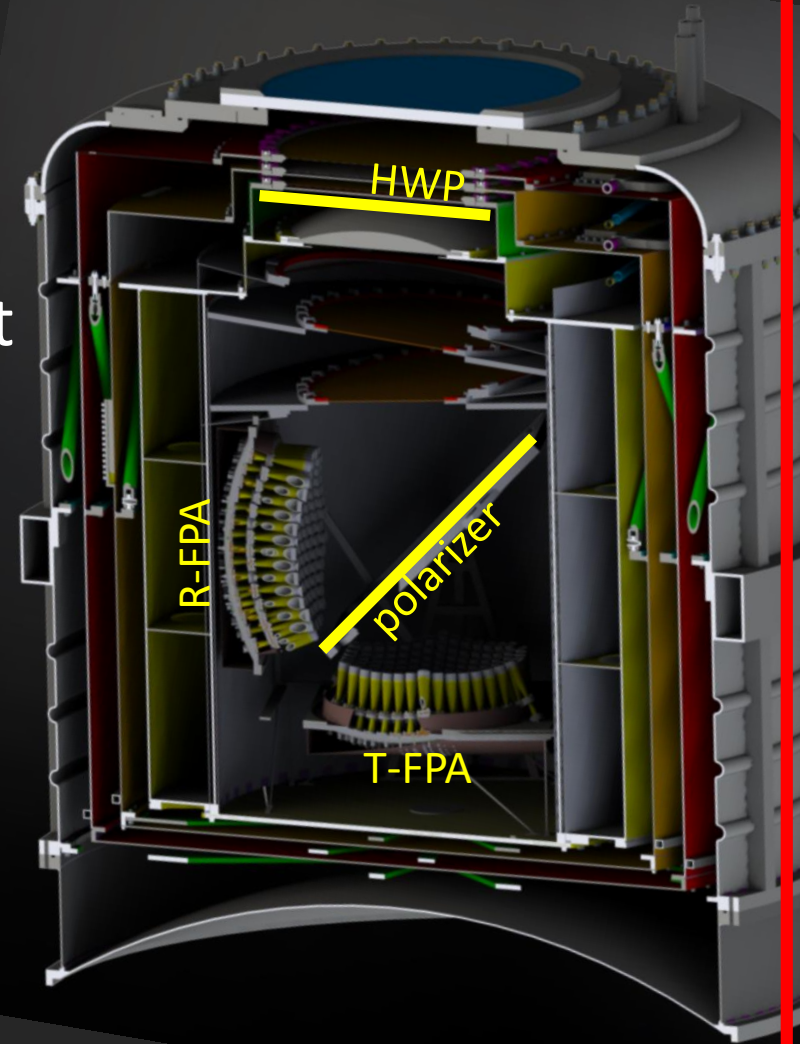
Reduction of the amplitudes of HWP-synchronous systematic effects

In a real Stokes polarimeter, the optical devices produce polarized emission, which can be in part modulated by the rotation of the HWP (e.g. Salatino & de Bernardis 2010, Columbro et al. 2019)

- Polarized emission/transmission of the lens, stop, field optics: mitigated using the HWP as the first optical element skywise.
- The HWP can have slightly different efficiencies for the fast and slow axes. This results in polarized emission & transmission of the HWP, modulated by the polarizer, i.e. a $2f_{\text{HWP}}$ signal (**5 mK !**). Mitigated by filtering the output signal (bandpass around $4f_{\text{HWP}}$)
- The polarizer emission can be reflected by the HWP and modulated: this results in a small $4f_{\text{HWP}}$ signal. Mitigated by reducing the temperature of the polarizer (here 1.6K, so **few μK**). Can be removed by a dedicated pipeline (e.g. Ritacco & 2017).
- The polarized emission of the HWP can be reflected by the polarizer and by the HWP. This is a small $4f_{\text{HWP}}$ signal. In our case is very small, since the polarizer is tilted 45° wrt the HWP.



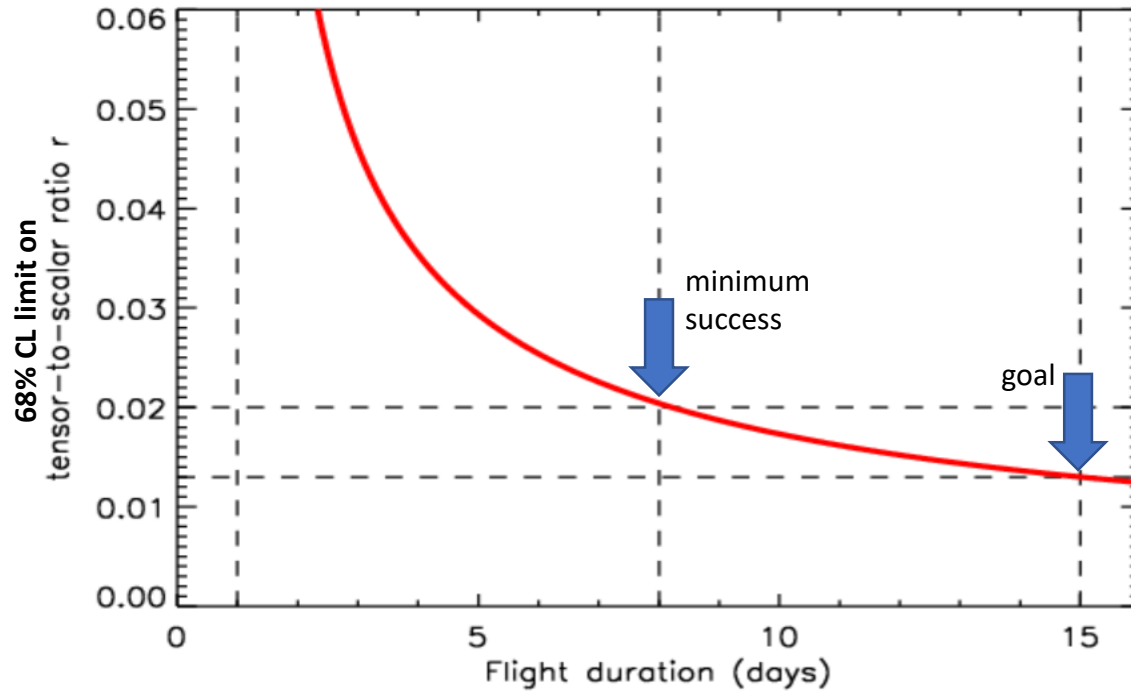
- There are other subtle systematic effects, an additional ones will be discovered.
- One of the main reasons of interest for this experiment is that we have the opportunity to study **experimentally** the performance of a Stokes polarimeter with cryogenic spinning HWP, a configuration which will be used in several ultrasensitive experiments, including LiteBIRD.
- Real experimental tests are badly needed, in addition to simulations, to validate a very difficult measurement !



LSPE: HW implementation & status

Mission Requirements:

SWIPE limits
(68% CL) to the
tensor to scalar
ratio versus
integration time
(including
foregrounds
separation):

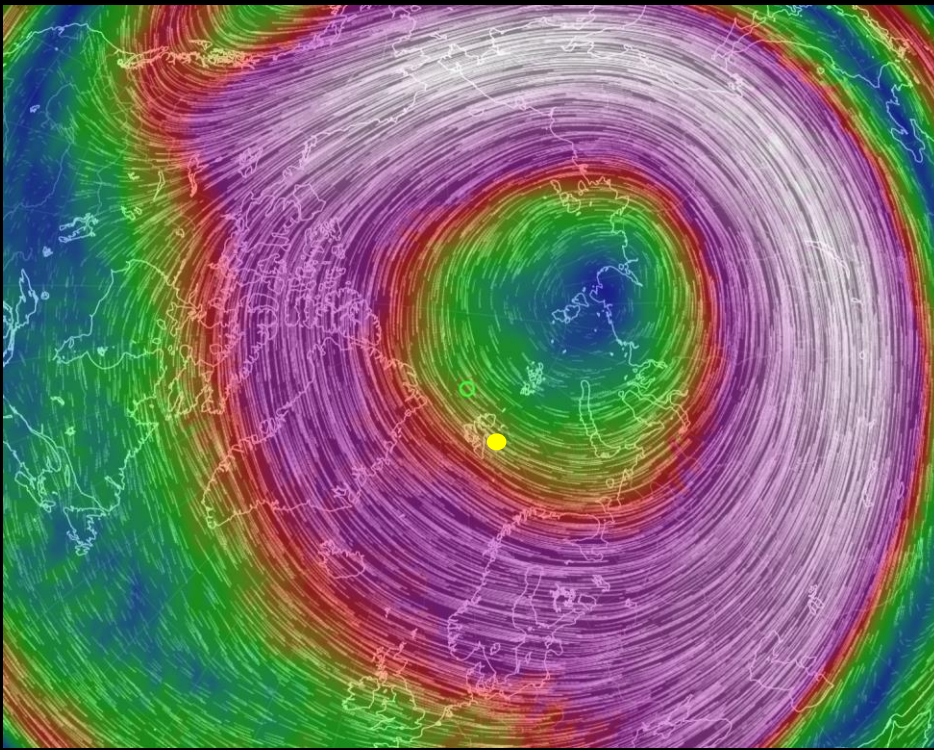


- Long integration time (8 days minimum, 15 days goal)
- Night flight (to cover a large sky fraction with a telescope spinning in azimuth)

LSPE/SWIPE : polar night flight

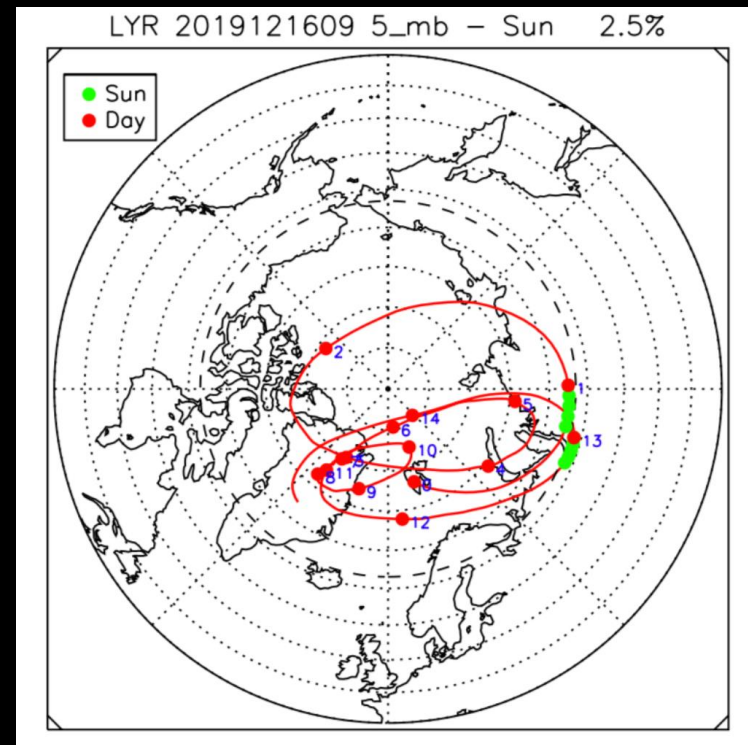
- Uses the winter stratospheric polar vortex
- Less stable than the summer vortex used in Antarctica
- Reliable forecast tools needed

16/Dec/2019: polar vortex



Credit: earth.nullschool.net

16/Dec/2019: flight forecast: 14 days



Credit: Piacentini

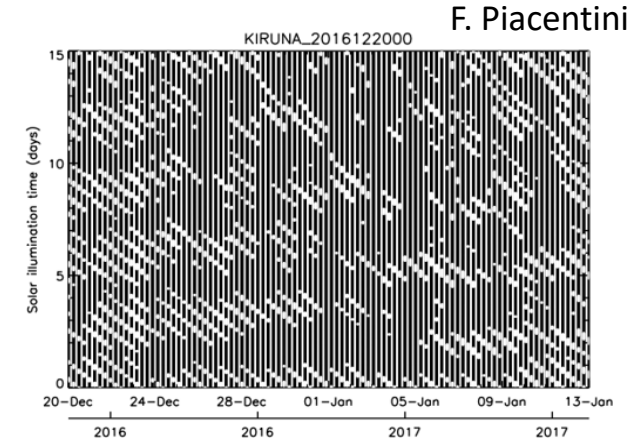
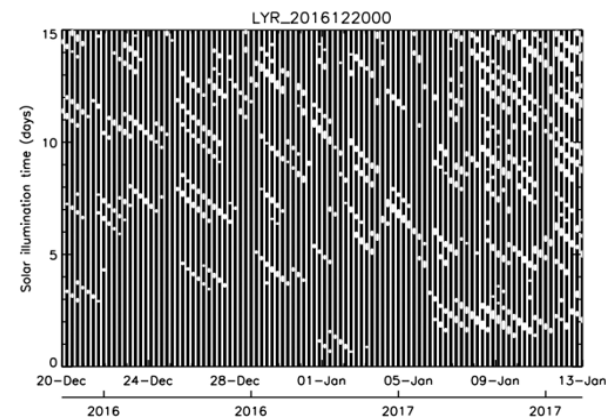
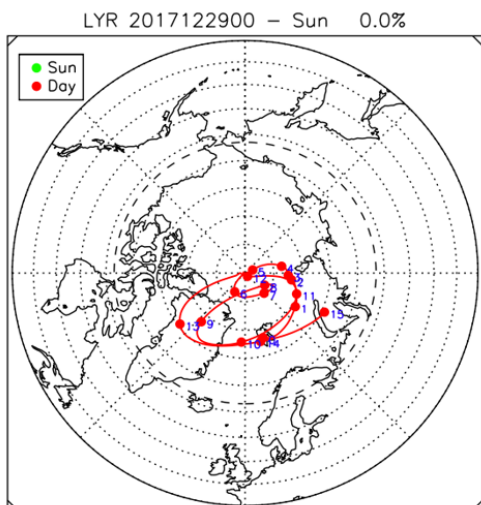
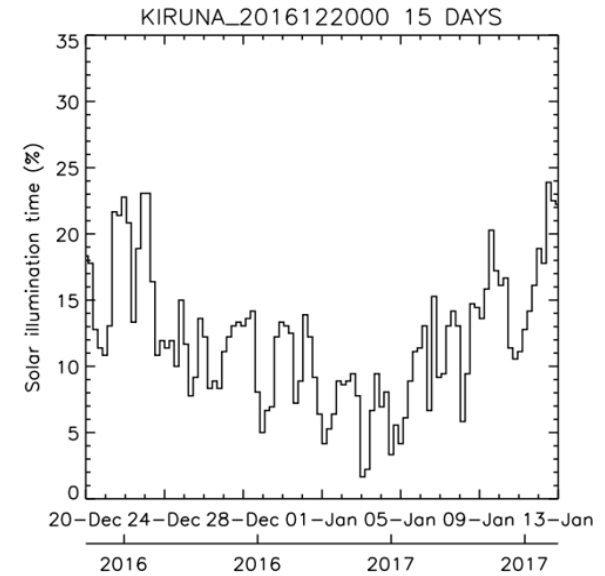
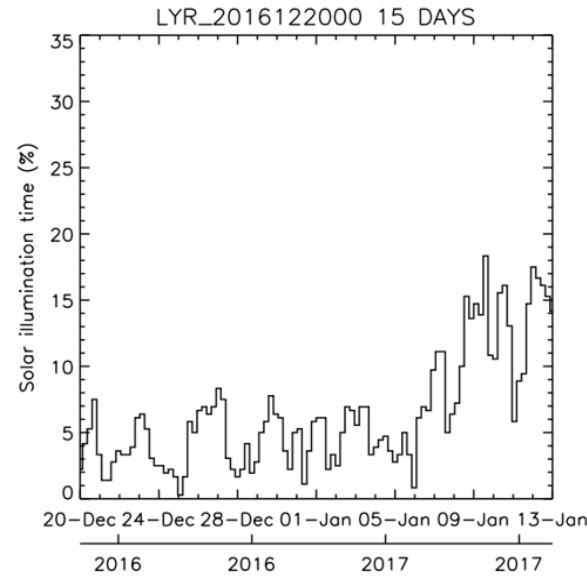
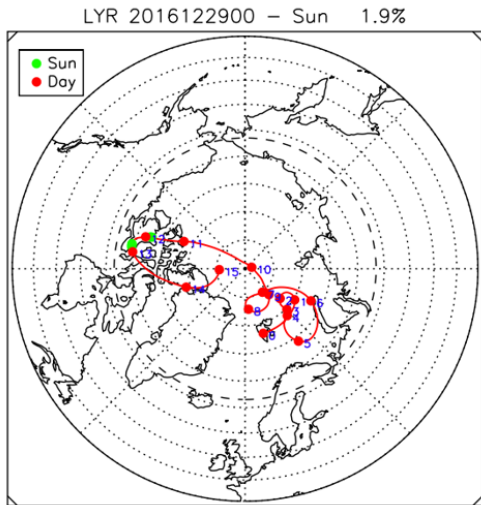
LSPE/SWIPE : night polar flight

- Flight managed by ASI, scheduled for end of 2021
- Longyearbyen – Svalbard or Kiruna Sweden
- Several test flights already carried out



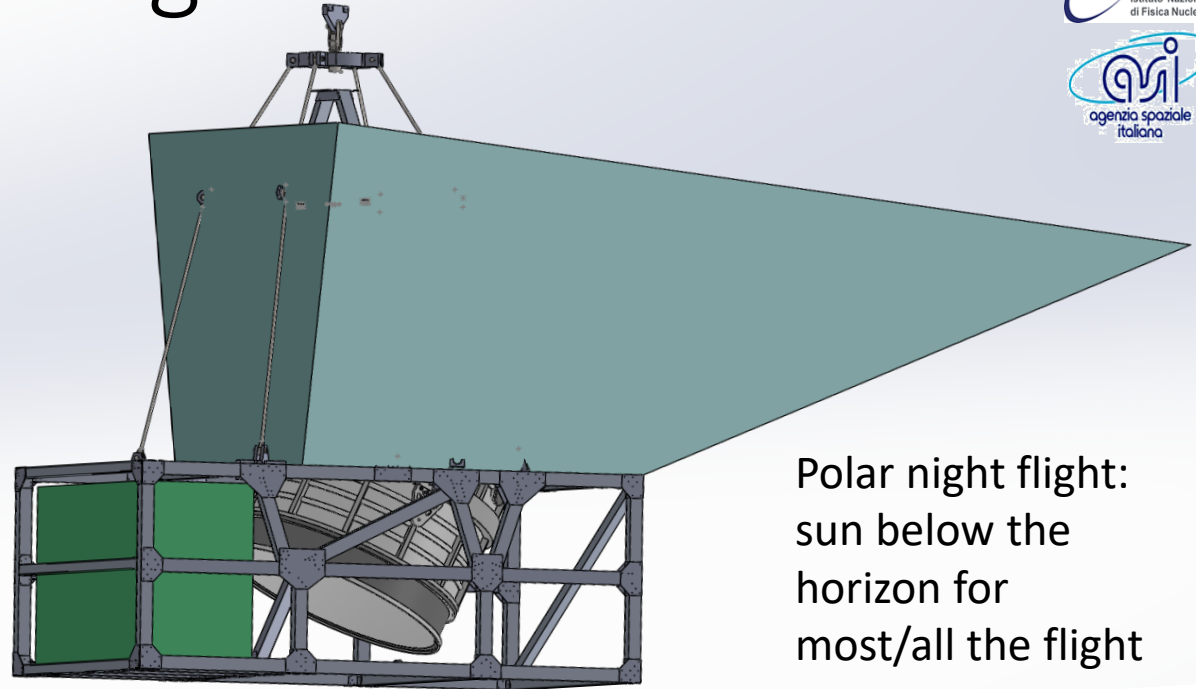
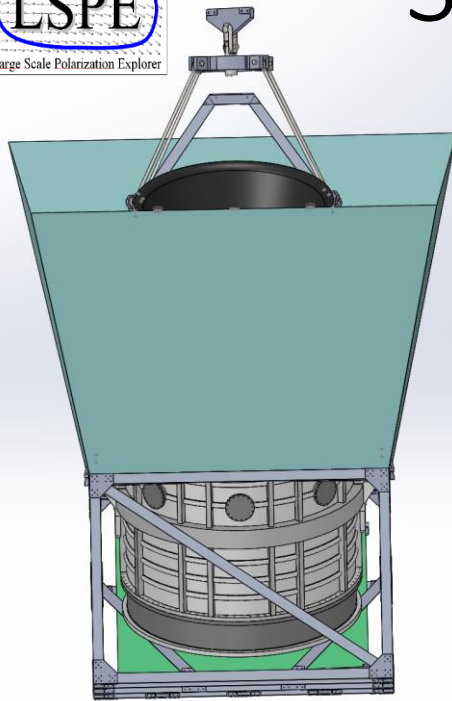
SWIPE: solar illumination issues

- With a careful choice of the launch date and launch site the length of the illuminated portions of the flight can be minimized
- We do not plan to carry out science measurements during these periods, but the instrument should be prepared to survive short solar illumination periods.



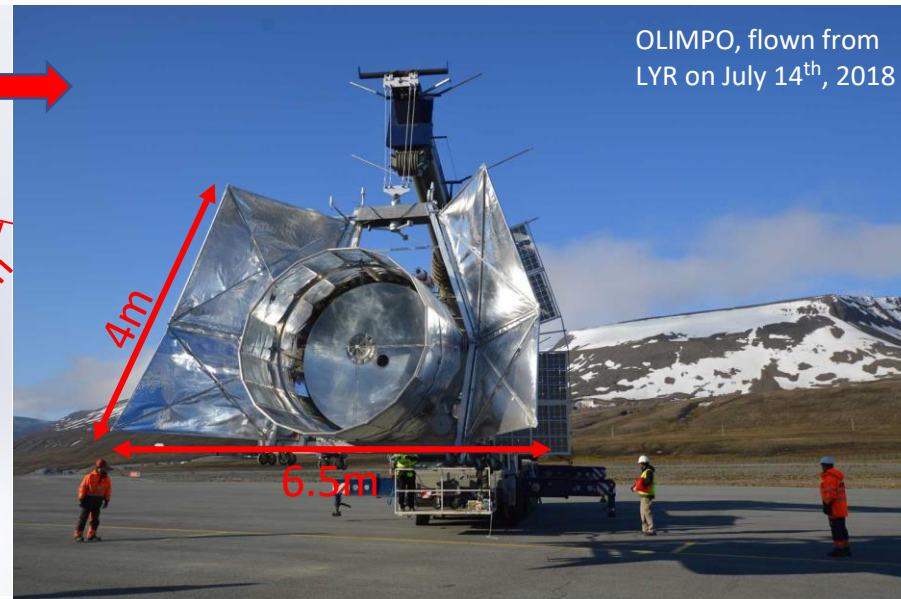
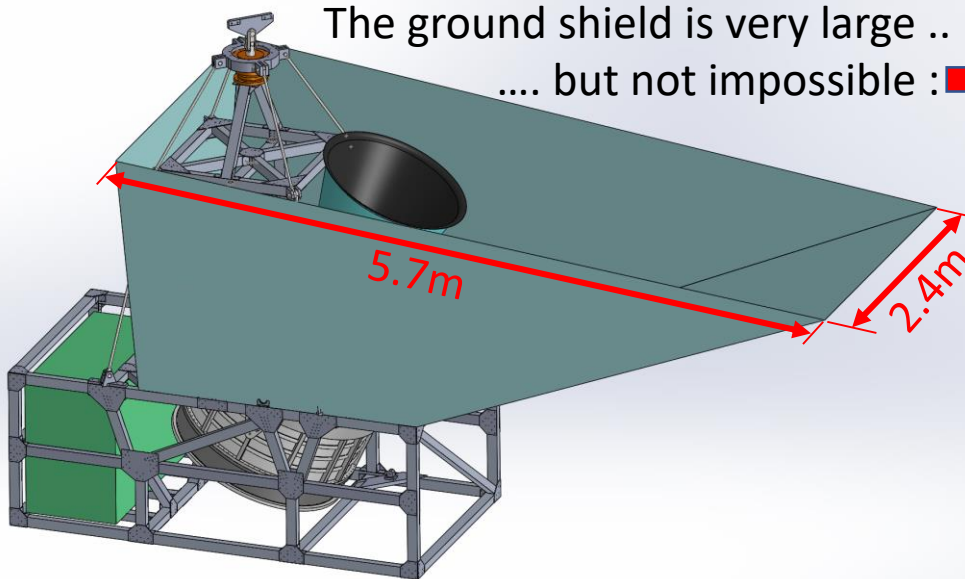
F. Piacentini

SWIPE: ground shield



Polar night flight:
sun below the
horizon for
most/all the flight

The ground shield is very large ..
.... but not impossible :

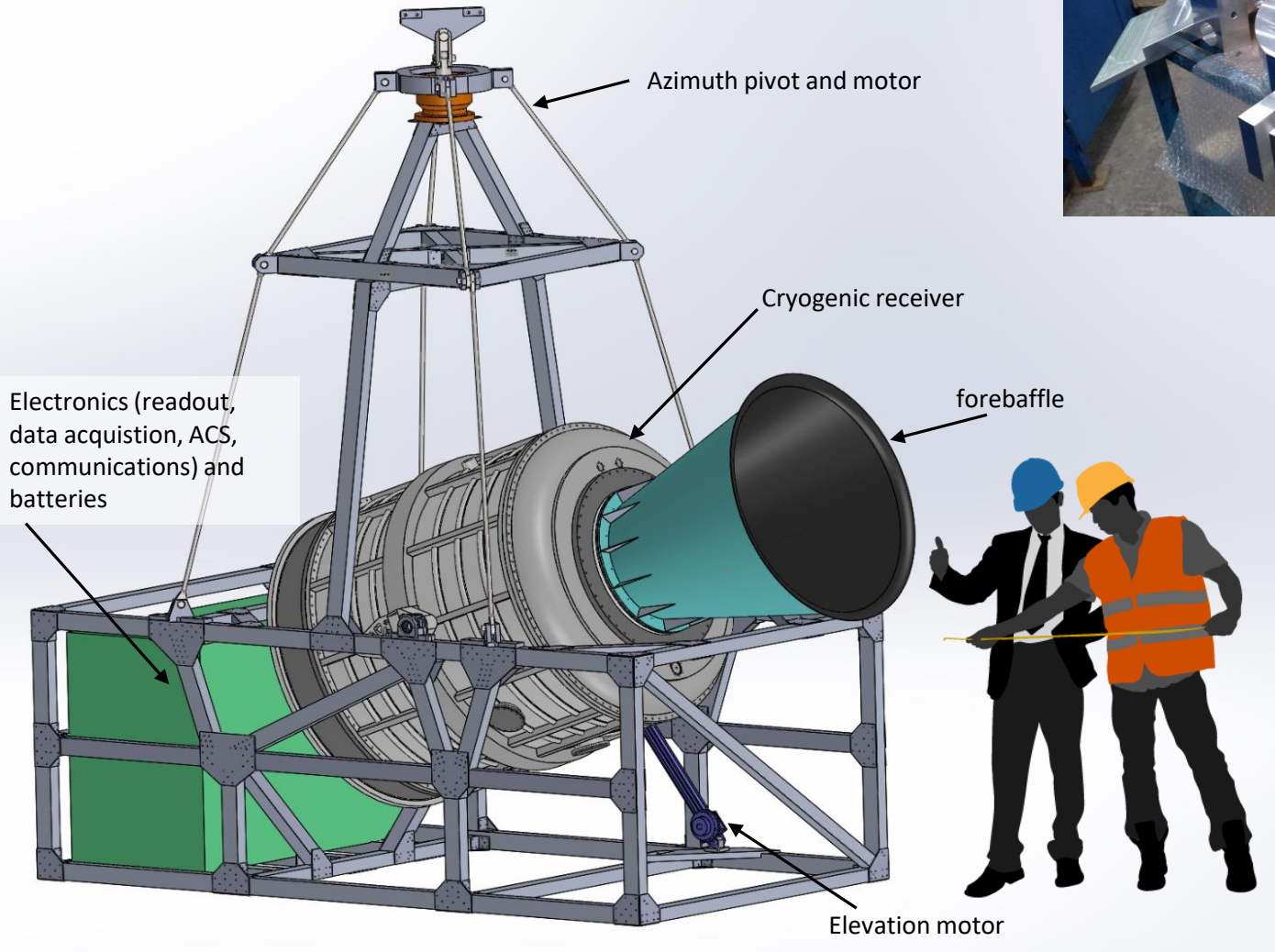
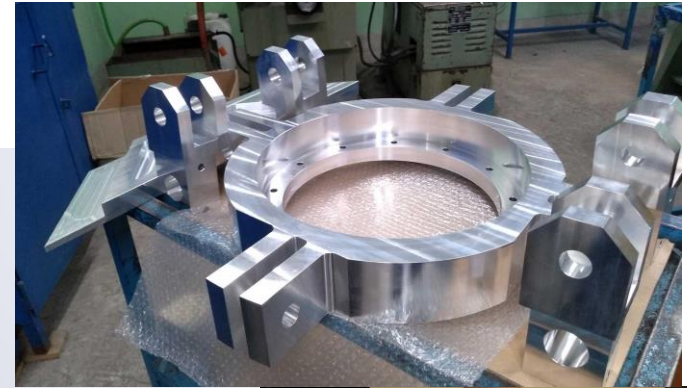


OLIMPO, flown from
LYR on July 14th, 2018

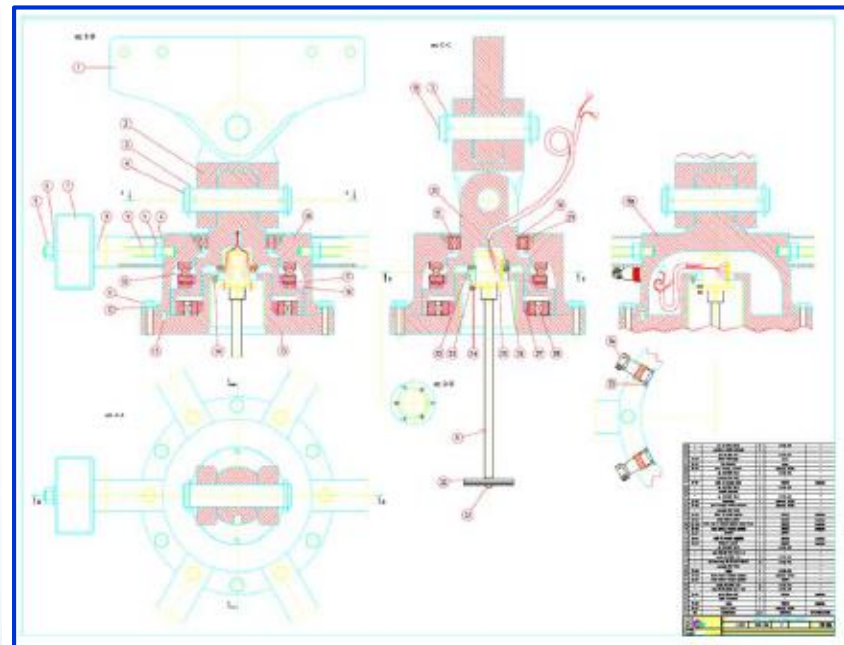
Rendering without ground/sun shields

1.6 tons payload

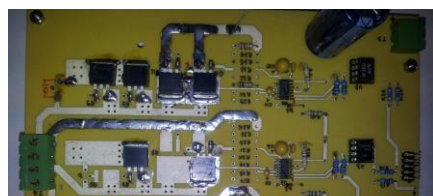
- Gondola design certified.
- Gondola parts being machined.



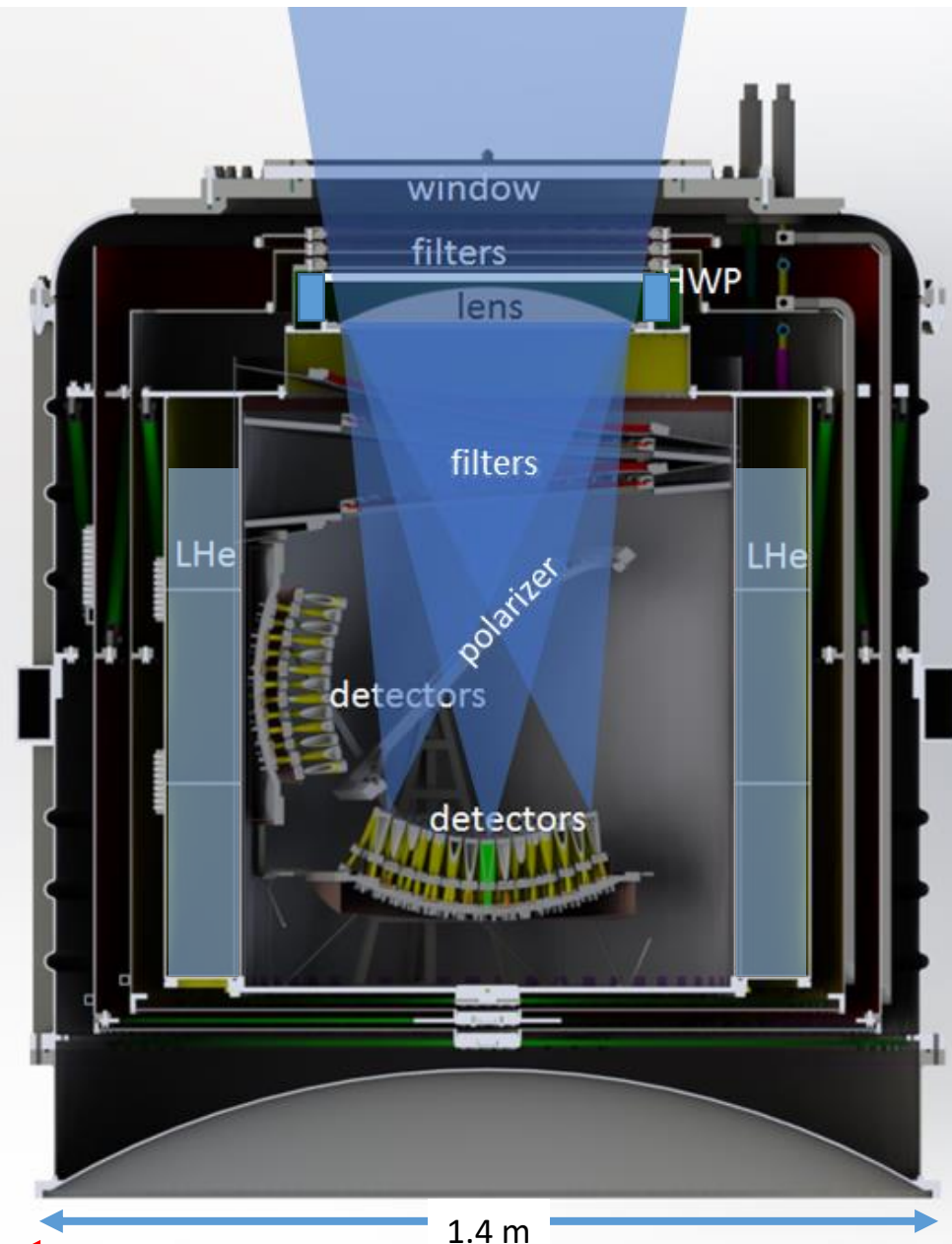
- ACS based on the successful pivot flown on BOOMERanG and OLIMPO.
- Azimuth spin of the entire payload up to 3 rpm (with 3A current for a 1600kg load).
- Attitude determination from the same gyros and star sensors flown on Archeops (Nati et al. *A fast star sensor for spinning balloon payloads* Review of Scientific Instruments, 74, 4169-4175, (2003))



Azimuth Pivot (Boscaleri, IFAC). Same as OLIMPO. Test @ 6 rpm

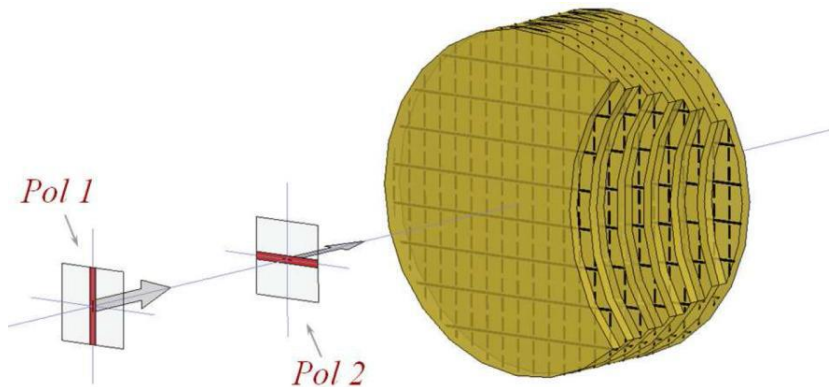
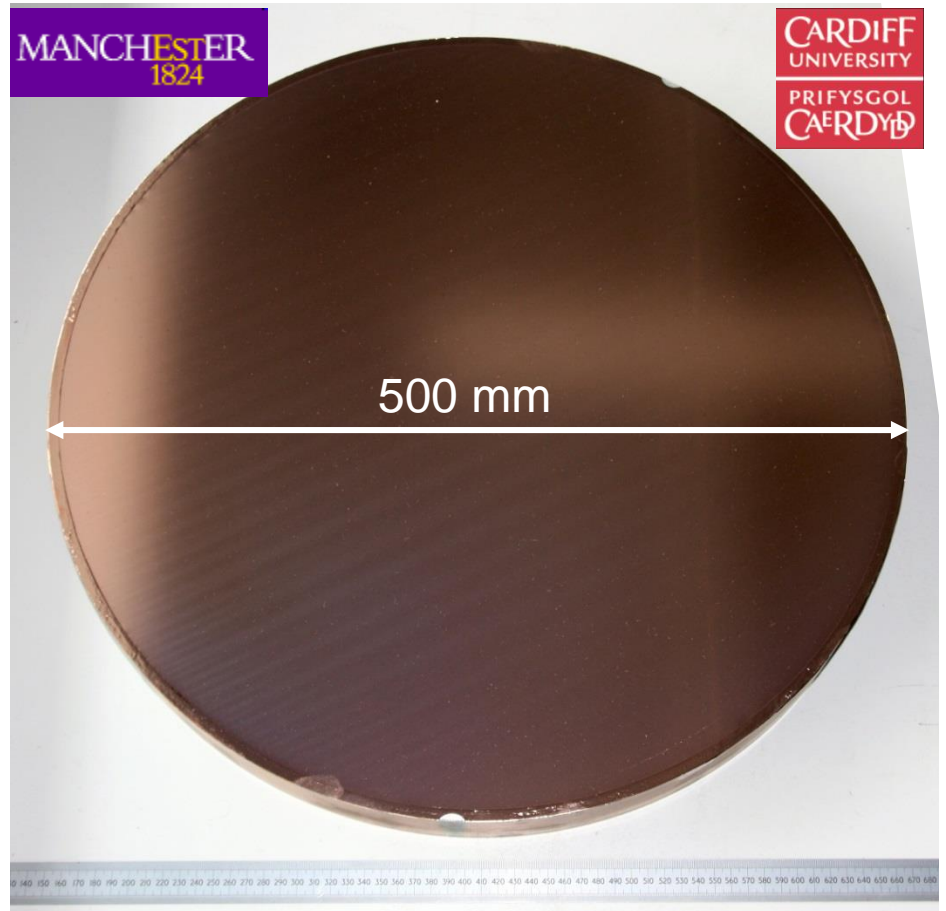


- A Stokes (HWP + polarizer + power detector) polarimeter, panoramic
- Simple implementation
- Two large focal planes (8800 modes), at 0.3K, in a large cryostat, cooling also the lens (490mm diam. and a 460 mm diam. cold stop) and the polarization modulator (HWP at about 10-15 K).
- FOV: 20° split by a 500mm diam., 45° tilted wire grid into 2 Focal Planes 300 mm diam (f/1.75)
- **Most components being machined, some ready**

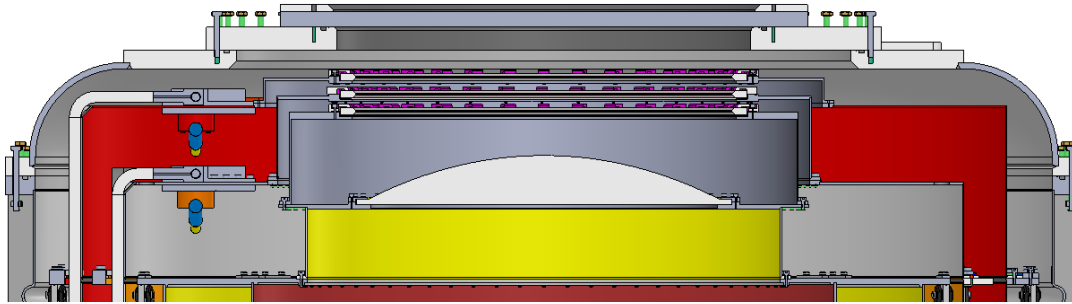


SWIPE – HWP

- Is a cold (2K), large (50 cm useful dia.), wide-band meta-materials HWP, placed immediately behind the window and thermal filters stack.
- HWP characteristics for the ordinary and extraordinary rays are well matched:
 $(T_o - T_e)/T_o < 0.001$, $X_{pol} < 0.01$, over the 100-300 GHz band.
- Simulations show that continuous rotation has advantages in terms of 1/f noise mitigation and angles coverage.
- A custom superconductive rotator has been developed.



Pisano et al., Proc. SPIE, Vol. 9153, id. 915317 (2014)



~670mm

Permanent magnet ring



High Temperature Superconductors

Pros

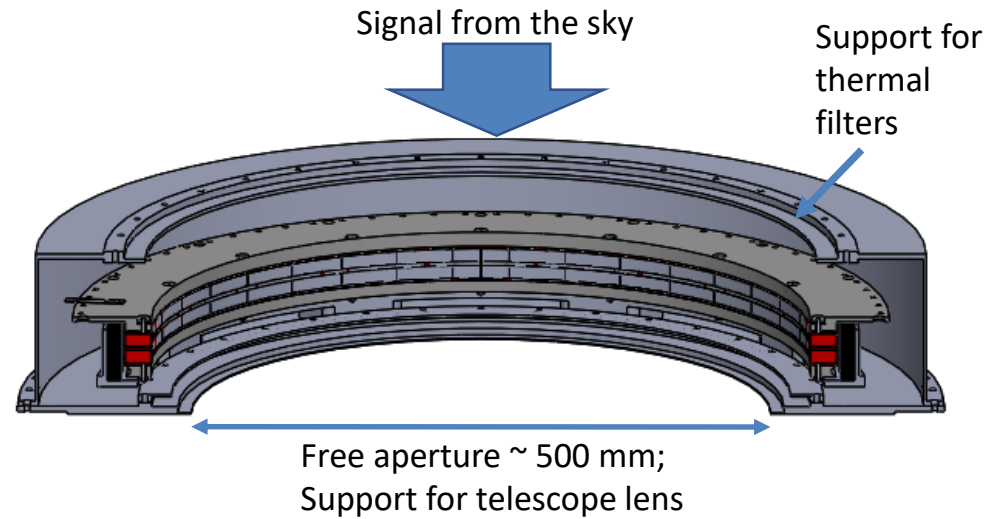
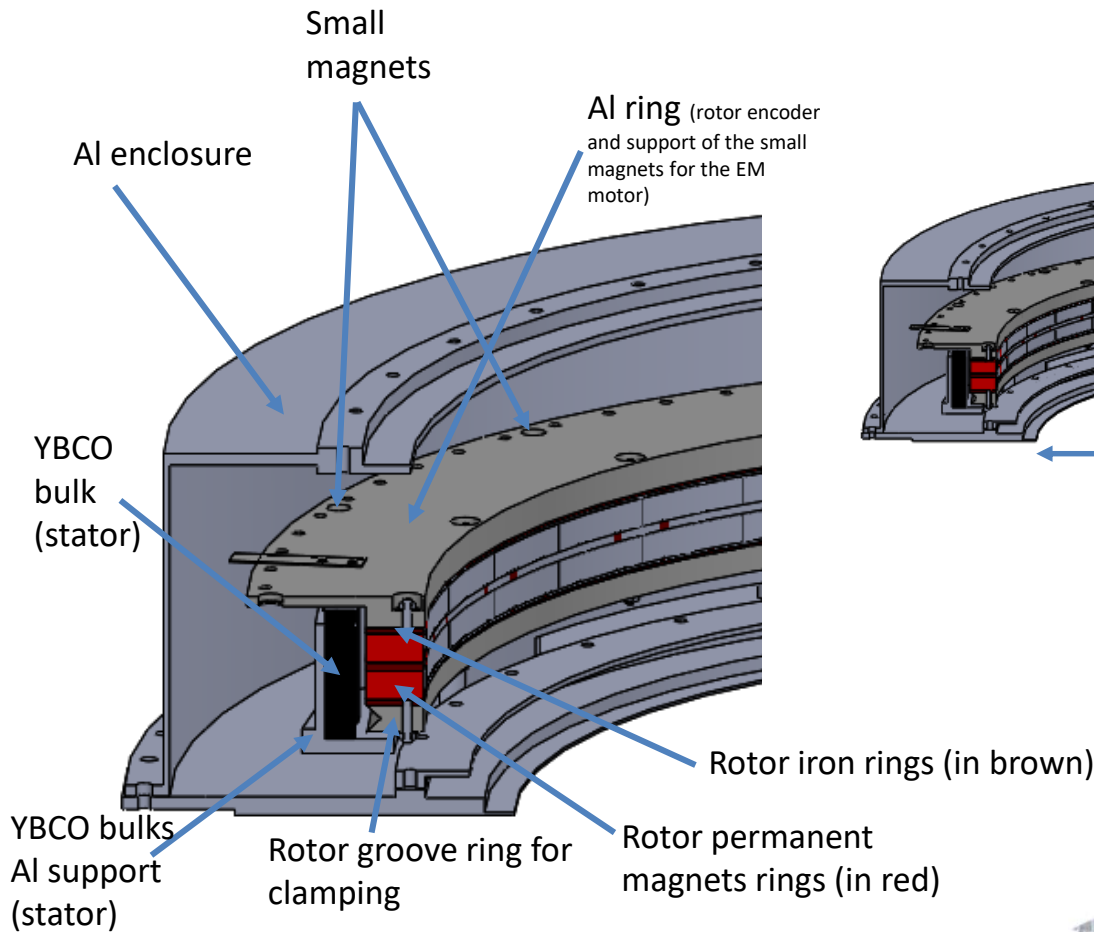
- NO stick-slip friction
- NO extra-effort to cool HTSs
- Passive stable levitation
- Low Coefficient of friction
- Continuous rotation (0-10Hz)

Cons

- Variable magnetic field
- Clamp mechanism at 4K

S. Hanany et al., IEEE Trans.Appl.Supercond. 13 (2003) 2128-2133

T. Matsumura et al., IEEE Trans.Appl.Supercond. 26 (2016)



1T field strength in the gap. Total mass 9 kg.

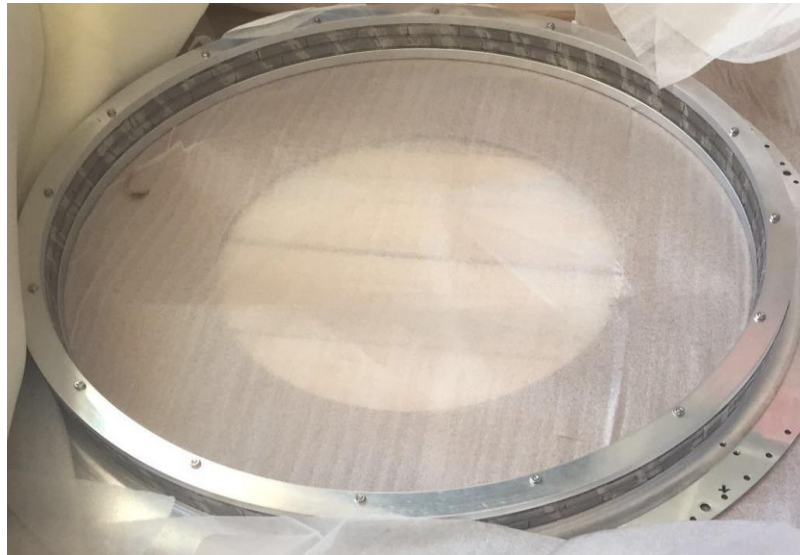
SWIPE – HWP rotator – parts procured



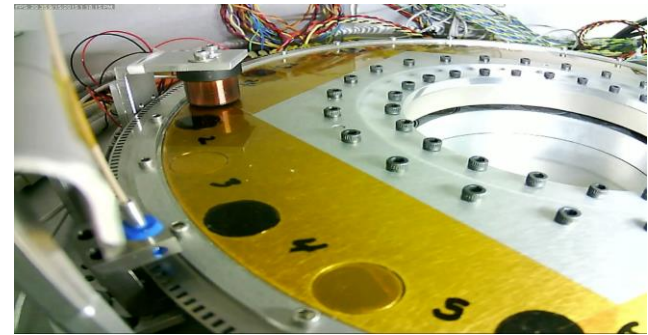
Groove ring
for C/R



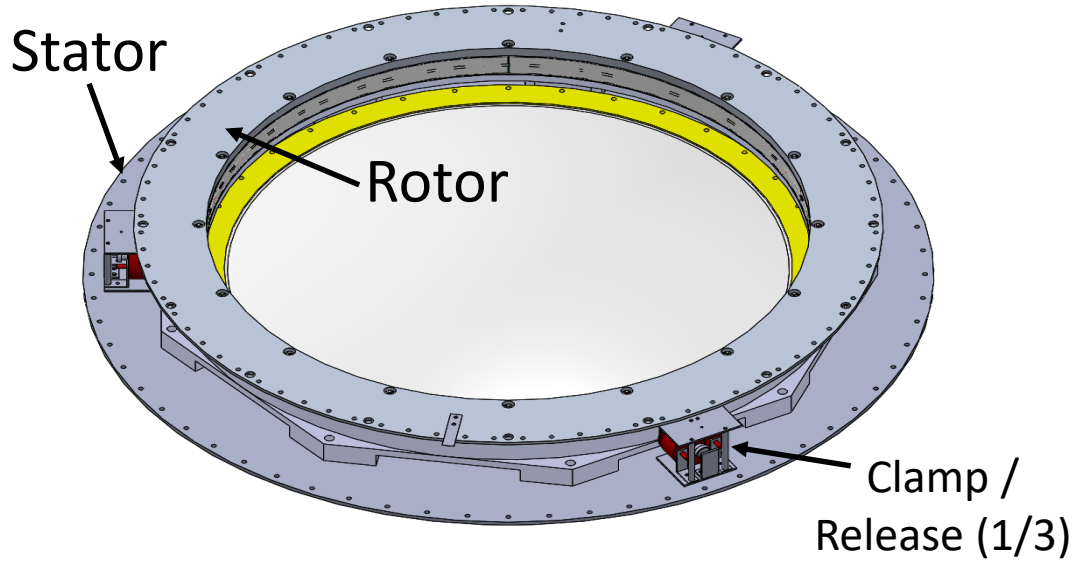
Stator with
YBCO bulks



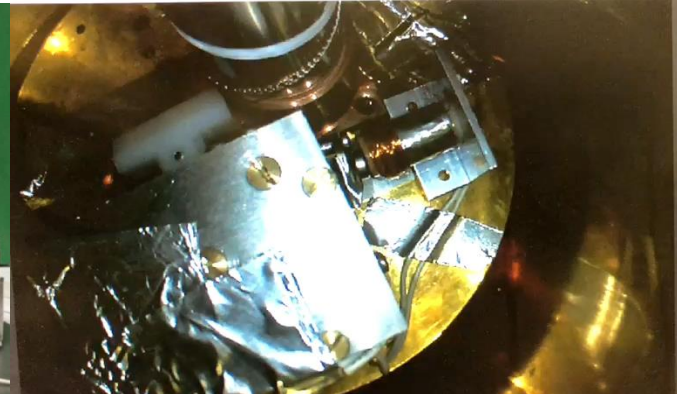
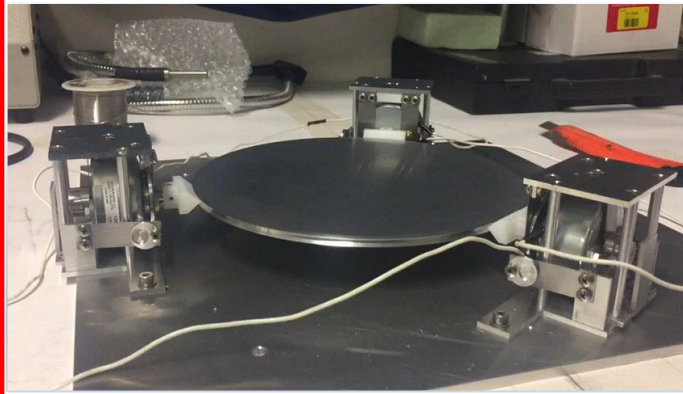
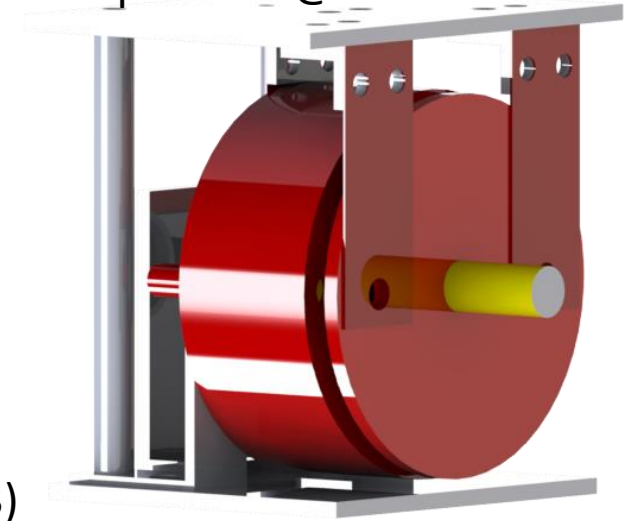
Rotor with
permanent
magnets



smaller
diameter
Prototype
arXiv:1706.05963v3

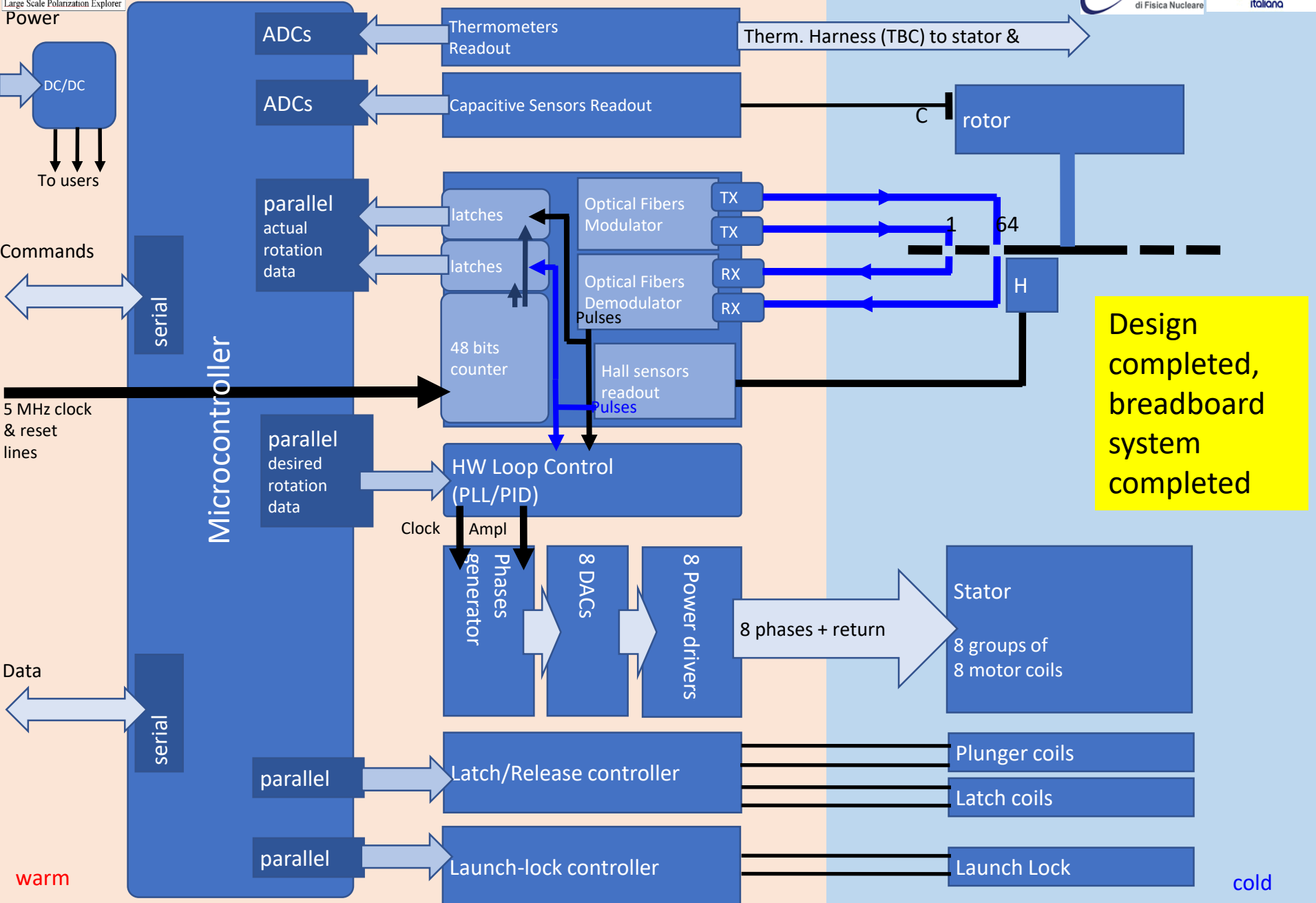


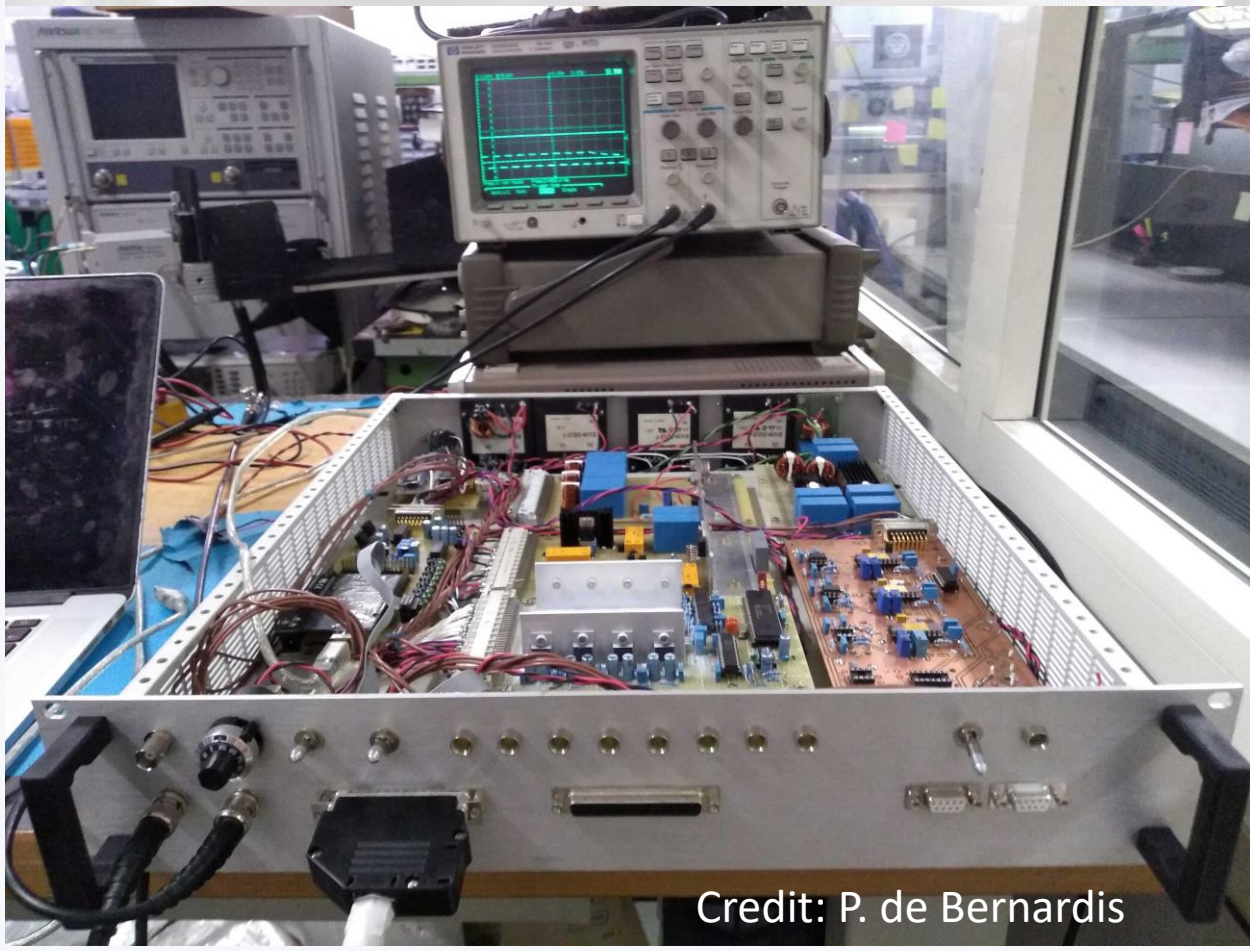
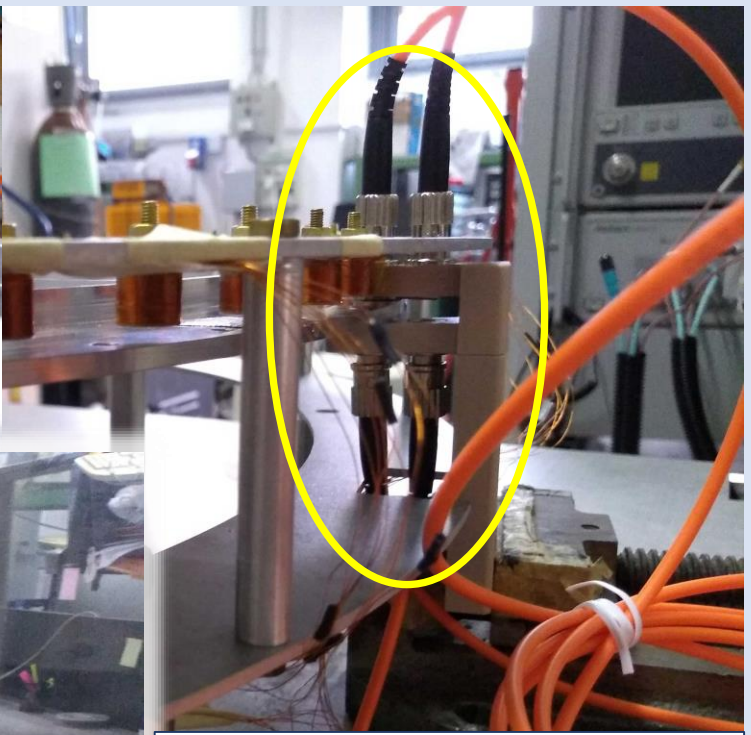
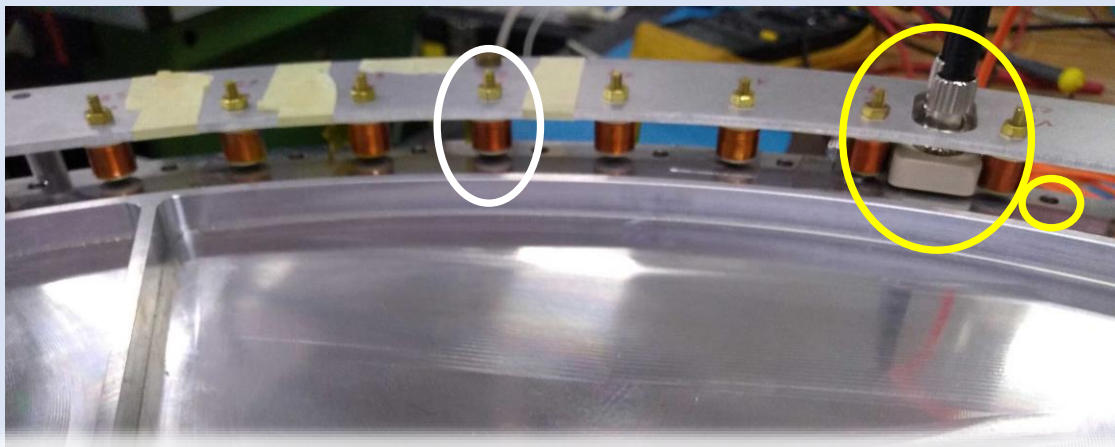
Frictionless actuator for operation @ 2K



Fabio Columbro, Paolo de Bernardis, and Silvia Masi
A clamp and release system for superconducting magnetic bearings
Review of Scientific Instruments 89, 125004 (2018)

Cryogenic PMU rotator – Control Electronics

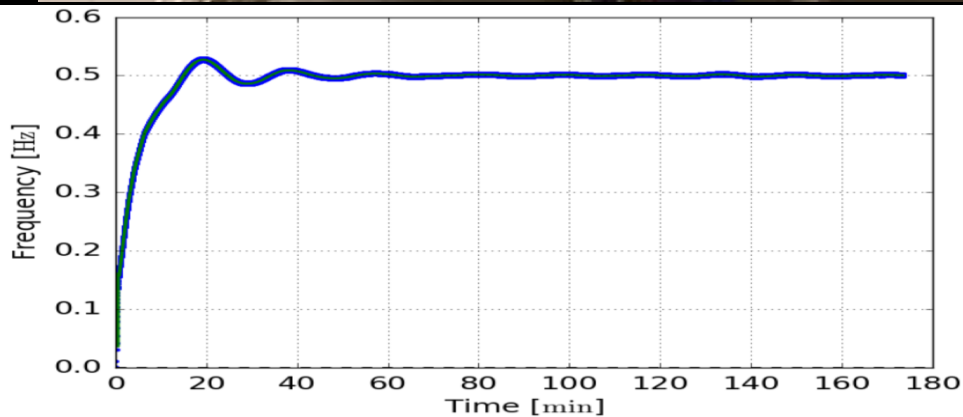




Custom brushless synchronous motor & control electronics:

- 8 phases
- 64 equalized coils (stator)
- 8 magnets (rotor)
- Smooth phased currents to minimize EMI & induced eddy currents
- 64-slits optical encoder
- High accuracy optical fibers readout ($\Delta t=50\mu s$)

Credit: P. de Bernardis



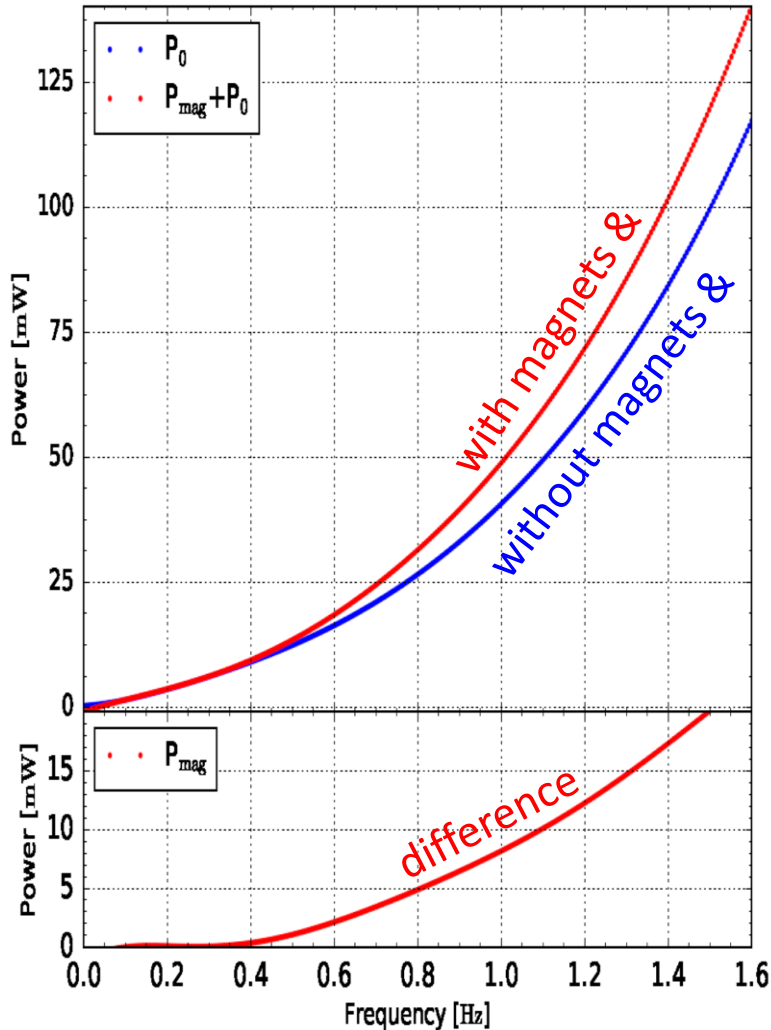
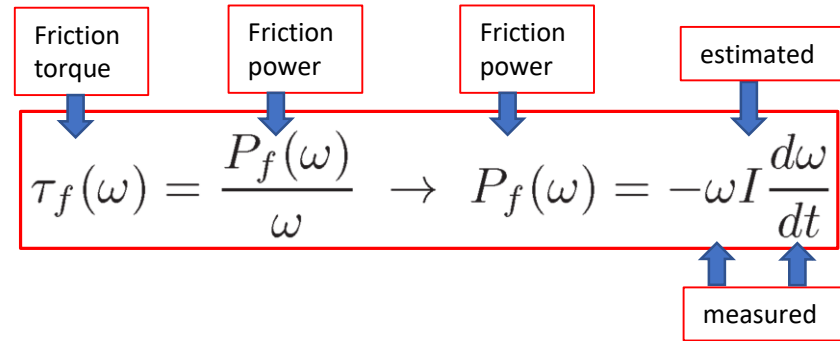
Room-T testbed for motor & control: OK

Working for :

- Optimization of start
- Optimization of feedback algorithm (frequency, phase and amplitude)
- Minimization of driving currents
- FPGA board for precision time stamping
- Thermal/vac test

Power Dissipation Tests @ room-T and extrapolation to cryo-T

From spin-down test :



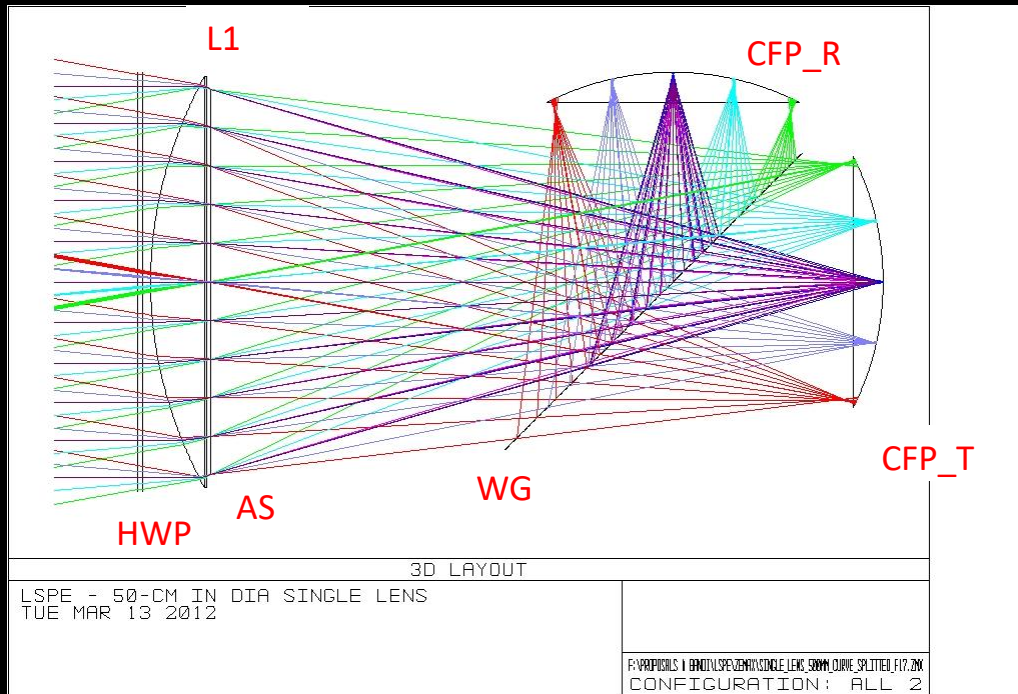
@ $f_{HWP}=1\text{Hz}$	P [mW] - 300 K		P [mW] - 1.6 K
	Measured	Optimized	Expected
8 magnets	9.2 $\xrightarrow{\text{G10 ring}}$	0.8 $\xrightarrow{\text{RRR Al}}$	2.2
Main magnet	6.2 $\xrightarrow{\text{No tilt}}$	1.3 $\xrightarrow{\text{RRR Al}}$	3.5
Hysteresis	-	-	10
Joule	1200 $\xrightarrow{\langle \tau \rangle \langle i \rangle \langle W \rangle}$	645 $\xrightarrow{\text{RRR Cu}}$	6.1
Harness	-	-	3.2
Bearing	41.5	41.5	-
Total	1260	690	25

Credit: Fabio Columbro



Based on a pulse-tube cooler

Single lens 490mm in dia: plano-convex lens curved focal plane



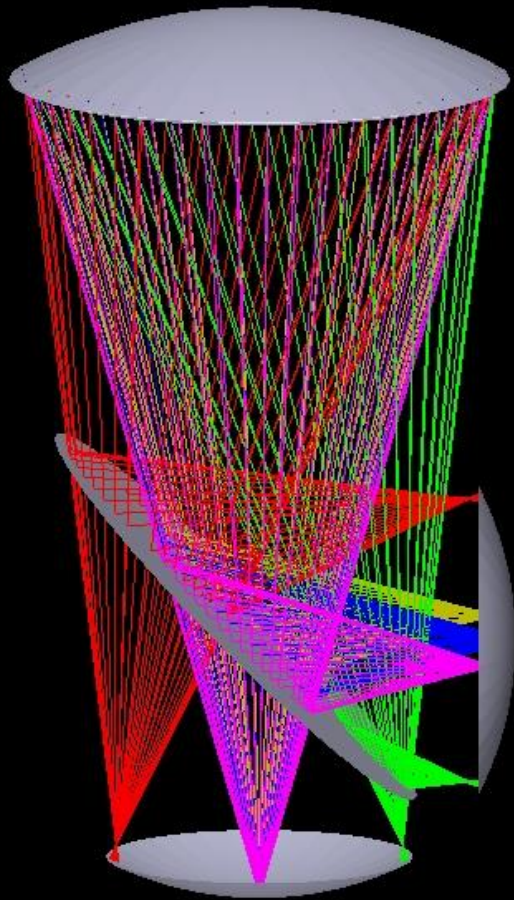
Dimensions:

HDPE Lens (L1) diameter = 480 mm
Aperture Stop (AS) = 440 mm
Entrance Pupil = 450 mm
FOV = 20 deg
f/1.88
Curved Focal plane (CFP_T o CFP_R)
diameter = 300 mm
Lens thickness = 65 mm
HDPE lens with AR by porous PTFE

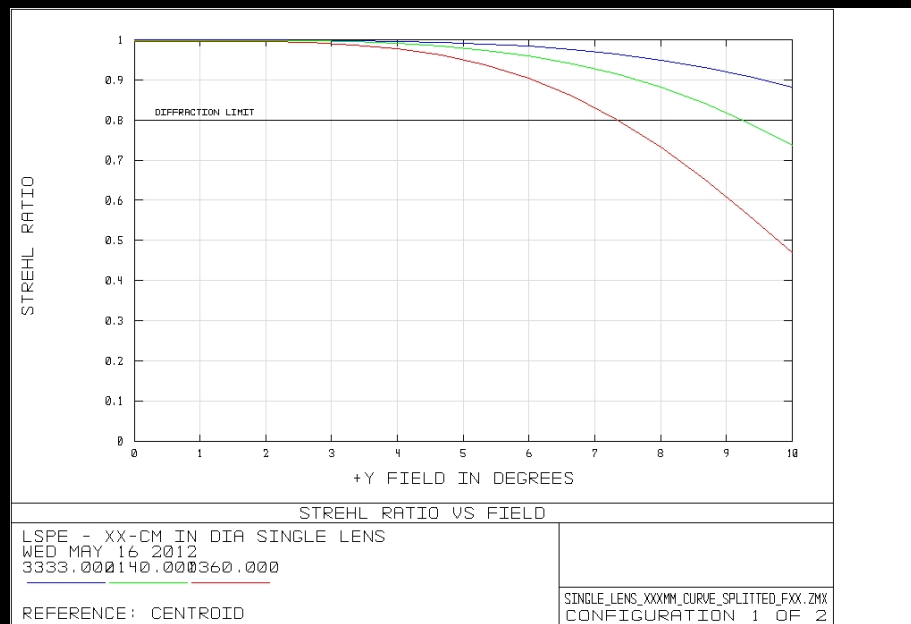
Constraints:

Thermal filters max c.a. diameter = 500 mm
Wire Grid (WG @45 deg tilt) max c.a. diameter = 500 mm
HWP max c.a. diameter = 500 mm

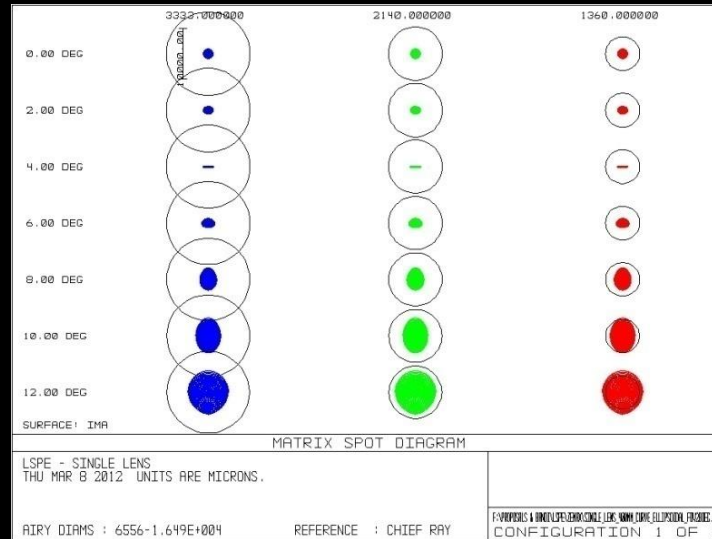
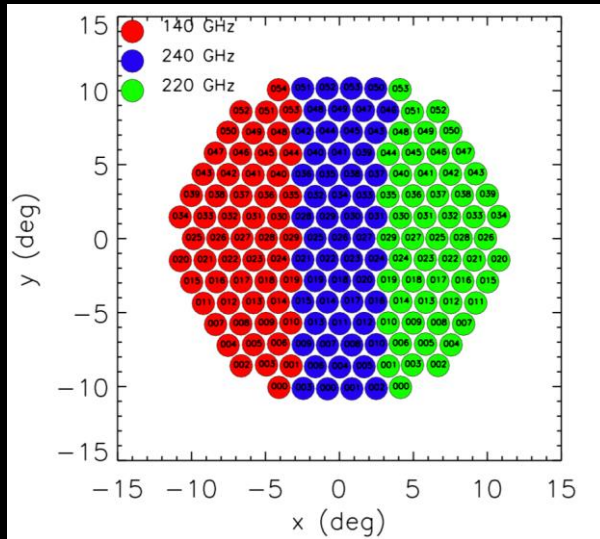
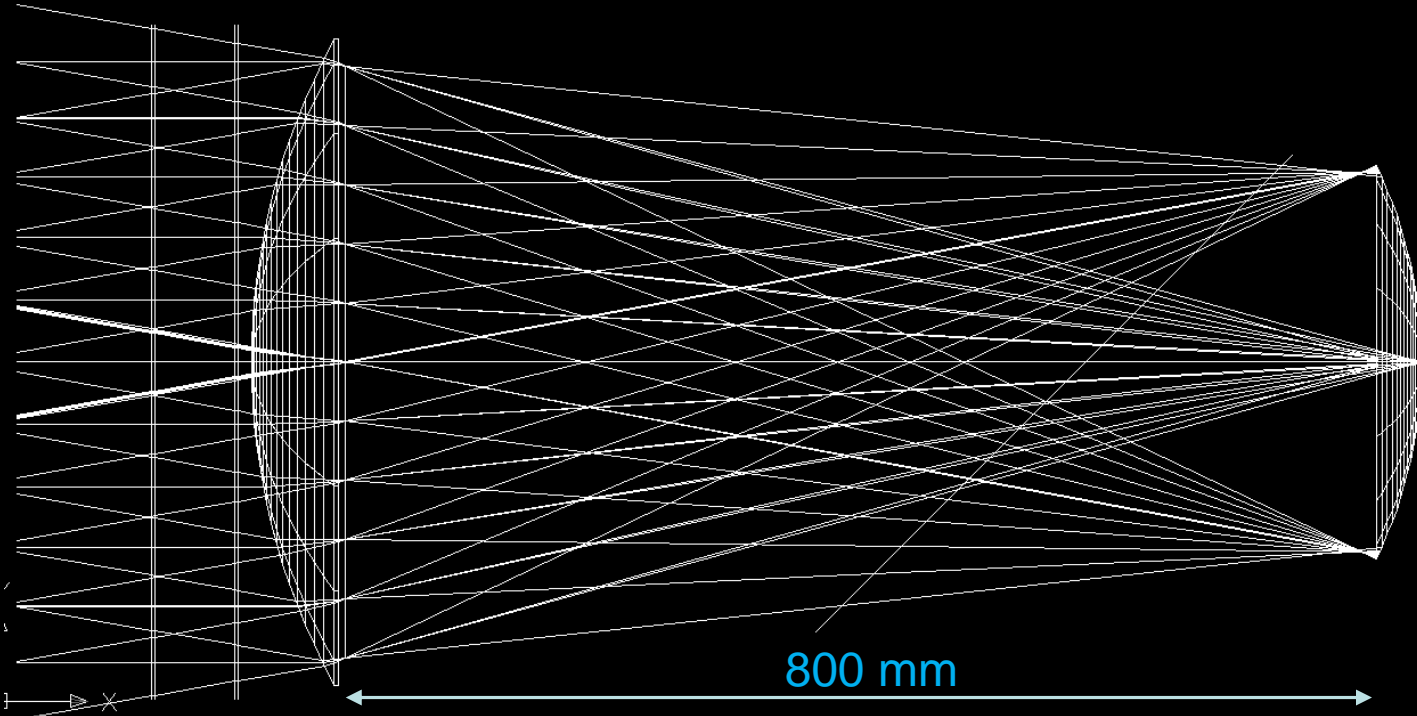
Single lens 490mm in dia: plano-convex lens curved focal plane



Corrected focal plane vs bands

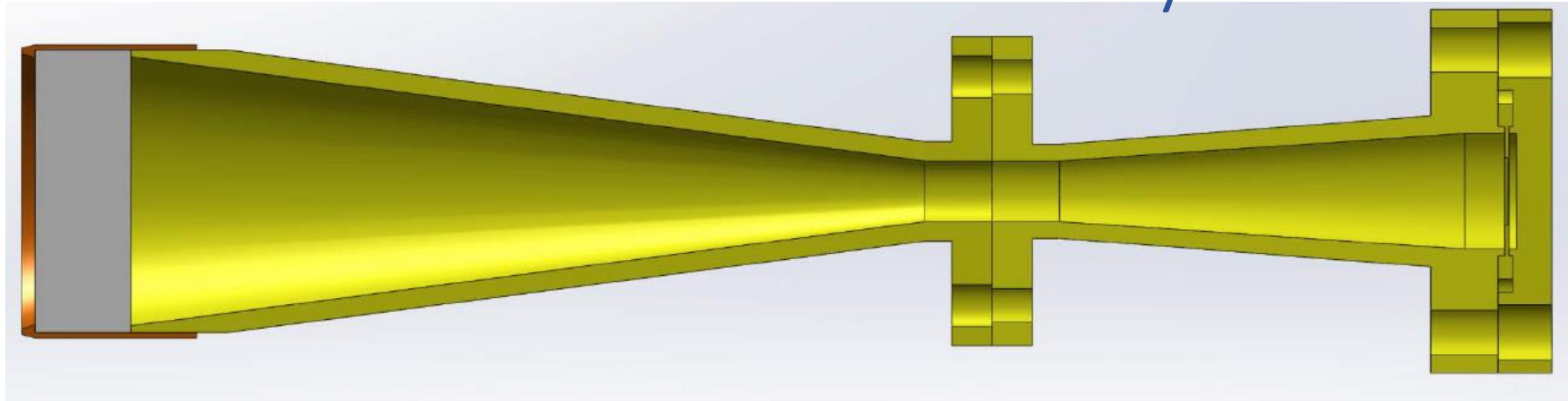


SWIPE: Simple Optical Design



M. De Petris

The SWIPE pixel multimode assembly



BP+FC

SCH

MSWG

STT

ABS+BS

Nominal <u>freq</u> (GHz)	Bandwidth	Min <u>freq</u> (GHz)	Max <u>freq</u> (GHz)
140	30%	119	161
220	5%	214.5	225.5
240	5%	234	246

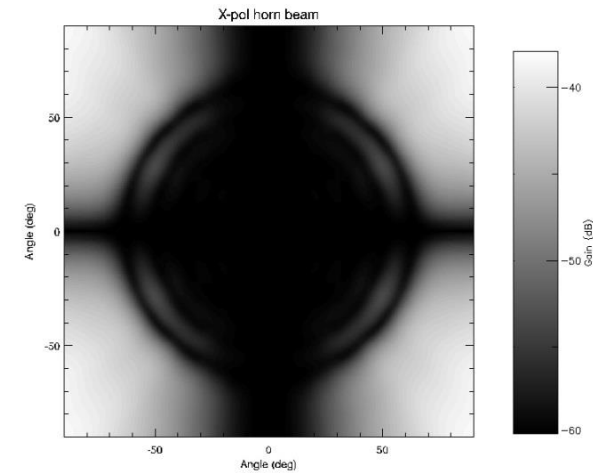
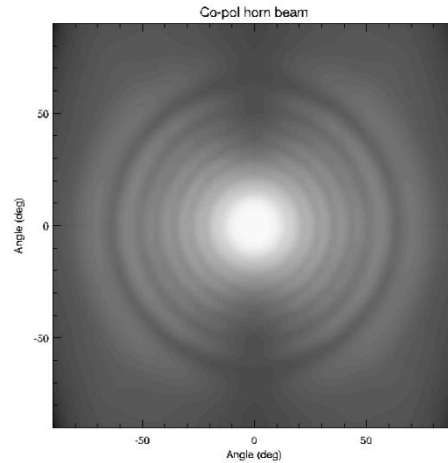
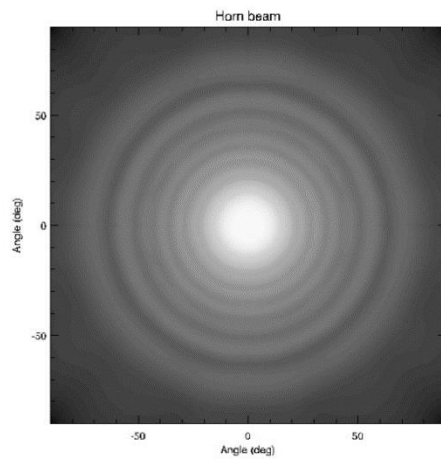
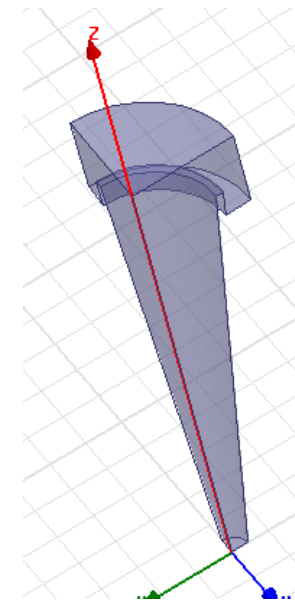
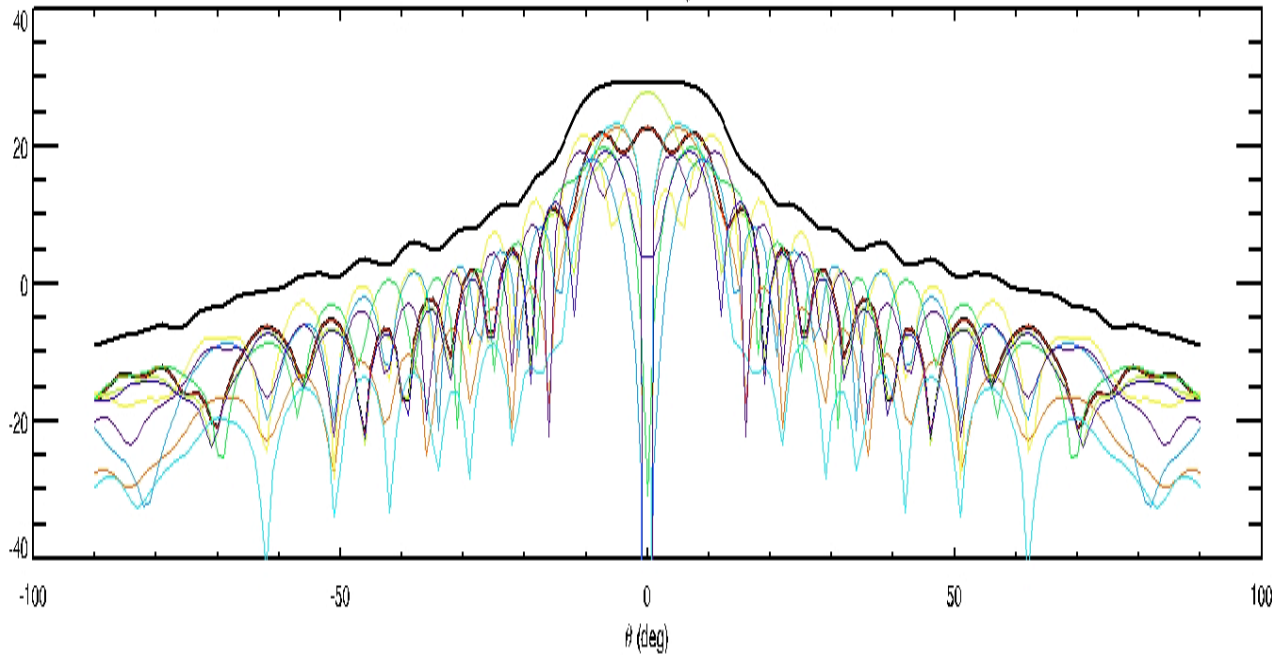
Table 1 – main features of the SWIPE bandpasses (source: C. Tucker, Cardiff Univ.)

Channel	ν_{\min} (GHz)	$N_{\text{modes}}(\nu_{\min})$	ν_{\max} (GHz)	$N_{\text{modes}}(\nu_{\max})$	ν_{eff} (GHz)	$N_{\text{modes}}(\nu_{\text{eff}})$
140	119	10	161	17	140	12
220	214	28	226	31	220	30
240	234	32	246	35	240	34

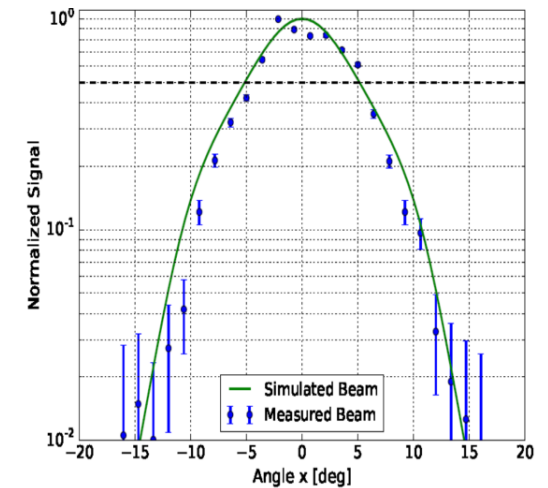
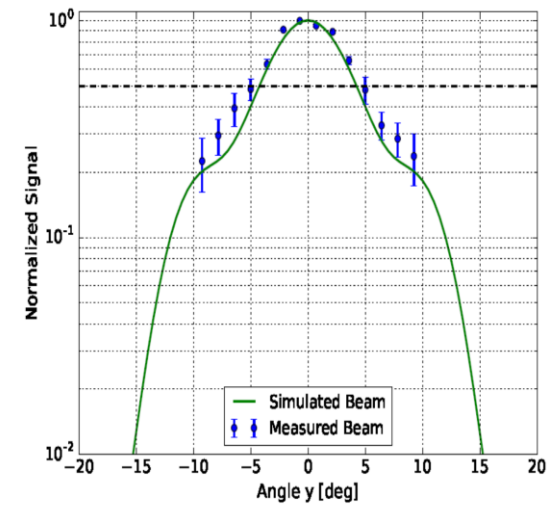
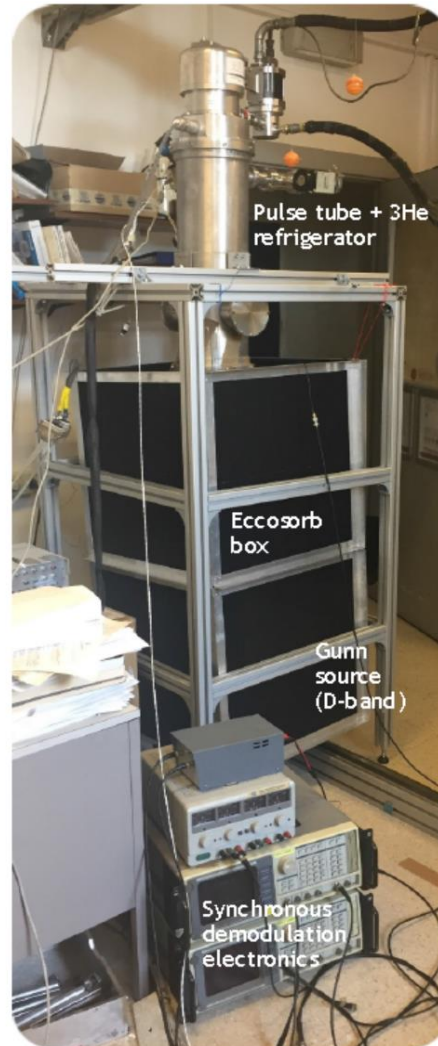
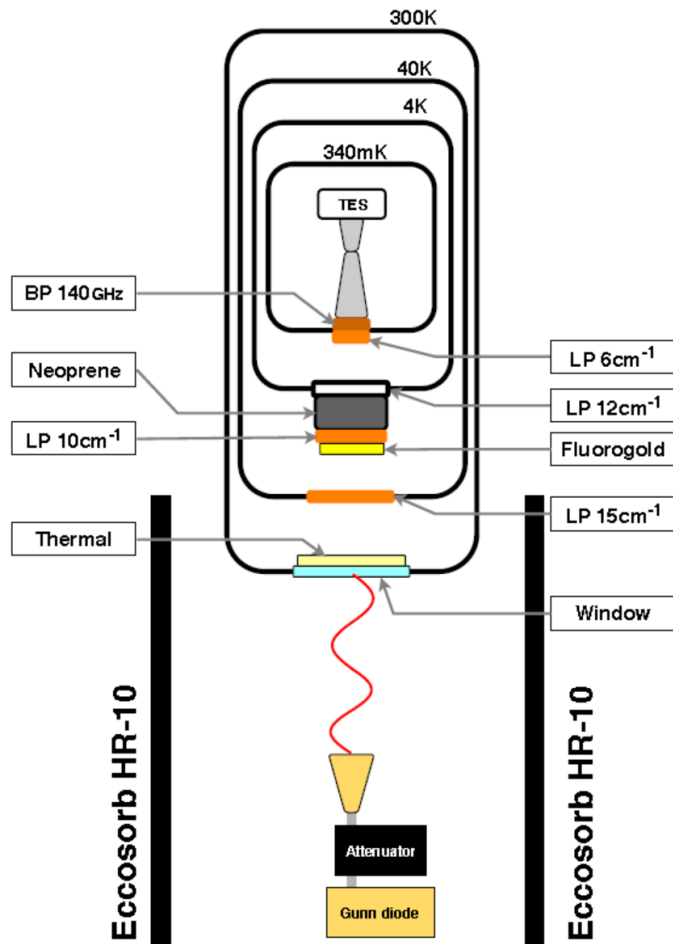
Table 2 – number of coupled modes N_{modes} at the center and at the edges of each SWIPE band. The total optical throughput at frequency ν is $N_{\text{modes}}c^2/\nu^2$.

SWIPE: Horn beam

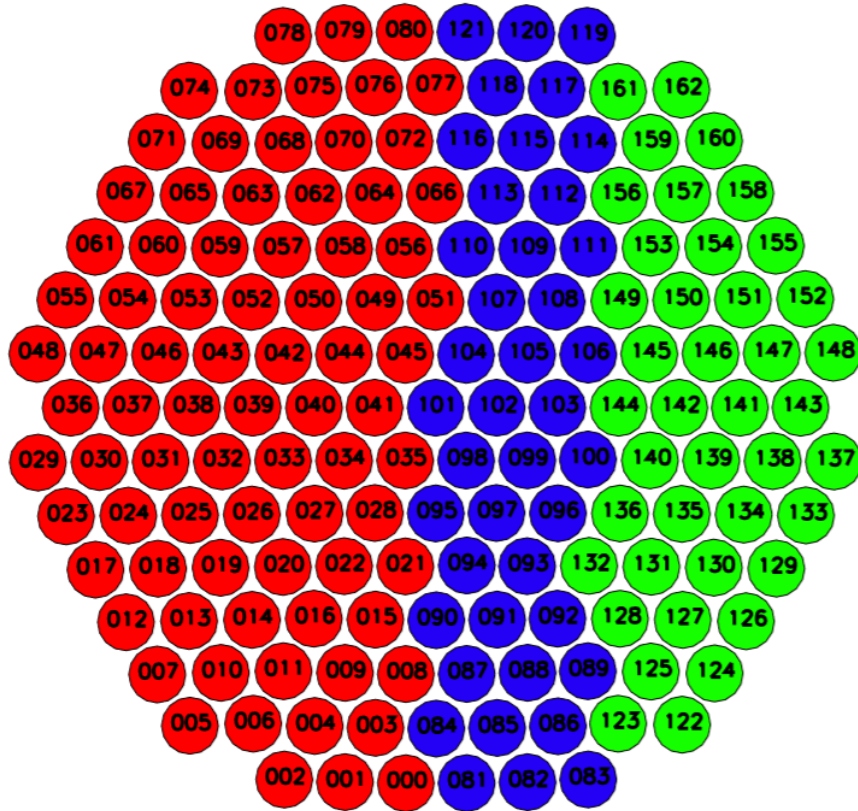
Winston horn gain, E_{θ} , $\phi=0$ deg



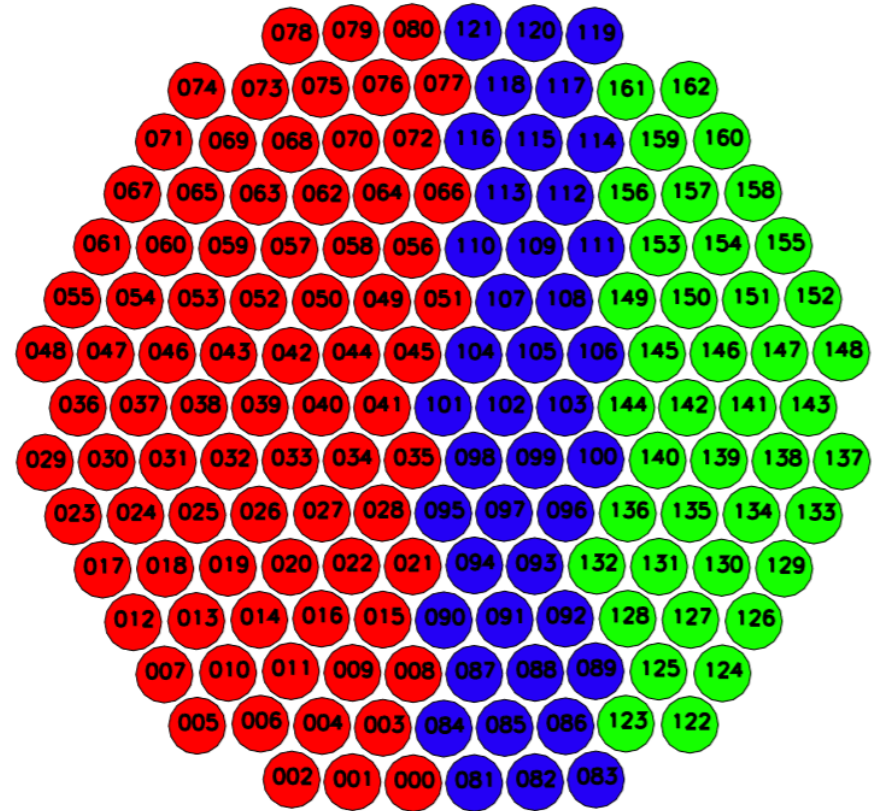
- Not an easy task. Custom cold absorber needed to limit radiative background
- Beam vignetted by test cryostat window. However, multimode regime demonstrated.
- Will be redone with the large flight cryostat.



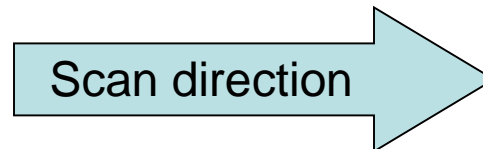
SWIPE focal planes : 50% 140 GHz, 25% 220 GHz, 25% 240 GHz
Total 330 detectors, with $A\Omega = 10\lambda^2, 21\lambda^2, 23\lambda^2 @ 140, 220, 240$



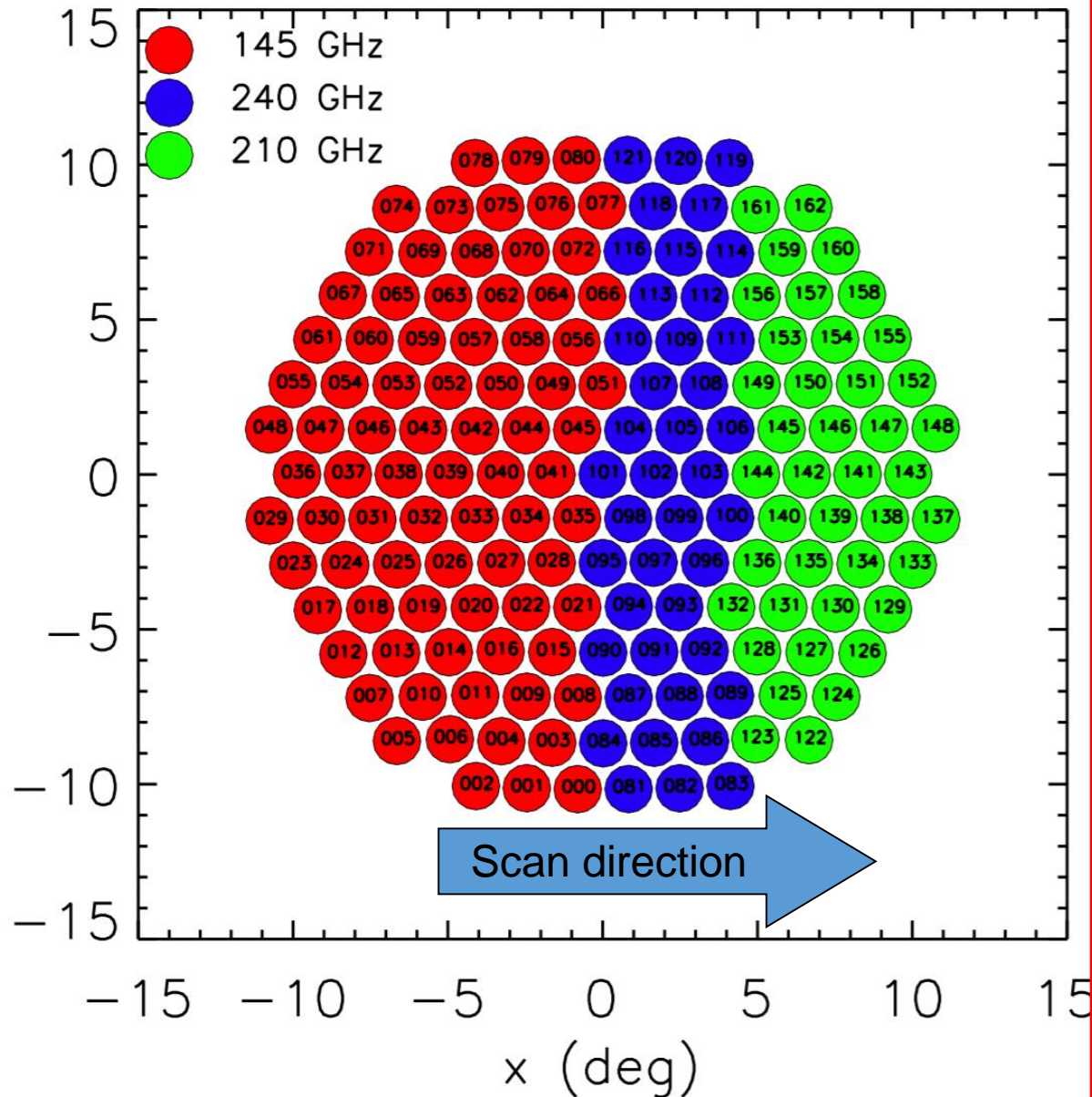
Reflected focal plane



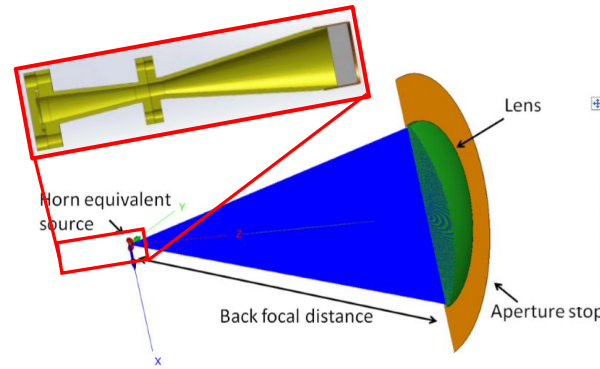
Transmitted focal plane



- The distribution of colors in the pixels has been optimized with a simplified scheme for foregrounds (dust) removal.
- This distribution provides sufficient precision to extrapolate the dust signal from high frequency down to 150 GHz
- This configuration totalizes 4400 radiation modes for each focal plane (transmitted and reflected).



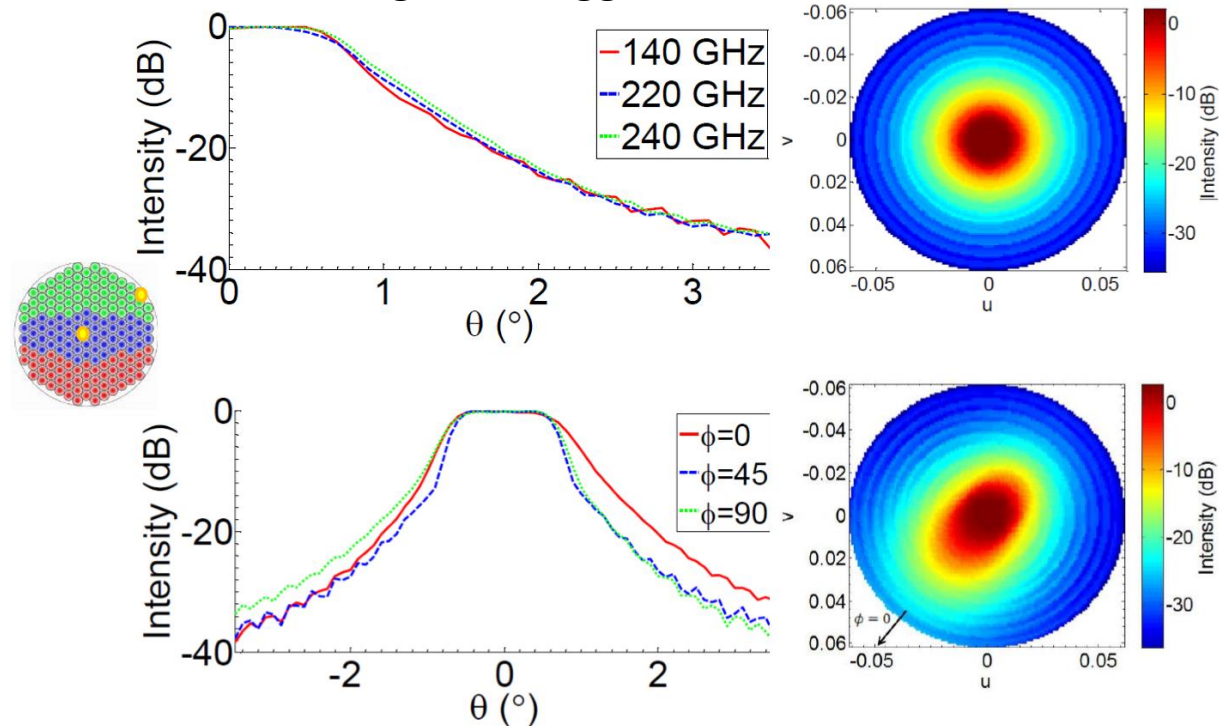
- Whole system multi-mode
- Full EM simulation described in: Legg, Lamagna, Coppi, de Bernardis, Giuliani, Gualtieri, Marchetti, Masi, Pisano, Maffei, *Development of the multi-mode horn-lens configuration for the LSPE-SWIPE B-mode experiment* Proc. SPIE 9914, Millimeter, Submillimeter, and Far-Infrared Detectors and Instrumentation for Astronomy VIII, 991414 doi:10.1117/12.2232400
- Resulting beam approximately top-hat. 1.5° FWHM.
- Good polarization properties.



Diameter (mm)	428
Centre thickness (mm)	60
Focal length (mm)	805
Refractive index	1.57
Conic constant	-0.54
Cold stop diameter (mm)	420

Coupling analysis – small angle beams

L. Lamagna, S. Legg



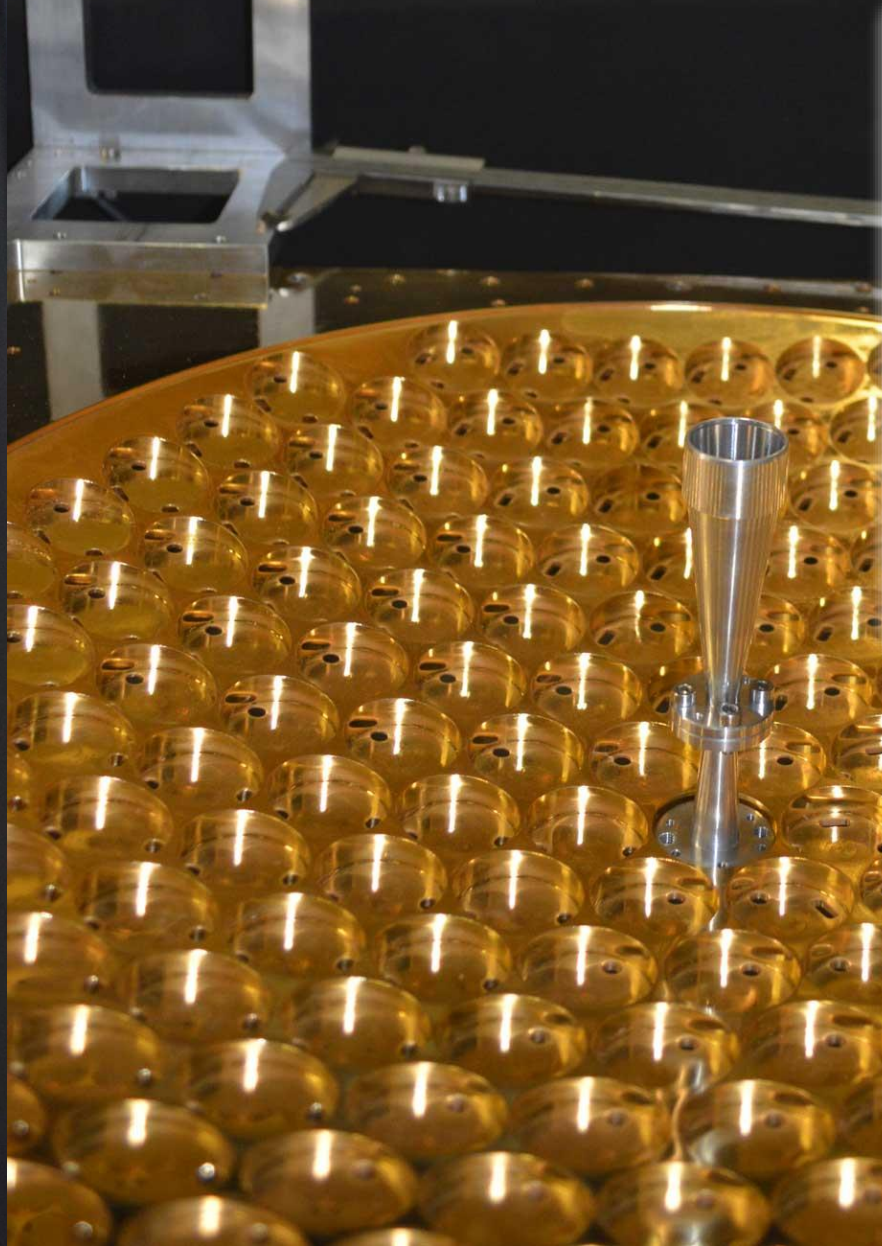
L. Lamagna. M. De Petris



LSPE horns & bolo holders

Large Throughput
multimode detectors:
8800 modes collected
by 330 sensors

Focal plane detector flanges
(gold plated Al6061, 40 cm side).



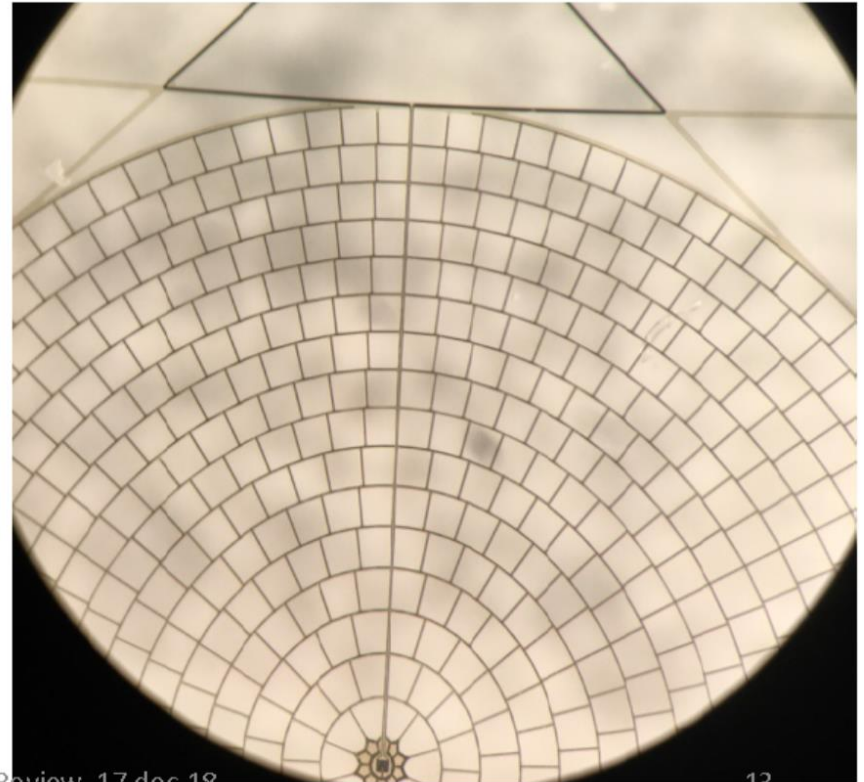
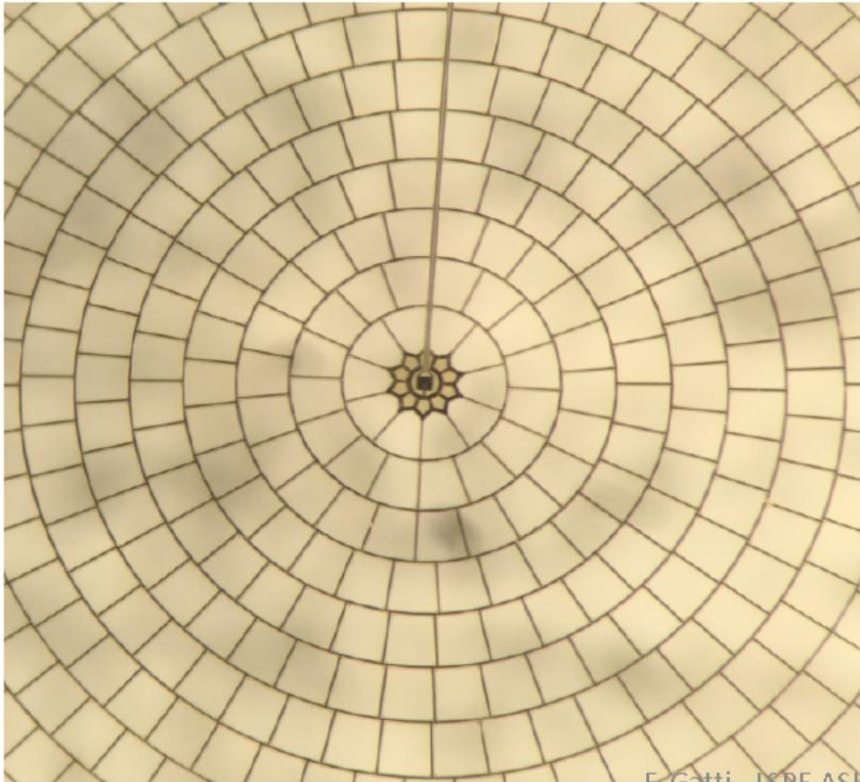
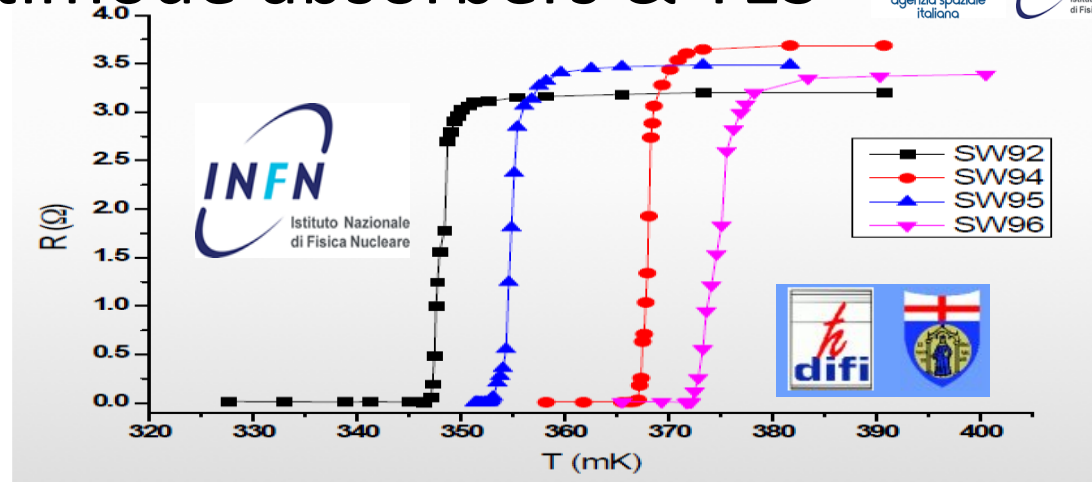
LSPE horns & bolo holders

Large Throughput
multimode detectors:
8800 modes collected
by 330 sensors

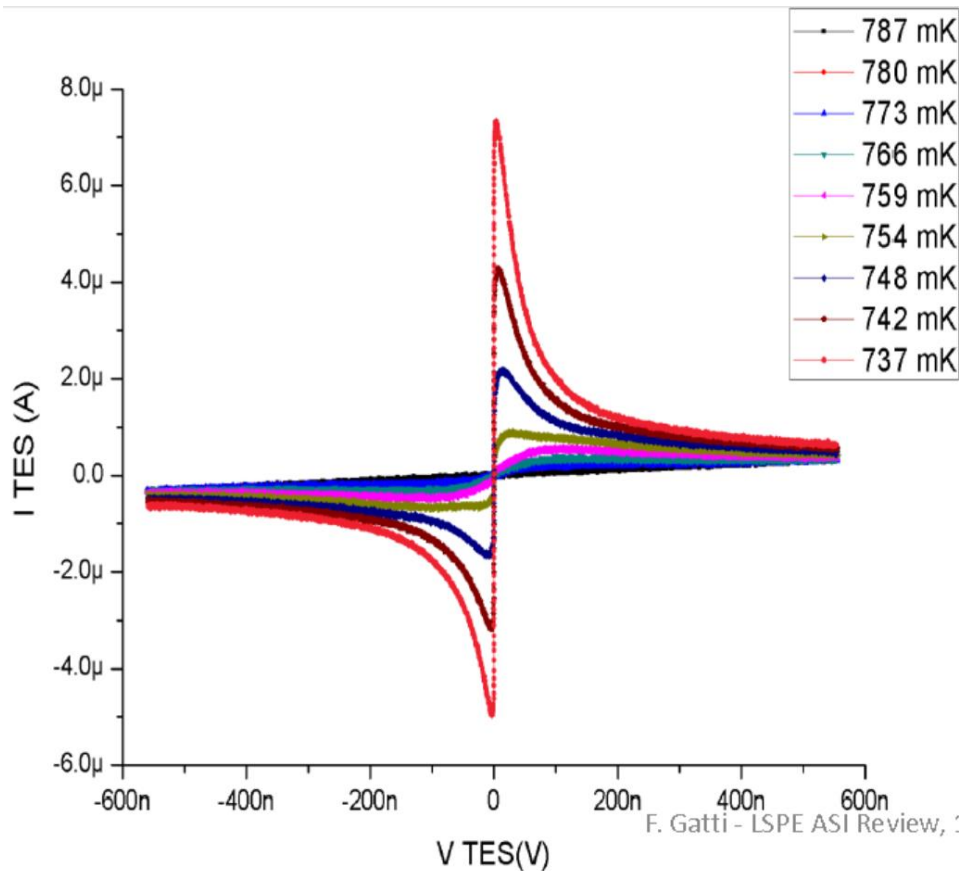
Focal plane detector flanges
(gold plated Al6061, 40 cm side).

SWIPE - multimode absorbers & TES

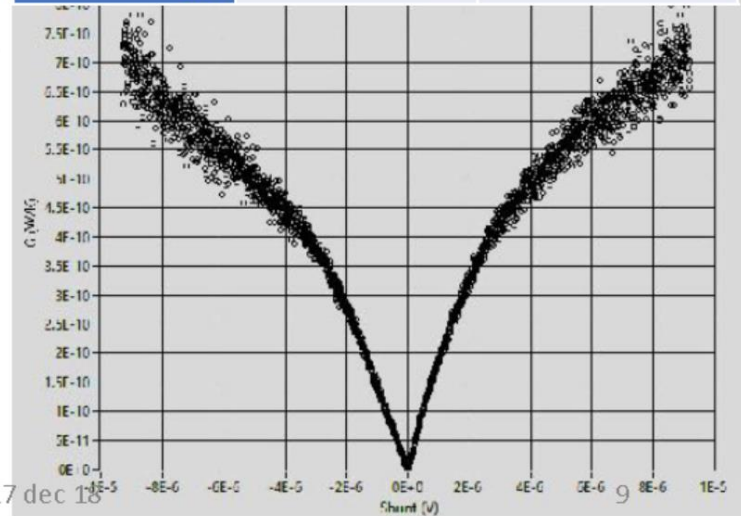
- The absorbers are large Si_3N_4 spider-webs (8 mm diameter, multimode)
- Sensors are Ti-Au TES
- Photon noise limited
- $\tau = 10\text{-}30$ ms



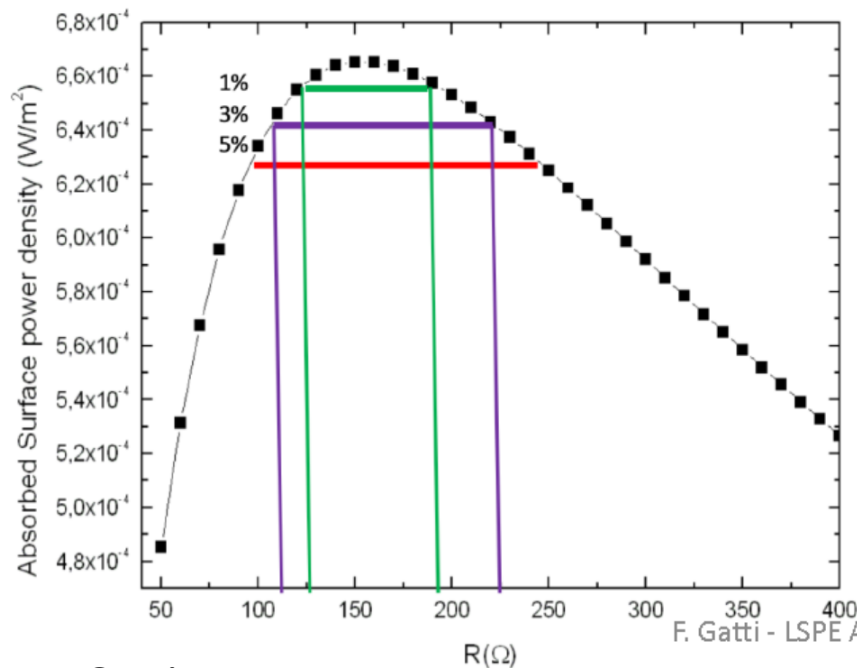
- IV curves acquired with SQUID VTT J3, with $M=36 \mu\text{A}/\phi$
- Voltage bias generated onto a shunt resistor of $7.34 \text{ m}\Omega$
- The analysis allows to calculate the effective thermal conductance G and the NEP, including the electro-thermal feedback



V_{bias} (μV)	G (10^{-11} W/K)	NEP 10^{-17} W/Hz $^{0.5}$
0.5	5	2.6
1.0	10	3.8
1.5	20	5.3
2.0	28	6.3



- Very large spider-web absorbers: long time constant, even with large electrothermal feedback
- Minimize heat capacity by using Bi metalization of the spider-web
- Optimization of resistance per square versus heat capacity
- Expected around 10-30 ms



F. Gatti - LSPE ASI Review, 17 dec 18

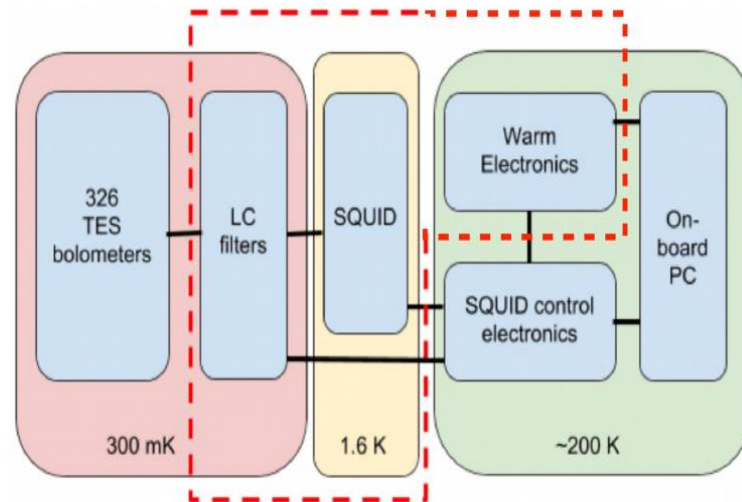
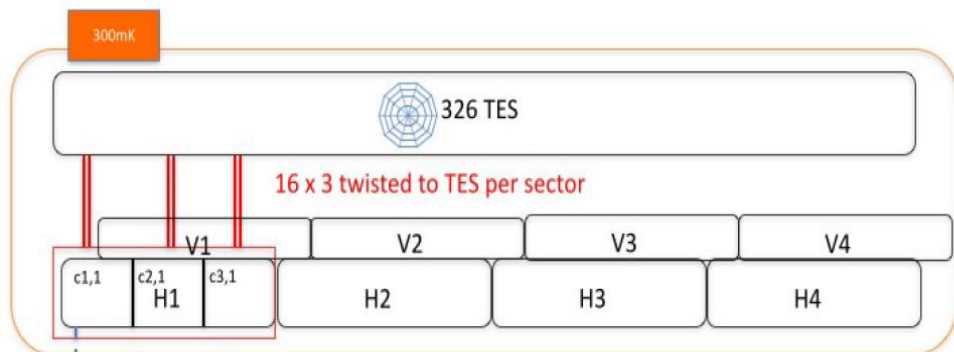
Parameters for Gold	Expct/meas. factor	Effect on heat capacity
RRR	1.5	1.5
3% Match. Fact.	1.8	1.8
G factor	2	-
Expctd Tau fact.	5	

Parameter for Bi over Gold	Expctd/meas. factor	Effect on heat capacity
Resistivity Ratio	50(expec.) - 70(meas.)	3,4(expec.)- 2,4(meas.)
Specific heat ratio	1/170	
G fact.	2	
Expectd. Tau fact	5(meas.)- 7(expec.)	

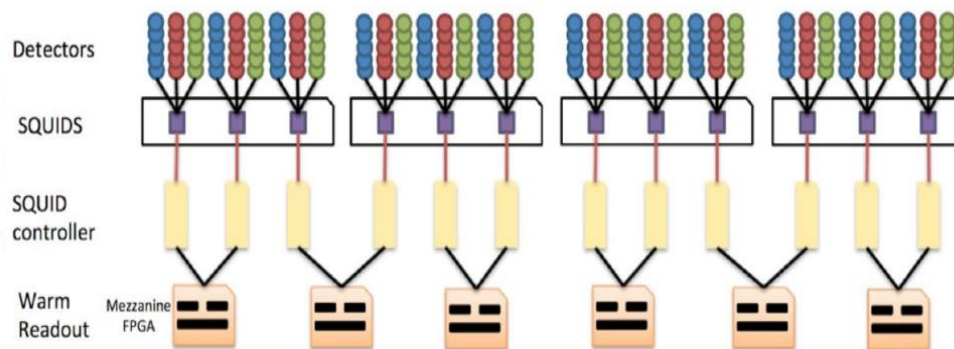
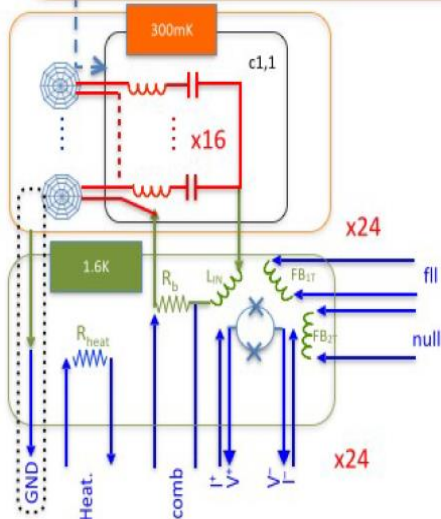
Cosmic Rays

- In the stratosphere: abundant primaries, and secondaries from both atmospheric and instrument interactions.
- Very rough estimate:
 - In BOOMERanG LDB in Antarctica: typical 8 mHz rate, for a spider web with 2.6 mm diameter and 5% filling factor (Masi et al. 2006, 2010).
 - Scaling from here, for a 8 mm diameter and 6% filling factor absorber with similar thickness, we expect a 90 mHz rate.
- Forecast basically confirmed by physics simulations carried out by the Pisa group (G. Signorelli et al. : 250 mHz).
- With a time constant of $\tau=30$ ms, and flagging data for 6τ for each event, this rate would result in a loss of $< 5\%$ of the data.

SWIPE - TES readout (mux)



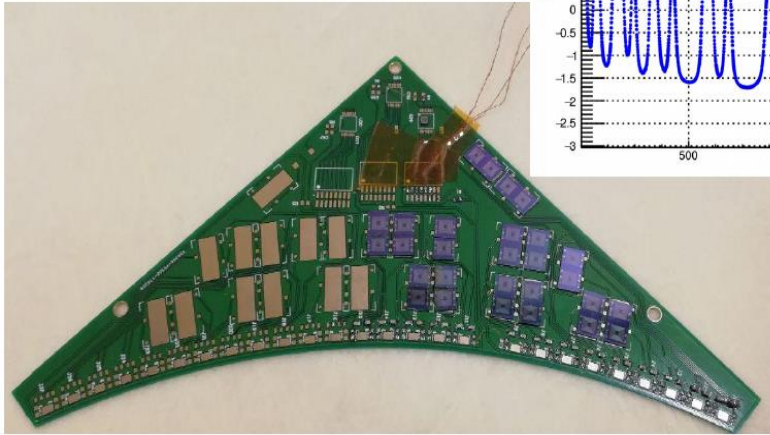
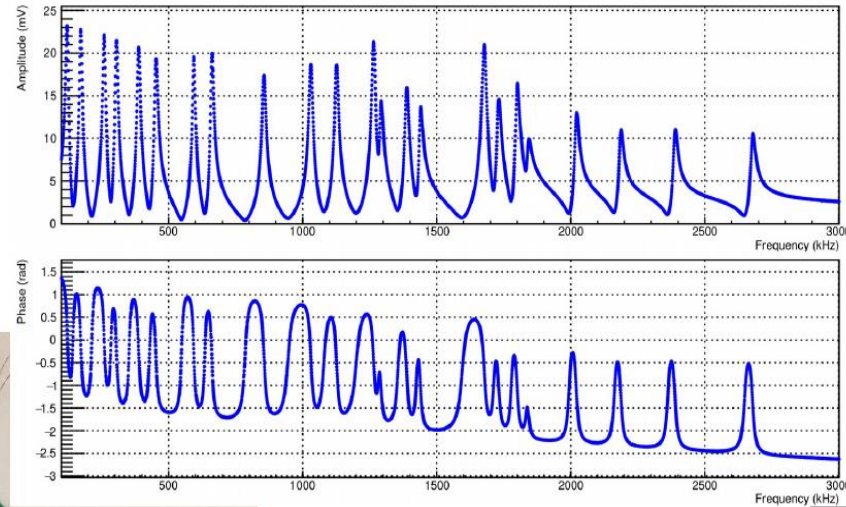
Wiring and connections from 300 mK to 250 K



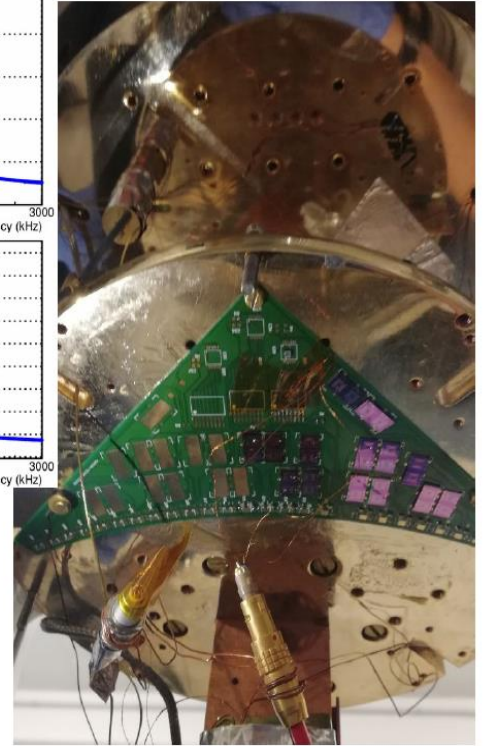
G. Signorelli

SWIPE - TES readout (mux)

- 14 Si chips, 2 Nb $15 \mu\text{H}$ inductors each, 5 open-circuited
- 28 SMD capacitors, ranging from 220 pF to 100 nF
- SMD resistors with $R = 1 \Omega$, $R_{\text{shunt}} = 100 \text{ m}\Omega$
- Readout with SQUID in FLL
- Tested @ 4 K



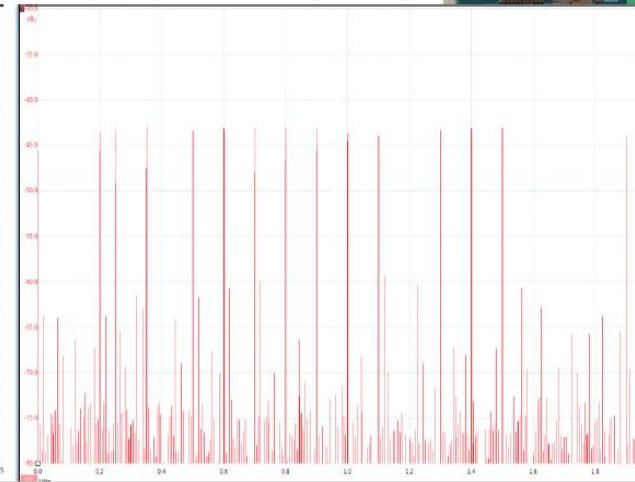
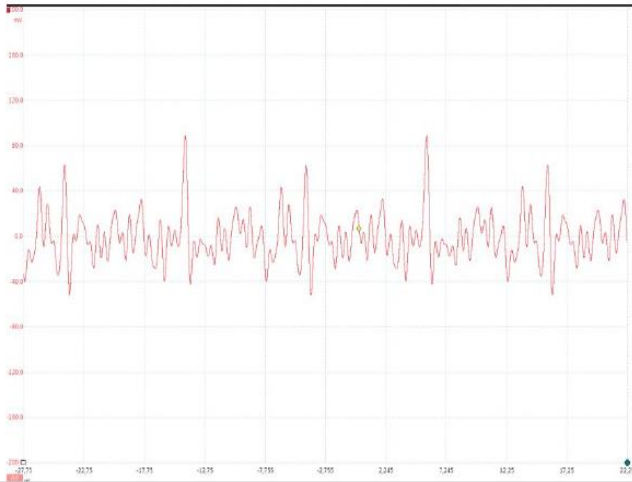
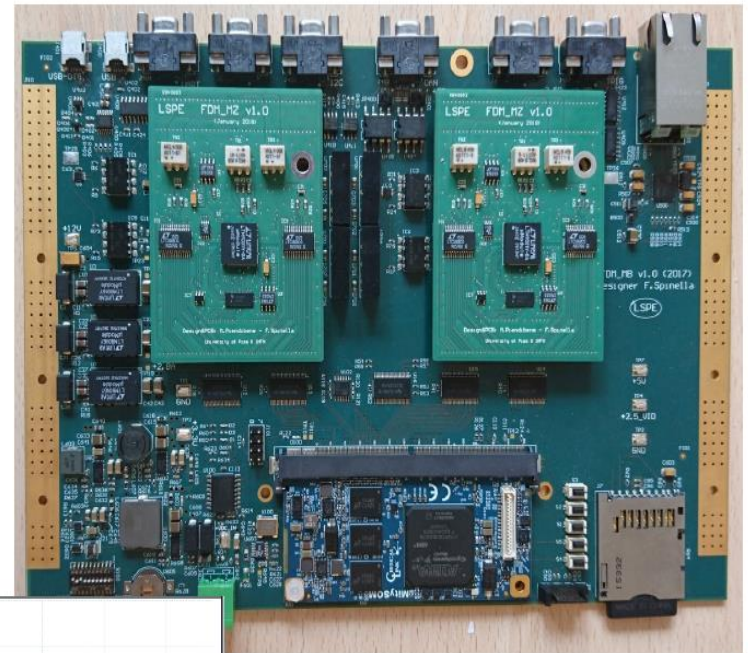
Test of a readout channel



G. Signorelli

SWIPE - TES readout (mux)

- **Altera Cyclone V SoC**
 - FPGA with 110'000 logic elements
 - 925 MHz dual-core micro-controller
- **Mezzanine plug-ins for DAC and ADCs**
 - 2 LTC1668 DACs (low noise, low power consumption)
 - 1 LTM9001-GA ADCs (16-bit, 25 MSPS)
- **Gbit interface** for data communication
- **CAN & I2C** interfaces to control low noise amps



FDM board tested and working

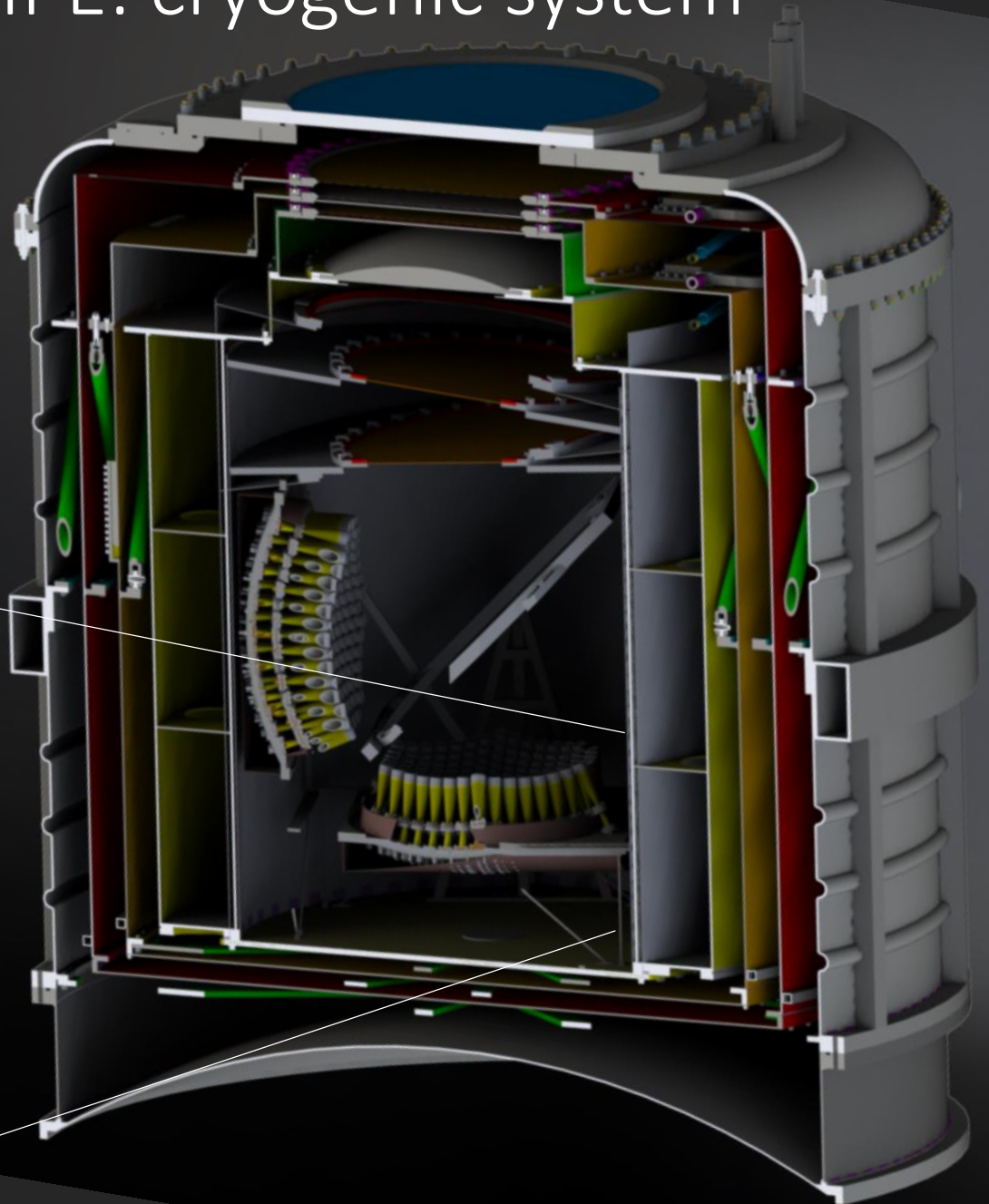
First comb generation algorithm

G. Signorelli

LSPE/SWIPE: cryogenic system

LSPE-SWIPE

- Aluminum cryostat
- Large cold volume (1m³)
- 2 vapor cooled shields
- Fiberglass support system
- 270L of superfluid ⁴He @ 1.6K
- > 15 days hold time
- ³He refrigerator 0.28K
(Coppi et al. 2016SPIE.9912E..65C)

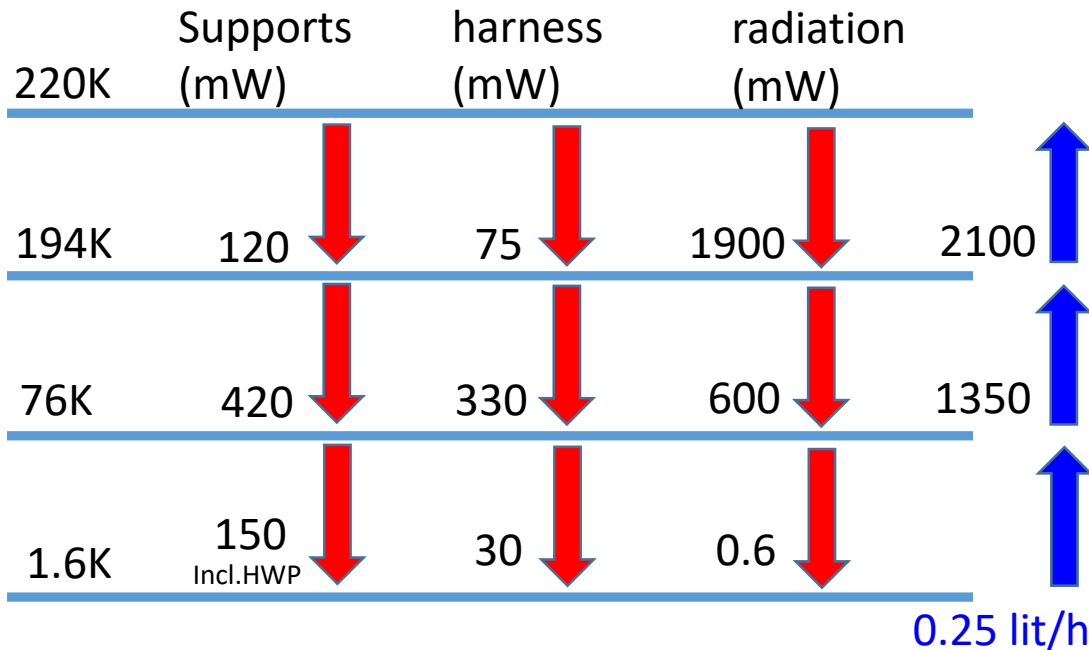


LSPE/SWIPE: cryogenic system

Expected performance versus gas exchange efficiency (30 s.i. shields)

T_{ext} (K)	Efficiency	T_{shield1} (K)	T_{shield2} (K)	Hold time (days)
290	0.7	106	270	13
290	0.8	100	255	15
290	0.9	93	250	16
220	0.7	76	194	22
220	0.8	71	190	25
220	0.9	67	187	27

Heat loads and heat lifts



Cryostat development

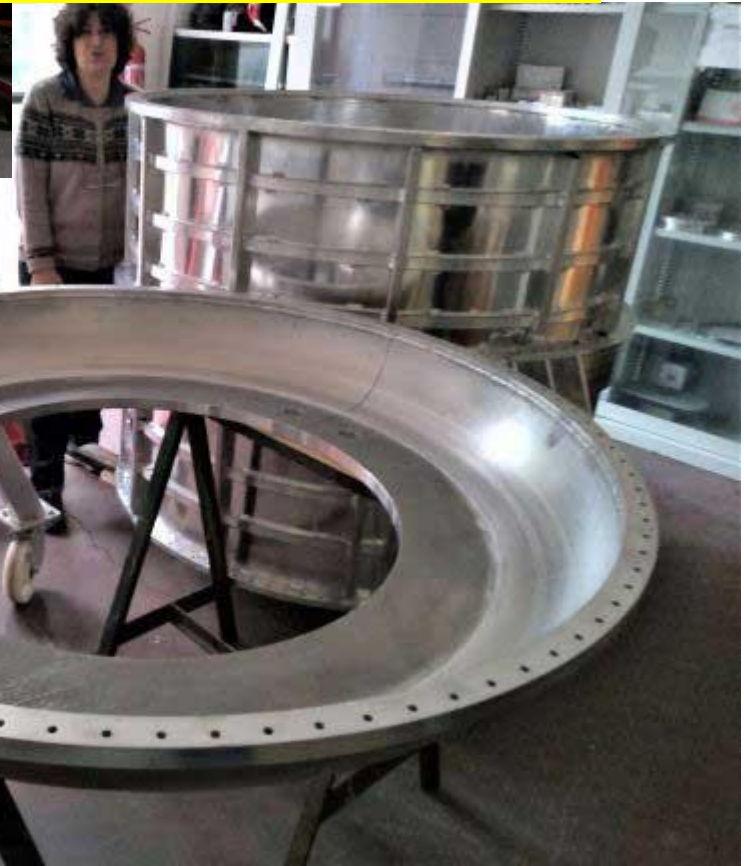
parts being machined



Main Cryogenic System



Outer shell assembled and vacuum tested to 10^{-10} mbar l s
Inner shell being welded.
Delivery in February 2020.

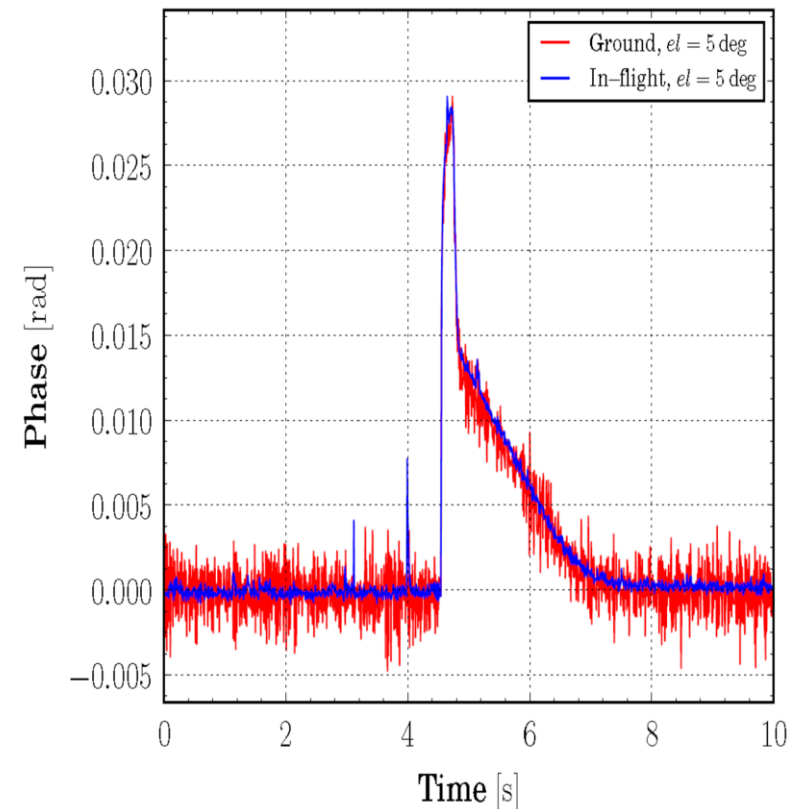


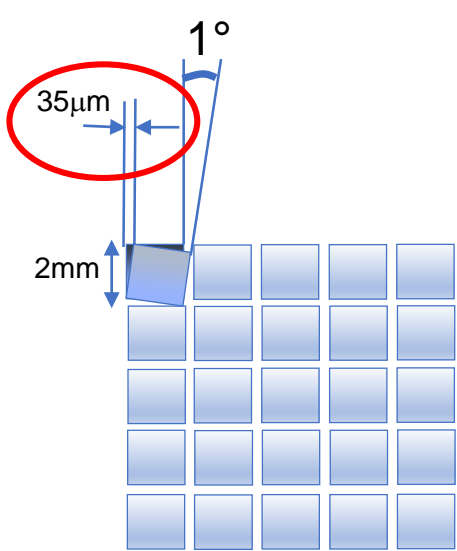
- Detectors harness defined
- Manufacturing started.
- Finalized in-synch with cryostat.

Calibration Plans

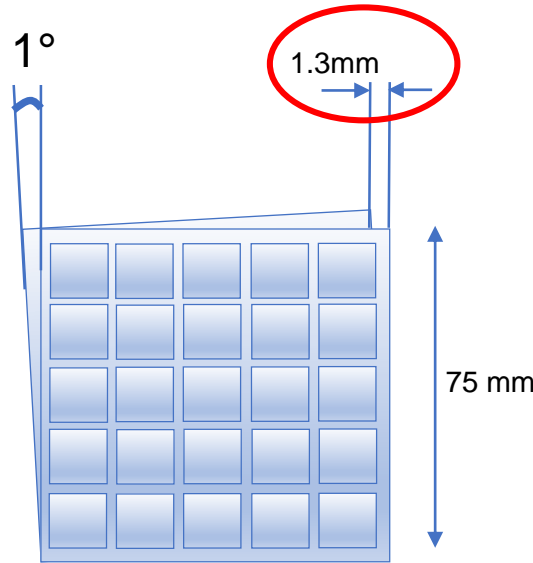
- τ calibration / ground
- Beam calibration/ ground
 - Gunn sources (G1: 145, G2: 210-240) in the far field (200-350 m), on a drone. High S/N
- Polarimetry calibration / ground
 - Full beam calibrator (+ NDF) see below
- Responsivity calibration / ground
 - Full beam chopper + NDF) + calibration lamp for calibration transfer
- Noise calibration / ground
 - Data acquisition with closed window, NDF, subsystems on/off

145 GHz	210 GHz	240 GHz
205 m	296 m	339 m
0.02 W	0.01 W	0.01 W
11.7 deg	12.1 deg	12.1 deg
5.89E-07 W	1.31E-07 W	1.00E-07 W

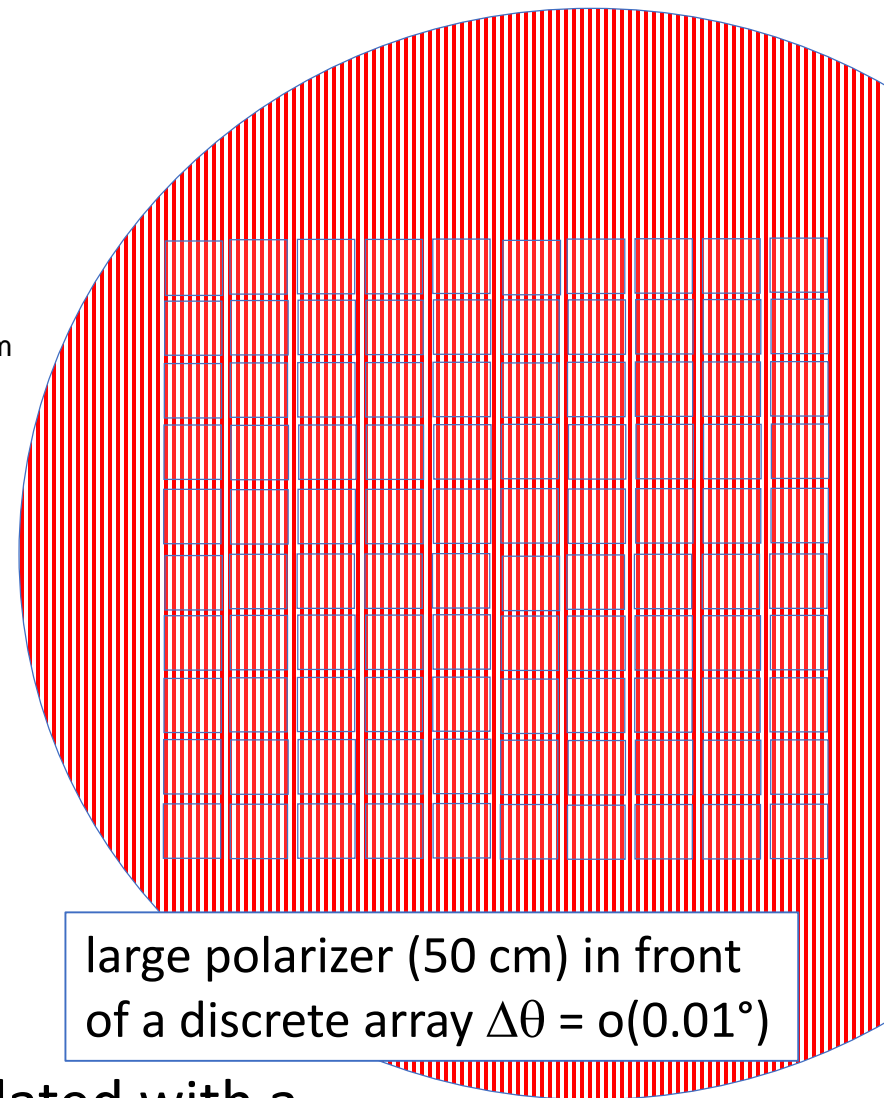




array of discrete elements.
 $\Delta\theta = O(1^\circ)$

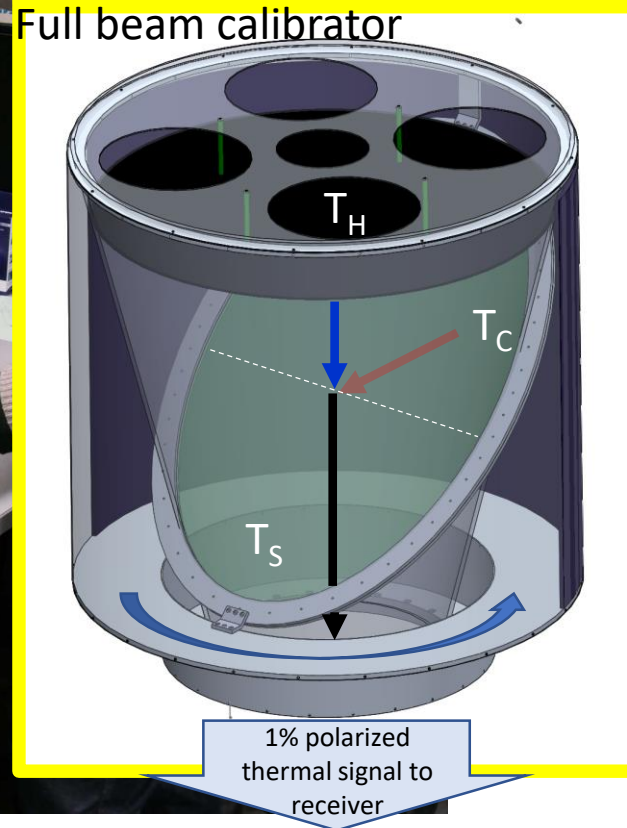
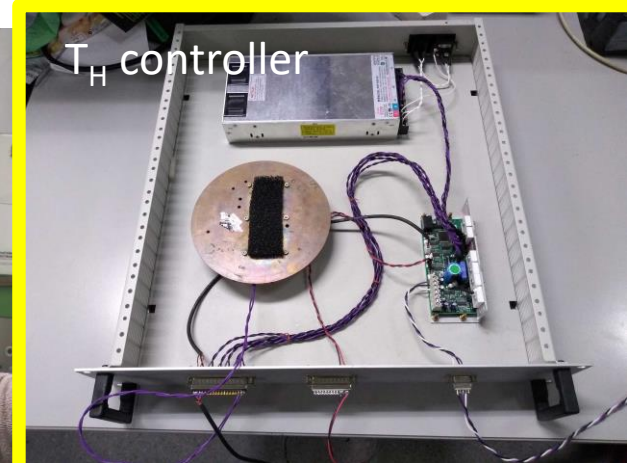
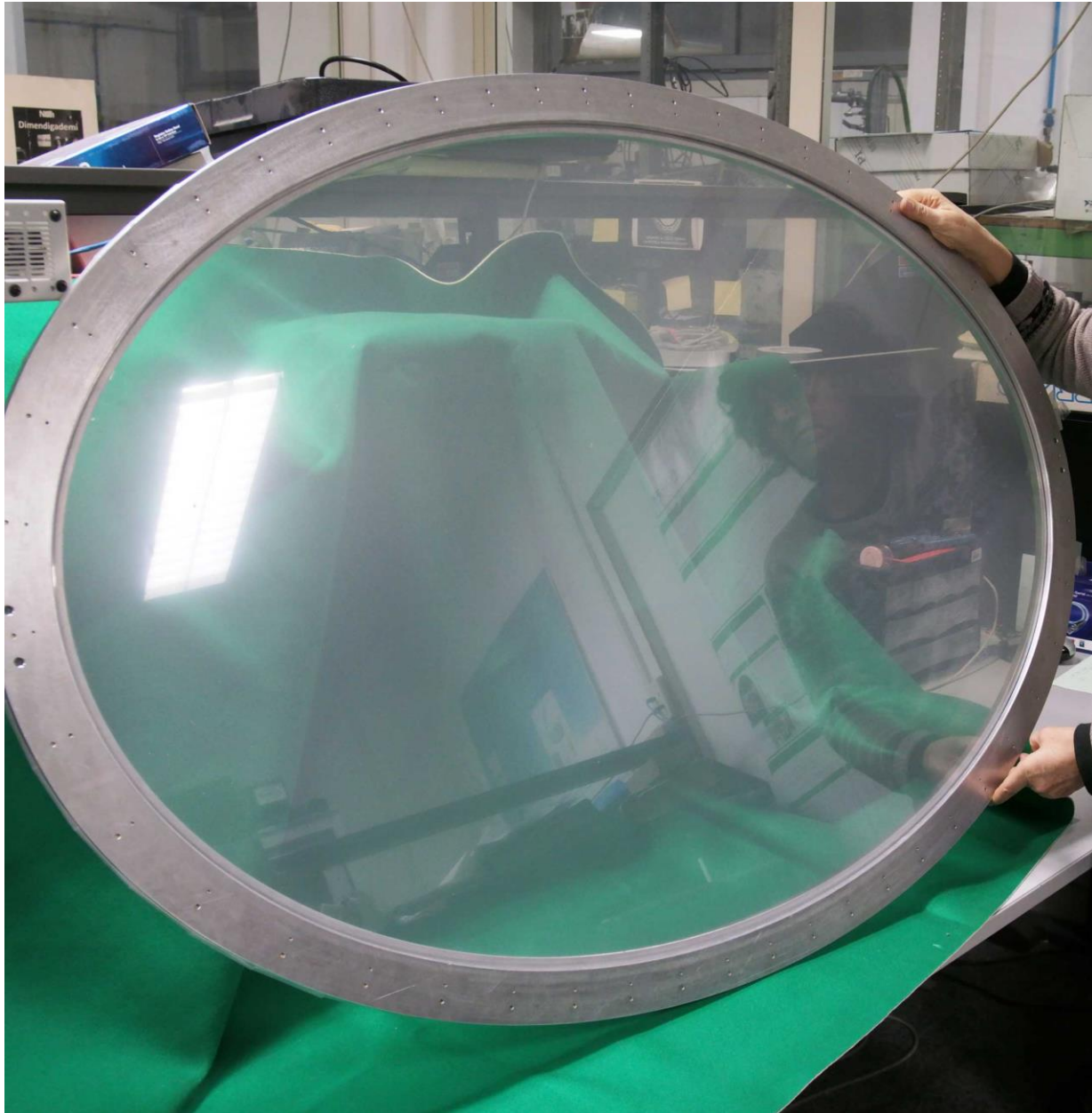


Photolithographed array – high precision within the tile.
 $\Delta\theta = o(0.1^\circ)$



This accuracy promise should be validated with a custom precision measurement

Full-beam Calibrator

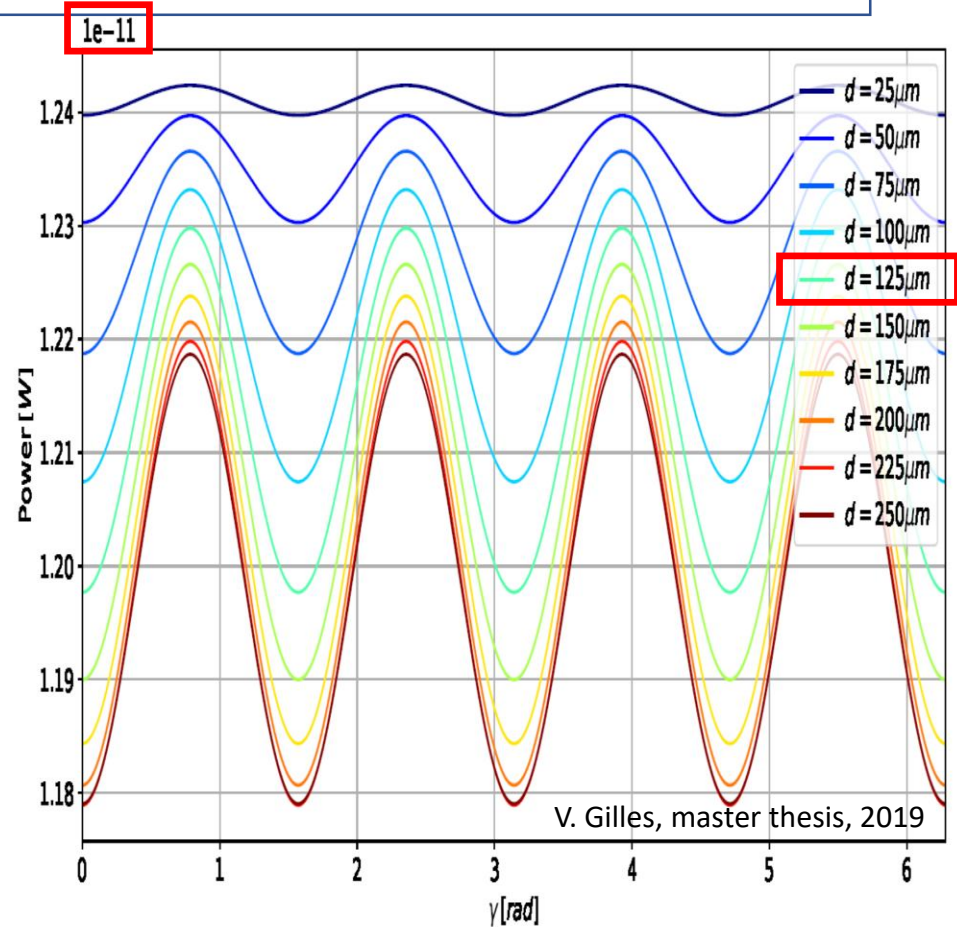
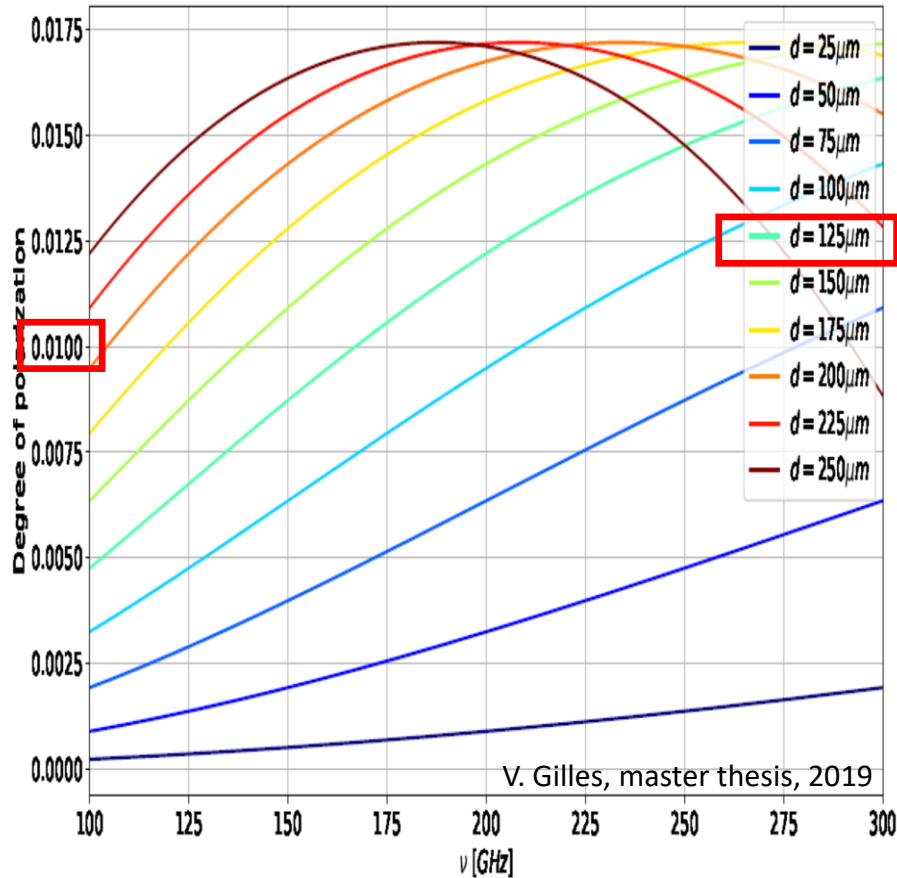


See e.g. O.Dell,
Swetz, Timbie (2003)

$$Q = T_H + (T_H - T_C)(R_{TE} - R_{TM}) + (T_S - T_C)(\epsilon_{TE} - \epsilon_{TM})$$

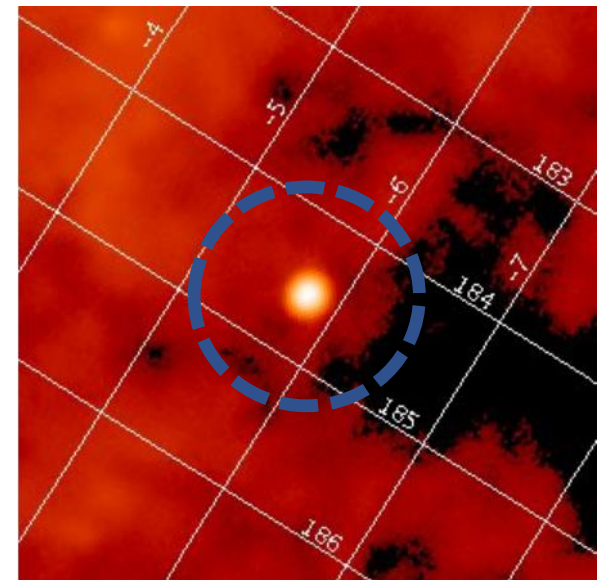
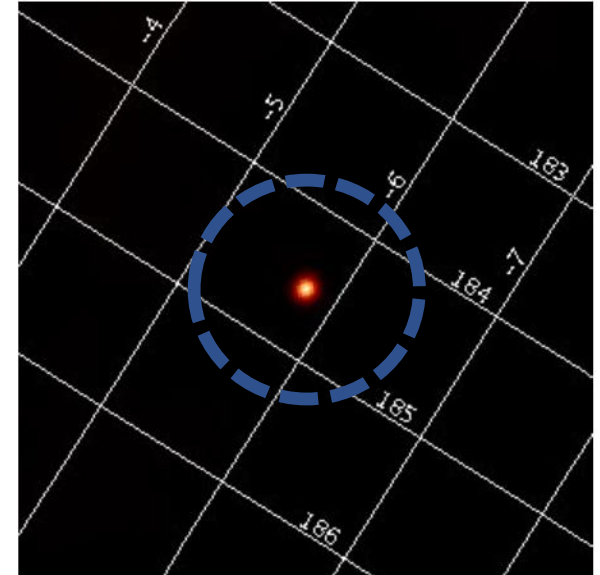
$$U = 0$$

TE // to dielectric sheet



Modulated polarized power expected on multimode detector (220 GHz band + 1% NDF, based on accurate measurements of 125 μm mylar sheet): 4×10^{-14} W : \gg NEP
 We expect to measure the direction of the polarimeter axis with 1' accuracy.

- Correlation with Planck T for gain calibration
- Crab nebula (culmination at 31°) to check the polarimetry calibration
- the Moon edges (if moon visible, culmination around 25°) can be used to check beam and polarimetry in the high-end of the dynamic range
- Edge polarization convoluted with main beam detected during the scan, needs modelling to recover both beam and polarization characteristics.



Summary

- LSPE (STRIP and SWIPE) will provide:
 - good internal foregrounds removal capabilities
 - good control of systematic errors
 - accurate calibration
- Sensitive polarization maps for CMB, synchrotron and dust, with high orientation accuracy
- Target $r = 0.01$ looks feasible and robust.
- Best way to learn how Stokes polarimeters with cryogenic spinning HWP work in the field.
- Commissioning in Tenerife for STRIP: end 2020
- Launch of SWIPE: end 2021
- Full data-set in hands: 2022